Transcriptomic characterization of the *B. napus – L. maculans* pathosystem

by

Michael Becker

A thesis submitted to the Faculty of Graduate Studies of

The University of Manitoba

in partial fulfilment of the requirements for the degree of

Doctor of Philosophy

Department of Biological Sciences

University of Manitoba

Winnipeg, MB

Abstract

Canola (*Brassica napus* L.) is one of the world's most valuable oilseed crops and sustains a multibillion-dollar industry. Currently, blackleg disease caused by the hemibiotrophic fungus *L. maculans* threatens the canola industry in Canada, Europe, and Australia and causes over $500 Million in crop loss per annum. Disease control relies heavily on crop resistance mediated by SOBIR1-interacting receptor-like proteins, such as Rlm2 and LepR1. Understanding the downstream plant immune responses activated by SOBIR1-RLP complexes is currently an area of interest in plant pathology. This work profiles the transcriptome of canola cotyledons from the initial stages of infection through to the necrotrophic stage of disease, in both compatible and incompatible (*Rlm2*, *LepR1*) interactions. A spatial dimension was added to this dataset through the application of laser microdissection and captured early signaling events during initial host colonization. Through transcriptomic interrogation I identified plant immune responses associated with resistance, such as jasmonic acid signaling, lignin and callose production, and calcium signaling. Additionally, I designed the program SeqEnrich to build regulatory networks and predict transcriptional control of these important immune processes. SeqEnrich has been made publicly available and will serve as a valuable resource to researchers studying transcriptional control of biological processes in *B. napus* and Arabidopsis. Further, sequencing data was functionally validated with mutant screens, microscopy, measurement of endogenous jasmonic acid concentrations, and physiological experiments with calcium channel blockers. This identified positive regulators of plant resistance, including uncharacterized receptor-like proteins, that are the focus of ongoing research. To my knowledge, this is the first study to apply LMD and RNA-Seq in combination to characterize early signaling events during a plant host-microbe interaction, and the first transcriptomic investigation into *LepR1*- and *Rlm2*-mediated

immunity. Together, this information will be valuable to researchers studying blackleg disease, regulation of transcription in plants, and plant host pathogen interactions in general.

Acknowledgements

First, I want to thank my supervisor Dr. Belmonte, whose guidance and motivation over the course of this PhD showed me how to successfully balance research, teaching, and service while maintaining a life outside of the lab. Over the course of my PhD I believe Mark and I have become colleagues and friends, and I can't thank Mark enough for the opportunities and support provided to me during my time under his tutelage.

Next, I have to thank everyone in the Belmonte lab, past and present, for making the lab a great place to work. I want specifically to thank those that contributed their time and ideas: Jacob Cavers, Ainsley Chan, Matthew Granger, Vanessa Hoi, Deirdre Khan, Jenna Millar, Rachel Robinson, Samantha Lee, Phil Walker, and Joey Wan. The cohesive environment in the lab is probably what I will miss the most from my time as a PhD student.

I also appreciate the collaborations that were built during my PhD with some excellent people. In particular, Dr. Dilantha Fernando and Dr. Xuehua Zhang; Dr. Teri de Kievit, Ms. Kelly Duke and Ms. Nidhi Shah; and Dr. Steven Whyard and Dr. Suresh Desai. I also thank Dr. Fernando, Dr. de Kievit, and Dr. Whyard for their time on my PhD advisory committee – I know this is an incredible commitment and I am grateful. Also, I would like to thank my supervisor Dr. Belmonte and co-supervisor Dr. Teri de Kievit for the countless reference letters provided during my time as a student (and most likely in the future too… sorry).

Finally, I would like to thank my friends and family for their support over and I would like to apologize for their neglect while writing this thesis and when research was a demanding force in my life. I would also like to thank my partner, Samantha, for her support during my PhD and for providing a much needed distraction from research. Although you probably delayed my graduation a few months, the joy you have brought into my life almost makes up for it.

Table of Contents

List of Tables

List of Figures

List of Appendices

Forward

This thesis follows the format outlined by the Department of Biological Sciences and Faculty of Graduate Studies at the University of Manitoba. It contains an introductory literature review, followed by three manuscripts, and general discussion and future directions. My second chapter has been published in The Plant Journal, my third chapter has been published in PLoS ONE, and my fourth chapter will be submitted to a peer-reviewed journal.

1 Literature Review

1.1 Introduction:

Blackleg disease, caused by the ascomycete fungus *Leptosphaeria maculans*, is a major disease of *Brassica napus* (canola) and a threat to canola markets. This fungus is endemic in Canada, Australia, and Europe, and causes an estimated global rapeseed loss of 15% or $900M USD (Fitt et al. 2008, Tollenaere et al. 2012). Current control methods include crop rotation and fungicide application; however, the most effective and utilized strategy is the cultivation of resistant varieties (Liban et al. 2016). It is only recently that the genes responsible for canola resistance against *L. maculans* have been more clearly identified and much about the molecular mechanisms that control these interactions are unknown. This first chapter will examine available information regarding the *B. napus-L. maculans* pathosystem. It will highlight gaps in knowledge and indicate where current biotechnology can be used to provide insights into the mechanisms underlying resistance.

1.2 Host Background:

1.2.1 Brassica species:

The Brassica genus, within the family *Brassicaceae*, contains a number of agriculturally relevant crops (Bhandari et al. 2015) including rapeseed (*Brassica napus*), cabbage, broccoli, cauliflower, kale (*B. oleraceae*), mustard seed (*B. nigra*) and turnip (*B. rapa*). These crops are divided into six cultivated *Brassica spp.* that were defined by Nagaharu U as three diploid species (U 1935), *B. rapa* (AA), *B. nigra* (BB), and *B. oleraceae* (CC), and three tetraploid hybrids, *B. napus* (AACC), *B. juncea* (AABB), and *B. carinata* (BBCC). The interconnected relationship between the above species and their genomes is known as the triangle of U.

Oilseed rape (*B. napus*) originated ~7500 years ago through the hybridization of *B. oleracea* and *B. rapa* (Chalhoub et al. 2014). Rapeseed oil was initially used as lamp fuel in ancient civilizations (Romanus et al. 2008) with documented use in India around 4000 years ago (Snowdon et al. 2007). In the 1940s, *B. napus* was heavily cultivated in Canada, as rapeseed oil was an excellent lubricant for the steam engines used in naval and merchant ships in World War II (Nieschlag and Regional 1970). Demand for industrial rapeseed oil fell after the war, pushing researchers to explore the use of rapeseed oil for human consumption and rapeseed meal as animal feed. Reports of rapeseed meal as a poultry feed began as early as 1944; however, the high level of glucosinolates in the meal produced a number of reported side effects including goitrogenicity (Pettit et al. 1944). As an edible oil its use was limited due to health concerns over the high levels of erucic acid (Stefansson and Hougen 1964). Conventional breeding programs led by Keith Downey and Baldur R. Stefansson at the University of Manitoba aimed at reducing glucosinolate and erucic acid content (Stefansson et al. 1961, Harvey and Downey 1964, Stefansson and Hougen 1964). A true success, the project led to the production of the first canola (Canadian oil low acid) varieties that were later approved for human consumption– with an erucic acid content of <1% in the oil and <30 mg/g of glucosinolates in the meal (Scarth et al. 1988).

1.2.2 National and Global Importance of Canola:

Since the introduction of canola, oilseed rape (canola and related Brassica species) has become the second-most cultivated oilseed globally (USDA, 2018), producing 13% of global supply. In Canada, 2017 marked the first year where canola acreage exceeded that of wheat, becoming the most cultivated national crop (Statistics Canada 2017; Fig. 1.1). The growth of canola can be explained by its high market value due to a high oil content (40%) and meals with

a high protein content of 35-45% (Khajali and Slominski 2018). The oil profile of canola is desirable, with an average of 60-65% monounsaturated fats and 30-35% polyunsaturated fats, rich in omega-3 fatty acids, and a high flash point (Kostik et al. 2013). Compared to other fats, a meta-analysis associated canola with lower cholesterol levels, improved insulin sensitivity, and a lower incidence of heart disease (Lin et al. 2013, Rajaram 2014). Breeding programs have effectively produced varieties of "designer" canola oils, with specialized oil profiles for frying, nutrition, biofuels, and lubricants (Von Cruz and Dierig 2015). As a result of its versatility of use and health benefits canola continues to gain popularity and global production is expected to increase by an average of 1.2% per annum for the next ten years (OECD-FAO, 2017).

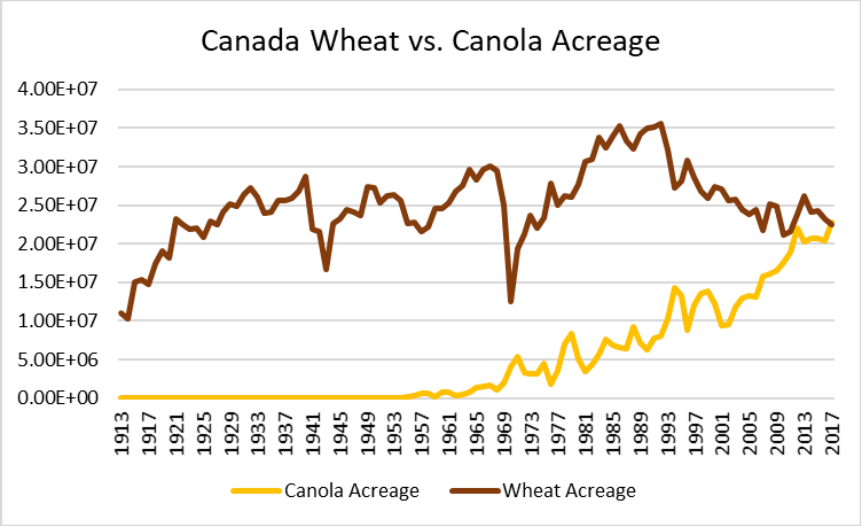

Fig. 1.1: Canola acreage trends 1913-2017, with wheat added for comparison. Note that 2017 marks the first year where canola acreage exceeds that of wheat. Graph constructed from data obtained from Statistics Canada (2017).

1.2.3 The *Brassica napus* genome:

Brassica napus L. was sequenced and annotated as part of a major collaborative effort because of its agricultural importance and the potential to provide insight into the evolution of polyploid plant species (Chalhoub et al. 2014). The genome of *B. napus* is considered large at 1.13 Gb and with 90,000-101,000 protein coding genes, compared to 135 Mb and 27,655 protein

coding genes in Arabidopsis (Cheng et al. 2017). Additionally, genes in *B. napus* are often multicopy (4-6 copies) due to allopolyploidy and historic genome duplication events (Parkin et al. 2003). The release of the *B. napus* genome created opportunities for next generation sequencing projects on canola, which previously relied on genomic data obtained from related *B. rapa* and *B. oleracea* species. This included a sudden emergence of transcriptome studies investigating canola development (Chen et al. 2015, Deng et al. 2015, Long et al. 2015, Wan et al. 2017) and defense against pathogens (Lowe et al. 2014, Kumar et al. 2016, Duke et al. 2017, Girard et al. 2018).

1.2.4 Diseases of *B. napus*:

The most economically relevant diseases of *B. napus* are caused by the ascomycete fungal pathogens *L. maculans* (blackleg) and *Sclerotinia sclerotiorum* (sclerotinia stem rot); however, both clubroot caused by the obligate protist *Plasmodiophora brassicae* and verticillium stripe caused by the fungus *Verticillium longisporum* are emerging threats to the canola industry (Peng et al. 2015, Depotter et al. 2016, Al-Daoud et al. 2018). Additionally, incidences of 'minor' diseases on cultivated canola have been recorded. This includes white leaf spot (*Pseudocercosporella capsellae*; Gunasinghe et al. 2017), downy mildew (*Peronospora parasitica*; Mohammed et al. 2017), Alternaria leaf/pod spot (*Alternaria brassicae;* Wouw et al. 2016a), powdery mildew (*Erysiphe cruciferarum;* Uloth et al. 2016), white blister rust (*Albugo candida*; Borhan et al. 2010), leaf white spot (*Pyrenopeziza brassicae*; Boys et al. 2007), Aster yellows (*Ca. Phytoplasma spp.*; Bahar et al. 2018), and Fusarium wilt (*Fusarium oxysporum*; Gaetán 2005). Of all these diseases, blackleg is often considered the most severe, largely due to the nature of its lifecycle, diversity, and global distribution (Wouw et al. 2018, Zou et al. 2018).

1.3 Blackleg disease of the Brassicaceae

1.3.1 Lifecycle of blackleg:

The lifecycle of *L. maculans* is outlined in Fig. 1.2. Infection of the host begins when sexual (ascospores) or asexual (pycnidiospores) *L. maculans* spores germinate on the surface of a host leaf or cotyledon. Fungal hyphae circumvent the epidermis through stomata or wounds on the foliar surface produced by mechanical damage or insect feeding (Hammond et al. 1985). Once inside, *L. maculans* grows biotrophically within intercellular and apoplastic spaces. This biotrophic stage can be divided into an initial establishment phase and a subsequent exploration phase as *L. maculans* spreads between intercellular spaces (Hammond and Lewis 1987). The fungus then transitions into a necrotrophic lifestyle producing necrosis-inducing proteins that activate host cell death forming lesions (Haddadi et al. 2016). *L. maculans* continues to reproduce in the necrotic tissue forming pycnidia, which can propagate the infection to nearby plants through rain splash (Travadon et al. 2007). The hyphae of the fungus penetrate the vasculature and migrate down into the stem of the host. Here, the fungus continues to grow, leeching nutrients from the host and restricting water along the shoot. In severe cases this leads to blackening of the stem (from which the disease receives its name), lodging, and host death. *L. maculans* can overwinter in the stubble and reproduce sexually producing pseudothecia that release wind-dispersed ascospores that can continue infection in the next growing season (Bousset et al. 2018). Further, *L. maculans* can infect pods, leading to contaminated seeds that produce infected seedlings. The debris from these plants can produce pseudothecia in the following growing season that serve as a new source of inoculum (Van de Wouw et al. 2016).

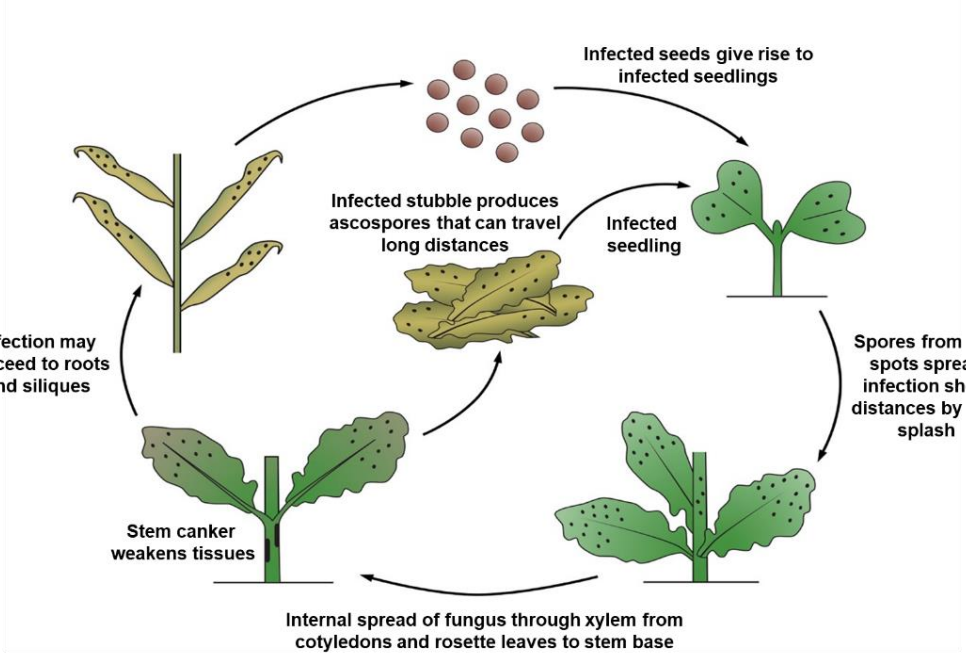

Fig. 1.2: Lifecycle of *L. maculans* on canola. During its lifecycle the fungus will produce sexual ascospores in the stubble, and asexual pycnidiospores in infected foliar tissue. The fungus can cause death of the plant through severe infection of the stems leading to lodging.

1.3.2 Transmission of *L. maculans* in Canada:

L. maculans can persist within stubble for three or more years (Baird et al. 2018). In Western Canada release usually occurs between May to August (West et al. 2001), with extreme spring weather conditions delaying sporulation on stubble (Petrie 1994). Production of *L. maculans* ascospores varies wildly each growing season based on a number of factors, but will generally be worse in years with mild temperatures and heavy rainfall (Guo and Fernando 2005, Aubertot et al. 2006). In Canada, evidence suggests transmission of blackleg relies heavily on asexual disease transmission through pycnidiospores in seasons with little or late ascospore production (Ghanbarnia et al. 2011); however, in Manitoba over the last six years there is no evidence that sexual reproduction has been inhibited (Fernando et al. 2018). Depending on

conditions, asexual reproduction may produce several rounds of infection in a single growing season, known as polycyclic infection (Li et al. 2006).

1.3.3 A brief history of blackleg disease of canola:

L. maculans can infect a wide range of hosts within the Brassicas, including *B. rapa*, *B. oleracea*, and *B. juncea*, along with other wild crucifers that may serve as a significant source of inoculum (Petrie 1994). It was first identified as a pathogen of cabbages (Tode 1791, Desmazières 1849), with several epidemics resulting in severe yield losses in the early 20th century (Henderson 1918). Although rare outbreaks occurred, *L. maculans* was not a major agricultural concern until the development of canola with its low levels of glucosinolates and erucic acid. Initially, two strains that caused blackleg disease were defined that were originally regarded as one species: an aggressive strain that produced the phytotoxin sirodesmin PL (Group A) and a non-aggressive strain that does not produce sirodesmin PL (Group B). They were eventually determined to be two species due to morphological differences in pseudothecia and no evidence for mating between the two groups (Toscano- Underwood et al. 2003). The aggressive strain was defined as *L. maculans* and the non-aggressive strain *L. biglobosa*. Although distinct species they are often found to coexist, and the life cycles of both are similar (Fernando et al. 2016).

Following commercialization of canola, blackleg epidemics were increasingly severe as cultivated varieties had no resistance. Blackleg disease nearly destroyed the Australian rapeseed industry during its early stages (reviewed in Salisbury 1995) and in the early 1990s average yield losses in France climbed as high as 40% (Ansan-Melayah 1997). Introduction of resistant varieties and 4-year crop rotations kept disease occurrences to a minimum until the early 2000s when tighter 2-year crop rotations became common due to the increasing economic benefits of

canola (Hegewald et al. 2017). Shifts to virulent *L. maculans* strains eventually rendered several commonly used resistance (*R*)-genes ineffective in Canada (Zhang et al. 2016).

The disease remains endemic in Australia, Europe, and Canada, despite wide variation in growing season, climate, and cultivars (reviewed in West et al. 2001). Alberta has incurred recent outbreaks of blackleg disease. Average incidence of blackleg disease ranged from 13.1-21.2% between 2015-2017 in Alberta, with severity in some fields reaching as high as 3.8 on a 5 point scale (Canadian Plant Disease Survey, http://phytopath.ca/publication/cpds/). Note; each unit increase in disease severity leads to an approximate decline of 17.2% of yield (Hwang et al. 2016). In Australia annual yield losses generally range from 10-15% (Wouw et al. 2016b). Only *L. biglobosa* has been detected in China, causing disease outbreaks that are less severe than those of *L. maculans* (Li et al. 2013), but can lead to measurable losses (Cai et al. 2018). The fear of introducing *L. maculans* into the country previously led to Chinese import restrictions on Canadian oilseed, cutting Canadian exports to China by half in 2010 (Zhang and Fernando 2018) and highlighting the political and economic impact of blackleg disease.

1.3.4 Strategies for control of blackleg disease of canola:

In addition to proper crop rotation practices, fungicides have been approved for control on the disease including seed treatments and a foliar spray. In Canada the foliar fungicide Quilt (Azoxystrobin & Propiconazole) is registered for control of blackleg and the active ingredients have been shown to limit disease symptomology (Peng et al. 2012). In 2012, the first foliar fungicide (Prosaro/prothioconazole & tebuconazole) was registered in Australia for blackleg control. In both countries, foliar fungicide application only shows an economic benefit under extreme disease pressure such as instances where grown varieties have a sudden breakdown of resistance (Wouw et al. 2016b, Zhang and Fernando 2018). Fungicide seed coatings (mainly

fluquinconazole) have been common in Australia since 2005 and have been shown to provide an economic benefit (Wouw et al. 2016b); however, the same benefit was not observed in Canadian-grown rapeseed (Zhang and Fernando 2018).

The main method of disease control is through the effective application of *R*-genes. To date, 16 resistance genes have been identified in the Brassicas (*Rlm1-Rlm11, RlmS, LepR1-LepR4*) and two have been cloned (*LepR3* and *Rlm2*), which are two alleles of the same gene (Delourme et al. 2004, Larkan et al. 2013, 2015, Raman et al. 2016). Of these, currently, *Rlm1, Rlm2, Rlm3, Rlm4, Rlm7, Rlm9, LepR1, LepR2, LepR3,* and *RlmS* are found in cultivated canola varieties (Wouw et al. 2016b, Zhang and Fernando 2018).

The efficacy of an *R*-gene can be quickly eroded over the first several years of its rotation – especially if seeded in succession. This process of initial potency followed by rapid breakdown of resistance is often referred to as a "boom and bust" cycle (Rouxel et al. 2003). For example, *Rlm1* was highly effective in Europe following its release in 1998, with 83% of European *L. maculans* isolates avirulent on *Rlm1* plants. By 2000, due to strong selection pressure less than 13% of isolates were avirulent and the *R*-gene was rendered ineffective (Rouxel et al. 2003). Similar situations were observed with *LepR3* in Australia (Sprague et al. 2006) and *Rlm3* in Canada (Zhang et al. 2016).

The strategy of rotating host *R*-genes to protect their efficacy against blackleg was proposed by Marcroft et al. (2012) and implemented in Australia. Using greenhouse and field trials Marcroft et al. (2012) tested spores from the previous year's stubble against cultivars with various *R*-gene complements to predict relative susceptibility. With this strategy, researchers predicted the breakdown of Hyola50 *Rlm1* and *LepR1 R*-genes in the Eyre Peninsula growing region and recommended cultivation of alternative varieties (Wouw et al. 2014). Similar

strategies of *R*-gene rotation have been recommended for Canada (Zhang and Fernando 2018) and Europe (Winter and Koopmann 2016).

1.3.5 The genetic basis of resistance:

Blackleg resistance is often simplified into a gene-for-gene relationship where *B. napus R*-genes correspond to individual pathogen *Avr*-genes, such that if both are present the reaction will be incompatible and infection will fail (Flor 1971). Although this often holds true, the interactions between host *R*-genes and pathogen *Avirulence* (*Avr*)-genes are more complicated as it has become clear that multi-gene interactions occur between the two species. For example, pathogen *Avr* genes can prevent the detection of other *Avr* genes. Host *Rlm3* recognition of effector *AvrLm3* is suppressed by a functional allele of *AvrLm4-7* (Plissonneau et al. 2016). Additionally, it was recently discovered that recognition of *AvrLm5-9* by host *Rlm9* was also suppressed by *AvrLm4-7* (Ghanbarnia et al. 2018). Further, *L. maculans AvrLm1* is recognized by two separate *B. napus R*-genes, *Rlm1* and *LepR3* (Petit-houdenot and Fudal 2017). These recent findings demonstrate that the intricacies of gene interactions in the *B. napus-L. maculans* pathosystem are only partially defined. These findings also have direct implications in disease management. For example, to protect the integrity of cultivars containing *Rlm1* or *LepR3*, these *R*-genes should not be cultivated immediately after one another. Additionally, as *Rlm3* and *Rlm9 R*-genes would select for fungal isolates containing *AvrLm4-7*, *Rlm7* cultivars may be effective if cycled immediately afterwards those containing *Rlm3* or *Rlm7*.

1.4 Plant immune responses to fungal pathogens

1.4.1 The plant immune system:

As sessile organisms with no adaptive immune response plants have developed extensive barriers to prevent pathogen entry and intricate signaling mechanisms to detect and eliminate invading pathogens. The first line of defense against pathogens consists of physical and chemical barriers including a waxy cuticle, cell wall, antimicrobial enzymes, and secondary compounds (Malinovsky et al. 2014, Serrano et al. 2014). Most fungal pathogens can penetrate the cuticle through secretion of digestive enzymes such as cutinase, or through mechanical rupture. Bacterial and fungal pathogens may also take advantage of natural openings of the plant – commonly the stomata (Zeng et al. 2010, Kale and Tyler 2011). If a pathogen overcomes these physical barriers they will be faced with sophisticated surveillance systems within the cell that detect invading pathogen and activate host immune responses.

Host immune pathways are often divided into PAMP (pathogen-associated molecular pattern)-triggered immunity (PTI) and effector-triggered immunity (ETI). PTI is the first tier of the immune system and is characterized by extracellular recognition of PAMPs, such as chitin or flagellin, through membrane-surface pattern recognition receptors (PRRs). Following pathogen recognition, plants often accumulate a variety of secondary metabolites with toxic or inhibitory effects, may reinforce cell walls with callose and/or lignin, and activate a variety of other defense responses to be discussed later in this review (Gill et al. 2015). PTI is thought to be effective against a broad range of pathogens and is largely responsible for nonhost resistance (Bigeard et al. 2015).

For successful infection pathogens will produce effectors that supress normal host PTI signaling causing effector-triggered susceptibility. In response, plants have evolved mechanisms known as ETI to directly or indirectly detect effectors within the cell. This is usually accomplished through intracellular receptors of the nucleotide-binding leucine-rich repeat (NB-

LRR) type (Lee and Yeom 2015). Commonly, these proteins will monitor the status (or guard) plant proteins and detect perturbations due to effector activity (Khan et al. 2016). Compared to PTI, the effects of ETI are rapid and associated with localized programmed cell death (PCD), referred to as the hypersensitive response, and activation of systemic-acquired resistance in the host (Künstler et al. 2016). ETI signaling is responsible for race-specific resistance, as the host and pathogen undergo a genetic 'arms race' that can become fairly complex. A well-studied example is the *R*- and *Avr*-gene interactions of the Arabidopsis – *Pseudomonas syringae* pathosystem. In this system RIN4, a regulator of basal defense, is phosphorylated by pathogen AvrB compromising PTI as commonly seen in effector-triggered susceptibility. In response, the plant protein RPM1 detects phosphorylation of RIN4 and activates ETI. Further in response, *P. syringae* produces AvrRpt2 to cleave RPM1, and in turn the plant detects this cleavage through another R-protein RPS2 (Axtell and Staskawicz 2003, Kim et al. 2005, Russell et al. 2015). It stands to reason that protein interactions in the *L. maculans – B. napus* pathosystem could be similarly complicated; however, details regarding the specifics are only now starting to emerge.

1.4.2 Defined immune targets of *L. maculans* effectors:

Currently, studies have identified the genomic location of eight *L. maculans Avr*-genes including *AvrLm1*, *2*, *3*, *4-7*, *5-9* (previously referred to as *AvrLmJ1*), *6*, *11*, and *AvrLepR1*. Currently, 8 genes coding for the following proteins have been cloned: AvrLm1 (Gout et al. 2006), AvrLm2 (Ghanbarnia et al. 2015), AvrLm3 (Plissonneau et al. 2016), AvrLm5/J1 (Van de Wouw et al. 2014), AvrLm6 (Fudal et al. 2007), AvrLm7 (Parlange et al. 2009), AvrLm9 (Ghanbarnia et al. 2018), and AvrLm11 (Marie- Hélène et al. 2013). All are small cysteine-rich secreted proteins, except AvrLm1 that only contains one cysteine residue (Gout et al. 2006). The only effector with a defined mode of action is AvrLm1. AvrLm1 has been shown to affect host

defense signaling by stimulating phosphorylation of Map Kinase 9. Evidence suggests this change in phosphorylation state leads to an increased propensity for cells to undergo programmed cell death (Ma et al. 2018).

1.4.3 Plant defense deviates from the ETI/PTI dichotomy:

The idea of a clear distinction between ETI and PTI has become challenged with a growing number of exceptions. For example, nonhost resistance can generate a hypersensitive response similar to ETI, leading to rapid PCD and systemic acquired resistance (Mishina and Zeier 2007, Naito et al. 2008, Klessig et al. 2018). Rather, it has been suggested that PTI and ETI act on a continuum where the intensity and nature of the response depends on the combination of signaling pathways activated or repressed (Thomma et al. 2011). Even large quantities of beneficial microbes can trigger system acquired resistance and are said to 'prime' the plant for future attack (Duke et al. 2017, Mauch-Mani et al. 2017, Vatsa-Portugal et al. 2017).

Additionally, a major exception to the ETI and PTI dichotomy are extracellular LRR receptor-like proteins (RLPs) that mediate host-specific resistance to apoplastic fungal pathogens such as *L. maculans*. Unlike the rapid onset of PCD commonly observed in gene-for-gene interactions, defense against apoplastic fungi results in delayed PCD and an overall response that better fits the definition of PTI. Because of the inability of this signaling mechanism to be classified as PTI or ETI a new term, effector-triggered defense (ETD), has been suggested (Stotz et al. 2014), and refers to RLPs that mediate resistance through a complex with the protein SOBIR1. A well-studied example of ETD are tomato Cf proteins that recognize the effectors of *Cladosporium fulvum*, the causative agent of tomato leaf mold (Rivas and Thomas 2005, Liebrand et al. 2013). Recently, the Tomato *I* gene was found to code for an RLP effective against Fusarium wilt (*Fusarium oxysporum*; Catanzariti et al. 2017) that complexes with

SOBIR1 and SERK3/BAK1. Blackleg R-proteins also fall under this definition. LepR3, an RLP, interacts with SOBIR1 to mediate resistance to *L. maculans* (Ma and Borhan 2015) and is allelic to Rlm2 (Larkan et al. 2015). Because of the relevance of this pathosystem and the unusual characteristics of ETD there is an incredible interest in understanding the pathways that regulate ETD against *L. maculans* and other apoplastic fungal pathogens

1.4.4 Signaling through the SOBIR1 complex:

Although SOBIR1 has been shown to be a core component of PTI and ETD, how it transduces signals into an appropriate immune response remains enigmatic (Liebrand et al. 2013). Resistance mediated by RLPs is dependent on SOBIR1 and BAK1 (Zhang et al. 2013, Ma and Borhan 2015) that form a tripartite complex upon ligand binding (Albert et al. 2015). This has been found to be widely conserved among plants, with roles in defense against a variety of pathogens including *Phytophthora infestans*, *S. sclerotiorum*, *Verticillium dahliae*, and *L. maculans* (Albert et al. 2015, Ma and Borhan 2015, Zhou et al. 2018). Overexpression of BAK1 or SOBIR1 leads to a constitutive immune response and spontaneous cell death (Gao et al. 2009, Domínguez-Ferreras et al. 2015) providing further evidence to their role as positive defense regulators. Additionally, *bak1* mutants fail to activate MAPK signaling in response to several elicitors (Heese et al. 2007, Gao et al. 2009, Albert et al. 2015). BOTRYTIS-INDUCED KINASE 1 (BIK1) or other receptor-like cytoplasmic kinases likely connect BAK1-mediated signaling to MAPK signaling cascades (Saijo et al. 2017, He et al. 2018). Signaling from other PRR receptors, such as chitin perception through CERK1, integrates into these MAPK signaling pathways to further coordinate the immune response (Saijo et al. 2017). Additionally, SOBIR1 homologs in cotton have been shown to directly phosphorylate and activate a bHLH transcription factor (Zhou et al. 2018), suggesting this complex can directly activate transcriptional

reprogramming during defense. SOBIR1 and BAK1 are known effector targets (Zhou et al. 2014, Wu et al. 2018), which is likely reflective of their central roles in immunity. Resolving how signaling the SOBIR1-BAK1 complex coordinates defense will be a fundamental step towards understanding resistance against *L. maculans*.

1.5 Physiological changes during plant defense

1.5.1 Role of cell death in effector-triggered defense against *L. maculans*:

Cell death results from nearly any host incompatible or compatible interaction, and the balance between pro-death and pro-survival pathways can ultimately determine host fate. Cell death is often induced by hemibiotrophic apoplastic fungal pathogens and precedes lesion formation in compatible interactions (Keon et al. 2007, Haddadi et al. 2016). It is unclear if the observed cell death during ETD has a defensive role or is simply the result of intense immune signaling surrounding the infection site.

Regulators of PCD are often targets of effectors from apoplastic fungal pathogens (Franco-Orozco et al. 2017, Ma et al. 2018) and *L. maculans* produces a number of toxins to induce cell death (Pedras and Biesenthal 1998, Haddadi et al. 2016). In Arabidopsis *accelerated cell death 2* mutants inoculated with *L. maculans*, lesion spread was observed within 48 hours compared to 14-21 days for wild type plants (Bohman et al. 2004). When Arabidopsis plants susceptible to the necrotroph *S. sclerotiorum* were transformed with the CED-9 anti-apoptotic gene, a resistance phenotype was recovered (Kabbage et al. 2013). Introduction of anti-apoptotic genes, such as CED-9, into susceptible *B. napus* could provide a new mechanism for the manipulation of this pathosystem and provide conclusive evidence as to the role of PCD in the containment of the hemibiotroph *L. maculans*.

1.5.2 Production of plant secondary metabolites during ETD against *L. maculans*:

ETD is generally associated with the accumulation of antifungal indole-glucosinolates (IGSs) and other phytoalexins. IGSs are derived from tryptophan and their biosynthesis is mainly executed by families of cytochrome P450s (Fig. 1.3). In Arabidopsis, the hypersensitive response to the hemibiotrophic fungi *Colletotrichum gloeosporioides* required the production of IGS (Hiruma et al. 2013). In addition, Arabidopsis mutants with compromised IGS metabolism demonstrate hypersensitivity to necrotrophs *S. sclerotiorum* and *Botrytis cinerea* (Kliebenstein et al. 2005, Stotz et al. 2014, Zhang et al. 2015). In vitro studies have shown isothiocyanates from *Brassica napus*, predominantly those derived from the glucosinolate sinigrin, to be toxic to *L. maculans* (Mithen et al. 1986). In response, *L. maculans* has also been shown to synthesize enzymes that detoxify glucosinolates such as Brassinin (Pedras and Jha 2006).

The phytoalexin camalexin shares a portion of its biosynthetic pathway with IGS (Fig. 1.3). In Arabidopsis (a nonhost to *L. maculans*), disruption of camalexin biosynthesis results in susceptibility to *L. maculans* (Bohman et al. 2004). Additionally, *L. maculans* cannot metabolize camalexin *in vitro* (Pedras et al. 1998). However, *B. napus* lacks the ability to produce camalexin (Staal et al. 2006), which we predict is through the loss of biosynthetic gene *PAD3*, which was not identified in the *B. napus* genome. Thus, it would be interesting to determine how the introduction of *PAD3* and restoration of camalexin biosynthesis in *B. napus* would affect host susceptibility to *L. maculans*.

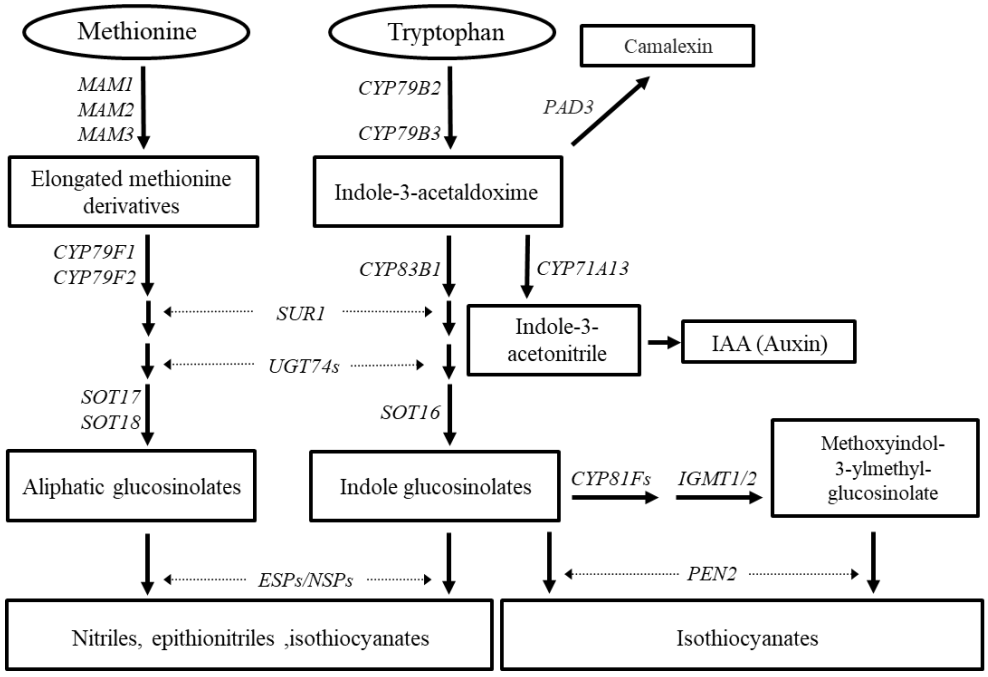

Fig. 1.3: Pathway for production of indole glucosinolates and related compounds in the Brassicaceae. Figure produced with data from Celenza et al. 2005, Liu et al. 2010, and Frerigmann et al. 2016. Products of this pathway have been shown to be toxic to L. maculans, including isothiocyanates and camalexin. Note; B. napus cannot produce camalexin through the loss of biosynthetic gene PAD3.

1.5.3 Calcium signaling during defense:

Calcium is an important secondary messenger involved in a number of stress responses in addition to growth and development processes. During plant-pathogen interactions, calcium flux is among the earliest detectable changes following pathogen recognition (Ranty et al. 2016). Calcium influx following activation of the SOBIR1-BAK1 complex may occur through interactions with BONZAI (BON1). BAK1 phosphorylates BON1 *in vitro* (Wang et al. 2011), and is a positive regulator of calcium channels Calcium ATPase 8 (ACA8) and ACA10 (Yang et al. 2017). Further, it has been shown that PAMP-induced calcium signaling requires PBL1 and BIK1 (Ranf et al. 2014), adding an additional layer of complexity that is currently not well understood.

It has been proposed that differences in amplitudes and timing of calcium flux fine tunes defense responses, which is supported by unique calcium signatures in response to effectors like flg22, eld18, Pep1, or chitin (Ranf et al. 2011). Because of its essential role initiating multiple cellular responses plants have evolved sensors that decode calcium signals. This includes calcineurin-B-like (CBL) proteins, calmodulin (CAM) and CAM-like proteins, calcium-dependent protein kinases, and CAM-dependent protein kinases (Ranty et al. 2016). The diversity of these sensors in their affinity for calcium, cellular location, and downstream targets ultimately allows for the interpretation of calcium signatures and elicitation of proper cellular responses. Crosstalk between calcium and other major defensive cues also coordinates the plant defense response. For example, at high intracellular calcium concentrations CAM1 stimulates nitric oxide (NO) and reactive oxygen species (ROS) production (Choi et al. 2009, Zhou et al. 2016). Although there is little direct evidence that calcium signaling contributes to resistance against *L. maculans*, it is suggested from its close association with SOBIR1-BAK1 signaling. Taken together, signaling through calcium and MAPK pathways following RLP detection of the pathogen leads to a variety of plant responses including transcriptional reprogramming (Fig. 1.4), hormone production and signaling, production of secondary metabolites, and callose and lignin deposition (Becker et al. 2017b).

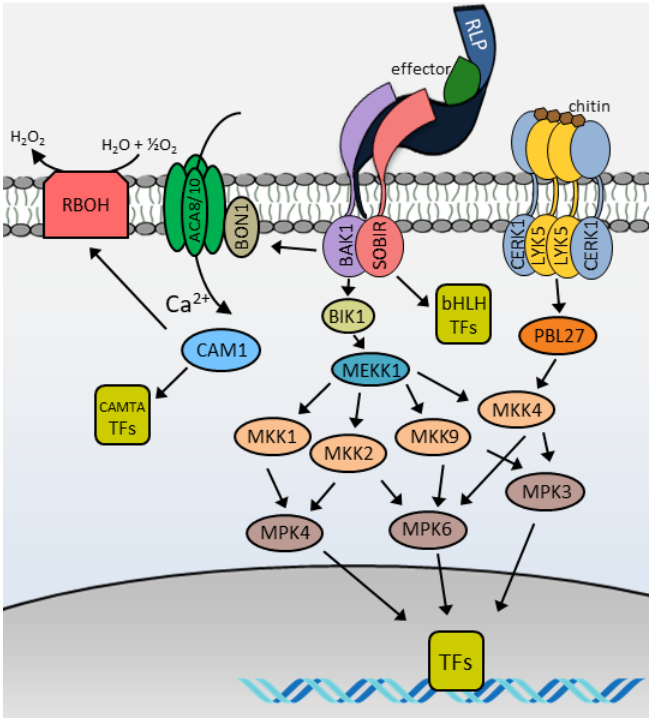

Fig. 1.4: Putative regulatory events following activation of the SOBIR1-BAK1 complex. Following recognition of pathogen effectors transcription factors may be activated directly, or indirectly through MAP kinase or calcium signaling. MAP kinase signaling cascades also integrate signals from PAMP receptors, such as CERK1.

1.6 Emerging technologies useful for study of host pathogen interactions

1.6.1 The use of laser microdissection in host pathogen interactions:

The use of specialized techniques to isolate targeted cells is necessary for researchers studying cell-specific transcriptional programming of biological processes. Laser microdissection (LMD) is one of the few tools in the plant biologist's toolbox that can be used to isolate homogenous populations of cells and tissues for molecular analysis. This technology can be coupled to downstream molecular techniques such as qPCR, microarray, and RNA-Seq to provide high-resolution gene expression data (Millar et al. 2015). Other methods, such as fluorescence-activated cell sorting, can be used to isolate specific cell populations, however this technique has a few notable drawbacks. First, the technique relies on production of transgenic

lines and requires knowledge regarding cell- and tissue-specific promoters that may be difficult to determine for host pathogen interactions (Carter et al. 2013). Second, the technique requires cell wall digestion to liberate protoplasts, which may result in activation of stress pathways (Bargmann and Birnbaum 2010). Together, this makes LMD the best technique for isolating cell and tissue populations during host pathogen interactions.

Several studies have demonstrated the utility of LMD for the investigation of host microbe interactions, with the majority focusing on symbiotic relationships including fungi (Balestrini et al. 2007, Gomez et al. 2009, Gaude et al. 2012, Giovannetti et al. 2012, Hacquard et al. 2013, Hogekamp and Küster 2013) and bacteria (Limpens et al. 2013, Roux et al. 2014). LMD has also been used to isolate infected and non-infected leaf and stem tissues in response to fungal pathogens including downy mildew (*Plasmopara viticola*), black wood of grapevine (*Candidatus Phytoplasma solani*), powdery mildew (*Golovinomyces orontii*), and blackleg of canola (Chandran et al. 2010, Santi et al. 2013, Lenzi et al. 2016, Becker et al. 2017b). An additional advantage of applying LMD to host pathogen interactions is the ability to increase pathogen sensitivity. Using this technology, Hacquard et al. (2010) isolated rust fungi (*Melampsora larici-populina*) at uredinial or biotrophic functional stages to identify gene networks involved in sporulation. Additionally, it has been used to monitor gene expression of the maize stalk rot fungus (*Colletotrichum graminicola*) during host during host colonization (Tang et al. 2006).

1.6.2 The genomics era of molecular biology:

New '-omics' technologies have made it possible to analyze expression data from tens, or even a single, eukaryotic or prokaryotic cell (Wang and Navin 2015). To our knowledge no studies have combined LMD and RNA-Seq in the exploration of host microbe interactions;

however it has been used to study developmental processes (Osaka et al. 2013) and to investigate the interactions between a parasitic plant and its host (Honaas et al. 2013). Commonly used methods to analyze host pathogen interactions following LMD are targeted gene profiling with qPCR (Santi et al. 2013, Lenzi et al. 2016, Becker et al. 2017b, Kooliyottil et al. 2017) or arrays (Klink et al. 2005, Chandran et al. 2010). This is likely due to the technical challenge of producing sequencing libraries from small amounts of tissue, which is currently not a service offered by many sequencing core facilities.

1.6.3 Studies using RNA-Seq to study ETD:

Transcriptomic investigation of biological systems was revolutionized by the introduction of RNA-Seq technologies. This holds true for host pathogen interactions, where RNA-Seq allowed for the analysis of gene expression within both the host and pathogen simultaneously, referred to as dual RNA-Seq. Over the last five years, hundreds of RNA-Seq experiments have emerged investigating plant defense and disease creating a wealth of information (Westermann et al. 2017).

The first investigation of the *L. maculans – B. napus* pathosystem was performed by Lowe et al. (2014) and investigated gene expression in susceptible cotyledons at 7 and 14 dpi exposed to *L. maculans* or *L. biglobosa*. Data showed an overall stronger response of the host to *L. biglobosa*, which may explain the non-aggressive nature of this species. Three additional RNA-Seq studies were published the following year exploring this pathosystem (Haddadi et al. 2016, Sonah et al. 2016, Becker et al. 2017b). Haddadi et al. (2016) investigated compatible interactions across the infection process at 0, 2, 4, 6, and 8 days post-inoculation, focusing heavily on the expression of putative *L. maculans* effectors and identifying a clear fungal biotrophic-necrotrophic transition period. Further, this study showed that *L. maculans* effectors

could suppress cell death in *Nicotiana benthamiana*. Building on this study, Sonah et al. (2016) analyzed pathogen gene expression in compatible and incompatible (*AvrRlm2*) interactions to further identify *L. maculans* effector candidates and providing additional support for a rapid necrotrophic transition of the fungus. To date, two studies have analyzed the transcriptomic response of plants during ETD– in tomato (Zuluaga et al. 2016) and canola (Becker et al. 2017b). In both studies, suites of regulatory molecules including kinases and TFs were transcriptionally activated during ETD and coincided with pronounced JA- and SA-related signaling in resistant plants.

1.6.4 Developing new tools for analyzing the *B. napus – L. maculans* pathosystem:

With a growing number of *B. napus* genomics studies, few tools have been developed to facilitate computational analyses of these data. Currently, databases exist that curate *B. napus* genome annotation information (Duvick et al. 2008) along with online tools for gene ontology (GO) term enrichment (Tian et al. 2017). Analysis of large *B. napus* datasets can be difficult compared to the model system Arabidopsis, which has a number of sophisticated databases (Rhee 2003, Austin et al. 2016), along with tools for data mining (Haas et al. 2004, Srinivasasainagendra et al. 2008) and building regulatory networks (Belmonte et al. 2013b, Chien et al. 2015, Chow et al. 2016, Zheng et al. 2016). Recently, we developed a new tool for *B. napus*, adapted from a pre-existing Arabidopsis program, SeqEnrich (Becker et al. 2017a), that builds TF regulatory networks from coexpressed *B. napus* gene sets.

1.6.5 Building transcription factor networks to understand complex bioprocesses.

Complex bioprocesses, including development, and abiotic and biotic stress responses, are all controlled by global shifts in gene expression mediated by DNA-binding TFs. Technologies, such as chromatin immunoprecipitation sequencing (ChIP-Seq) and DNA affinity

purification sequencing (DAP-Seq), have provided a means to efficiently identify TF binding sites (Aparicio et al. 2004, O'Malley et al. 2016). As a result, the binding sites for nearly all Arabidopsis TFs have been elucidated with 2.7 million binding sites in the Arabidopsis genome (O'Malley et al. 2016). By combining data on DNA promoter sequences, TF binding sites, and gene functions we can develop tools to predict overarching regulation of bioprocesses. In Arabidopsis, these strategies have improved our understanding of seed development (Belmonte et al. 2013b, Khan et al. 2015), secondary cell wall biosynthesis (Taylor-Teeples et al. 2014), starch biosynthesis (Bumee et al. 2013), plant defense (Tsuda and Somssich 2015), drought (Laxmi 2015), photosynthesis (Yu et al. 2014), and circadian rhythm (Kulkarni et al. 2018). With the development of new software, a similar approach can be used to investigate the transcriptional reprogramming that occurs following activation of *B. napus* R-proteins effective against L. *maculans*.

1.7 Current developments in the *B. napus – L. maculans* pathosystem:

While we are starting to gather information on the genetics underlying resistance in the *B. napus – L. maculans* pathosystem, much about the downstream defense responses that facilitate ETD remains elusive. With current developments that suggest receptor complexes can directly modulate transcriptional regulators, experiments should look towards understanding transcriptional reprograming that occurs in resistant host cells. To accomplish this, new programs should be developed that predict transcriptional reprogramming during complex plant bioprocesses such as defense. Further, as few experiments have examined the earliest stages of ETD (or host pathogen interactions in general), technologies such as LMD that can isolate the first cells responding to the pathogen will provide unparalleled resolution into the genetic and molecular mechanisms underpinning plant resistance.

1.8 Research Objectives:

This research aims to investigate the *B. napus – L. maculans* pathosystem using modern technologies such as RNA-Seq and LMD. To accomplish this, research will be divided into three main objectives:

1. **To analyze *B. napus* effector triggered defense against *L. maculans* across infection and identify key regulators of resistance:**

   An overview of host defense against *L. maculans* is presented to identify key regulators of ETD. Using RNA-Seq technology I tracked global gene expression and monitored the bioprocesses elicited by the pathogen in resistant plants carrying the *R*-gene *LepR1*. Using this information, candidate genes involved in host plant resistance were identified. The utility of LMD coupled with qPCR in characterizing this pathosystem showed that gene expression is regulated spatially as one migrates away from the infection site.

2. **To develop new tools for efficient and detailed analysis of gene expression data from *B. napus*:**

   Using all existing data on *B. napus* regulatory sites, TFs and TF families, metabolic pathways, and gene ontology, I developed a program to facilitate the analysis of large *B. napus* gene sets. This involved extensive data curation and consolidation, database building, genome annotation, and testing and optimization. Further, this program will serve as a valuable resource for any researchers using RNA-Seq to explore gene expression in *B. napus* or Arabidopsis, and is modeled after the highly cited Arabidopsis program ChipEnrich (Belmonte et al. 2013).

3. **To investigate *B. napus* resistance signaling during initial infection stages and directly at the host pathogen interface.**

This analysis will focus on the earliest stages (1 and 3 dpi) of the *AvrRlm2-Rlm2* interaction. This provides unprecedented resolution of how the first cells of the host plant are reprogrammed to defend against invading fungal pathogens. Using our newly developed program SeqEnrich, I will build regulatory networks using gene expression data to better understand the complex TF-DNA interactions that coordinate the complex cellular responses to disease.

2 Transcriptome analysis of the *Brassica napus-Leptosphaeria maculans* pathosystem identifies receptor, signaling and structural genes underlying plant resistance

Michael G. Becker[1,†], Xuehua Zhang[2,†], Philip L. Walker[1], Joey C. Wan[1], Jenna L. Millar[1], Deirdre Khan[1], Matthew J. Granger[1], Jacob D. Cavers[1], Ainsley C. Chan[1], Dilantha W.G. Fernando[2] and Mark F. Belmonte[1,*]

[1]Department of Biological Sciences, University of Manitoba, Winnipeg, MB R3T2N2, Canada,

[2]Department of Plant Science, University of Manitoba, Winnipeg, MB R3T2N2, Canada

[*]For correspondence (e-mail mark.belmonte@umanitoba.ca).

[†]These authors contributed equally to this work.

Author contributions:

Michael Becker conceptualized RNA-Seq study, contributed to library prep and alignments, performed data visualization, conceptualized and led mutant screens, conceptualized laser microdissection experiments, performed qPCR experiments, contributed to the writing of the introduction and the material and methods, wrote the results and discussion, and prepared Figs. 2.2, 2.3, 2.4, 2.5, 2.6, Table 1, Appendix II, IV, V, VI, VII, VIII, IX. Xuehua Zhang conceptualized RNA-Seq study, identified cultivars for analyses (Appendix 1), contributed to library prep and alignments, performed lignin staining, contributed to the writing of the introduction and the material and methods, and contributed to Fig. 2.1, Fig. 2.6, and Appendix III. Joey Wan, Philip Walker, and Matthew Granger contributed to mutant screens. Jenna Millar, Deirdre Khan, and Ainsley Chan contributed to microscropy and interpretation. Jacob Cavers contributed to laser microdissection experiments and qPCR. Mark Belmonte and WG Dilantha Fernando conceptualized the study, supervised students and the experiments, and edited the manuscript.

2.1 Abstract:

The hemibiotrophic fungal pathogen *Leptosphaeria maculans* is the causal agent of blackleg disease in *Brassica napus* (canola, oilseed rape) and causes significant loss of yield worldwide. While genetic resistance has been used to mitigate the disease by means of traditional breeding strategies, there is little knowledge about the genes that contribute to blackleg resistance. RNA sequencing and a streamlined bioinformatics pipeline identified unique genes and plant defense pathways specific to plant resistance in the *B. napus–L. maculans LepR1–AvrLepR1* interaction over time. We complemented our temporal analyses by monitoring gene activity directly at the infection site using laser microdissection coupled to quantitative PCR. Finally, we characterized genes involved in plant resistance to blackleg in the Arabidopsis–*L. maculans* model pathosystem. Data reveal an accelerated activation of the plant transcriptome in resistant host cotyledons associated with transcripts coding for extracellular receptors and phytohormone signaling molecules. Functional characterization provides direct support for transcriptome data and positively identifies resistance regulators in the Brassicaceae. Spatial gradients of gene activity were identified in response to *L. maculans* proximal to the site of infection. This dataset provides unprecedented spatial and temporal resolution of the genes required for blackleg resistance and serves as a valuable resource for those interested in host–pathogen interactions.

2.2 Introduction:

Brassica napus (canola, oilseed rape) is the second most widely produced oilseed crop worldwide and is under constant threat of blackleg disease caused by the hemibiotrophic fungal pathogen *Leptosphaeria maculans* (Fitt et al. 2006). Currently, mitigation of crop loss relies largely on race-specific resistance (*R*) genes and their corresponding pathogen avirulence (*Avr*) genes (Larkan et al. 2015). Interaction between the products of *R* and *Avr* results in an incompatible host–pathogen interaction and pathogen restriction from host tissues. Absence of either the *R*- or the *Avr*-gene results in a compatible host–pathogen interaction and colonization of the host. Each interaction is probably governed by large sets of genes activated over time and under the control of cellular receptors and signal transduction cascades that determine host fate. Although *R*-genes conferring blackleg resistance have been identified in canola (Marcroft et al. 2012, Larkan et al. 2013), it is unclear by which mechanisms these genes effectively inhibit *L. maculans* colonization. Previous transcriptome studies of the *B. napus–L. maculans* pathosystem limited analyses to compatible interactions and focused on pathogen virulence and effectors (Lowe et al. 2014, Haddadi et al. 2016). Thus, there is a critical need to identify the genes facilitating host resistance against *L. maculans* and define how the host defense response is controlled in both space and time.

Plant defense response mechanisms are commonly subdivided into two immune pathways: pattern-triggered immunity (PTI) and effector-triggered immunity (ETI) (Thomma et al. 2011, Jones et al. 2016). PTI is characterized by the detection of pathogen-associated molecular patterns (PAMPs) via extracellular membrane receptors such as receptor-like proteins (RLPs) and receptor-like kinases (RLKs), while ETI is characterized by the detection of pathogen effectors or their perturbation of host molecules by intracellular nucleotide-binding–

leucine-rich repeat (NB-LRR) receptors (Dangl et al. 2013). Both immune pathways share cellular machinery to elicit a defense response; however, PTI is associated with non-host resistance and ETI (in conjunction with PTI) with host incompatibility (Bigeard et al. 2015). Although it is a useful model, this ETI/PTI dichotomy cannot be effectively applied to the Arabidopsis- or *B. napus–L. maculans* pathosystems. Not only are effector-triggered NB-LRR receptors required for Arabidopsis non-host resistance to *L. maculans* (Staal et al. 2006), but the recently cloned *B. napus R*-gene, *LepR3*, has been identified as a transmembrane RLP (Larkan et al. 2013). Thus, effector-triggered defense (ETD) was proposed by Stotz et al. (2014) and refers specifically to RLP-triggered incompatible interactions. Unlike the rapid cell death observed in ETI, ETD is often associated with a delayed onset of cell death, as observed in *B. napus–L. maculans* incompatible interactions (Stotz et al., 2014). As *L. maculans* grows apoplastically, the ability of *R*-gene products to detect pathogens in the extracellular space is logical and supports the ETD paradigm.

Following the recognition of hemibiotrophic pathogens, early defense responses such as the activation of mitogen-activated protein kinases (MAPKs) are triggered within the cell (Meng and Zhang 2013). Subsequently, large-scale transcriptional reprogramming contributes to the regulation of phytohormone signaling pathways (Denancé et al. 2013). Jasmonic acid (JA) and abscisic acid (ABA) are both involved in Arabidopsis non-host resistance to *L. maculans* (Kaliff et al. 2007), and JA, ethylene (ET) and salicylic acid (SA) signaling pathways are activated during the *B. napus–L. maculans* host–incompatible interaction (Sašek et al. 2012). Although hormone signaling has been described temporally across the plant defense response to fungal pathogens (reviewed in Mishra et al. 2012), there are no data on the spatial partitioning of these genes following ETD in host tissues.

Downstream plant defense responses in hemibiotrophic pathosystems may involve the deposition of callose (Ellinger et al. 2013). Callose deposition is typically triggered by PAMPs, and PAMP-induced callose deposition has been used as a marker for PTI activity in Arabidopsis (Luna et al. 2011). Indole glucosinolates (IGS), bioactive secondary metabolites with anti-fungal capabilities, also promote the production of callose (Clay et al. 2009). In Arabidopsis, resistance to hemibiotrophic fungi can be dependent on the production of IGS (Hiruma et al. 2013) or callose deposition (Staal et al. 2006, Kaliff et al. 2007); however, their role in the *B. napus–L. maculans* pathosystem remains unclear.

We profiled the transcriptome of *B. napus* cotyledons inoculated with *L. maculans* across a 2-week infection period to explore the activation of ETD pathways and identify specific regulators and genes contributing to host resistance. Detailed anatomical observations complement our molecular analyses and clearly show the delayed onset of cell death indicative of ETD. Genes activated exclusively in resistant cotyledons were disrupted in Arabidopsis and positively identify uncharacterized receptors, negative cell death regulators and activators of sulfur metabolism that contribute to *L. maculans* defense in the Brassicaceae. We explored the activity of these genes and defense markers directly at, and proximal to, the infection site. Data show tightly controlled spatial transcriptional gradients developed during ETD that are associated with pathogen detection, IGS production, and hormone signaling. Taken together, our data provide a global transcriptome analysis of ETD against *L. maculans* and show early activation of defense pathways in resistant cotyledons that are controlled in space and time.

2.3 Material and Methods:

2.3.1 Plant and fungal materials:

Susceptible *B. napus* cultivar Westar and *B. napus* line DF78 (*Rlm3, LepR1*) were inoculated with *L. maculans* isolate D3 (*AvrLm5, AvrLepR1*; Zhang et al., 2016). Canola seedlings were grown in controlled environments with a 16-h photoperiod (16°C dark, 21°C light). Plants were grown in Sunshine mix #4 (SunGro Horticulture, http://www.sungro.com/). Fungal inoculum was prepared according to Zhang et al. (2016). Seven-day-old seedlings were point-inoculated with 10 µl of D3 pycnidiospore suspension (2×10^7 pycnidiospores ml^{-1}) or sterilized distilled water (mock).

2.3.2 Microscopy, lignin and callose deposition:

Cotyledons were processed for light microscopy exactly as reported in Chan and Belmonte (2013) using the Leica Historesin embedding procedure (Leica Microsystems, http://www.leica-microsystems.com/). Sections cut 3 µm thick were stained with periodic acid-Schiff's (PAS) and counterstained with toluidine blue O (TBO) for general structure. For trypan blue/aniline blue staining of fungal hyphae, fresh canola cotyledons were cleared in acetic acid: ethanol (1: 3, v/v) and stained with 0.01% trypan blue or 0.05% aniline blue in lactoglycerol (lactic acid:glycerol:distilled H2O = 1:1:1, v/v/v). To visualize lignified plant materials, canola cotyledons were cleared in 95% ethanol and stained in phloroglucinol-HCl (a saturated solution of phloroglucinol in 20% HCl). Callose deposition was visualized using aniline blue staining. Cotyledons were incubated in K2HPO4 buffer for 30 min and incubated in 0.05% aniline blue using fluorescence microscopy (near UV, 395 nm). All sections and tissues were visualized on a Zeiss Axio Imager Z1 (https:// www.zeiss.com/). Scanning electron micrographs were captured

using the Hitachi T-1000 to examine fungal infection on the surface of freshly collected canola cotyledons without tissue fixation.

2.3.3 Construction of RNA sequencing libraries:

RNA was collected from three biological replicates of infected and two mock inoculated *B. napus* cotyledons at 0, 3, 7 and 11 dpi. Total RNA was isolated by using PureLink® Plant RNA Reagent (Ambion, https://www.thermofisher.com) and treated with a TURBO DNA-freeTM Kit (Ambion) according to the manufacturer's instructions. RNA quality and integrity were measured using the 2100 Bioanalyzer (Agilent Technologies, http://www.agilent.com/) with the Agilent 2100 PicoChip. RNA-Sequencing libraries were prepared according to an alternative HTR protocol (C2) developed by Kumar et al. (2012), except for a library PCR enrichment of 11 PCR cycles. The RNA sequencing libraries were validated using high-sensitivity DNA chips on the Agilent Bioanalyzer and quantified using the Quant-iT dsDNA Assay kit (ThermoFisher Scientific, http://www.thermofisher.com/). Fifty base pair single-end RNA-Sequencing was carried out at the UC Davis genomics core facility (Davis, CA, USA) on the Illumina HiSeq 2500 platform in high-throughput mode. All data have been deposited in the Gene Expression Omnibus (GEO) data repository (accession GSE77723).

2.3.4 Data analysis:

Barcode adaptors from the RNA sequence reads were clipped and low-quality reads removed (read quality <30) using TRIMMOMATIC software (Bolger et al. 2014). Quality control of each sample was performed with FastQC reports (http://www.bioinformatics.babraham.ac.uk/projects/fastqc/). RNA sequence reads passing the quality filter were aligned to the *B. napus* genome (v.4.1; Chalhoub et al., 2014) with TOPHAT2 of the Tuxedo pipeline (Trapnell

et al., 2012) allowing no more than two mismatches, in high-sensitivity mode, using *B. napus* reference annotation v.5.0 as a guide (Chalhoub et al. 2014), and otherwise using default settings. Identification of unannotated transcripts was performed using CUFFLINKS v.2.2.1 and CUFFMERGE (Trapnell et al. 2012) and transcript sequences were extracted using BEDTOOLS. Novel transcripts were identified and are defined in Data S4. Open reading frames (ORFs) were identified using TRANSDECODER (http://transdecoder.github.io) with alignment against Arabidopsis TAIR10 using NCBI BLAST (Altschul et al. 1990). The BLASTp function was used when a predicted protein sequence was available, with an E-value cutoff of 10^{-10}. For those without a predicted ORF, or no hit, BLASTn was used to identify potential orthologs (E-value 10^{-10}).

CUFFQUANT, CUFFNORM and CUFFDIFF were used to generate normalized counts in FPKM (also known as RPKM in single-ended sequencing; Mortazavi et al., 2008; Trapnell et al., 2012) and to identify DEGs (pooled dispersion method/standard settings). Genes were considered as significantly differentially expressed with a corrected P-value of <0.05 (false discovery rate = 0.05). Raw counts were obtained from BAM files using the HTSeq Python Framework with the following command: 'htseq-count -m union -f bam –stranded=no input.sam bnapusannotation.gff3'. Following, clustering was performed using the averaged raw counts of genes differentially expressed in one or more treatment groups. Clustering was performed with the DESeq software package (Anders et al. 2015). Principal component analysis was also performed with DESeq using raw counts from each individual sample and it validated clustering analysis (Appendix VIII).

2.3.5 GO term enrichment

GO term enrichment was performed according to the methods of Orlando et al. (2009). A hypergeometric distribution test was used to identify statistically enriched GO terms overrepresented in lists of DEG sets and assigned a P-value. GO terms were considered statistically enriched at $P < 0.001$. GO attributes were assigned to *B. napus* genes by transferring GO attributes of their closest putative Arabidopsis homolog (TAIR10; www.arabidopsis.org). Output from GO term enrichment can be found in Data S3.

2.3.6 Tissue processing for laser microdissection, RNA isolation, cDNA synthesis and qPCR:

Inoculated cotyledons were collected and processed for LMD according to the methods of Belmonte et al. (2013). Briefly, infection sites were cut parallel to the cotyledon petiole-like structure on either side of the lesion between 11 a.m. and 2 p.m. to minimize the time of day effect. A minimum of 16 infection sites per biological replicated were collected from the four treatments were fixed in 3:1 (v/v) ethanol:acetic acid and fixed overnight at 4°C. Tissues were then rinsed and dehydrated in a graded ethanol series (75, 85, 95, 100, 100%) followed by xylene infiltration (3:1, 1:1, 1:3 ethanol:xylene (v/v), 100% xylenes, 100% xylenes) at 4°C overnight. Tissues were washed with 100% xylene and paraffin chips were added to the xylene-infiltrated tissue and kept at 4°C overnight. Paraffin chips and tissues in xylenes were then allowed to come to room temperature (~21°C) and incubated at 42°C for 30 min followed by 60°C for 1 h. Three changes of 100% paraffin were made every hour before embedding.

Cotyledon tissues were sectioned using a Leica RM2125RT rotary microtome at 10 µm under RNase-free conditions and mounted on Leica PEN Membrane slides before being deparaffinized in xylene twice for 30 sec per wash. Histological sections 0–200, 200–400 and

400–600 µm from the edge of the infection site were collected in 60 µl of lysis buffer (Ambion, Origin). RNA was isolated from sections totaling at least 9,000,000 m^2 (ranging from 115 to 200 microdissected sections) from at least seven individual plants exactly as reported in Belmonte et al. (2013). RNA quality and yield were determined using microcapillary electrophoresis (with an Agilent 2100 bioanalyzer using an RNA 6000 pico chip). Several examples of RNA traces used to assess RNA quality can be found in Appendix IX. All LMD-collected tissues were of sufficient quality for downstream transcriptome profiling as described in Millar et al. (2015) and Chan et al. (2016).

Isolated RNA was converted to cDNA using the Maxima First Strand cDNA synthesis kit (ThermoFisher Scientific). Directed qPCR was carried out using a Bio-Rad CFX ConnectTM Real-Time System with SYBR® Green Supermix (Bio-Rad, http://www.bio-rad.com/) as per the manufacturer's instructions in a 10-µl reaction volume. Conditions for the reaction were as follows: 95°C for 3 min, 39 cycles of 95°C for 30 sec, 53°C for 30 sec and 72°C for 30 sec. Melt curves (0.5°C increments in a 55–95°C range) for each gene were performed to assess the sample for non-specific targets, splice variants and primer dimers. A list of the primer sequences used in these experiments is given in Data S5. The ΔΔCt method was used to analyze relative transcript abundance, normalizing to the endogenous housekeeping gene Actin and using Westar inoculated with H_2O as a reference sample.

The ΔΔCt method was used to analyze relative mRNA abundance (Rieu and Powers 2009). The results are based on three repeats in three independent experiments. Each biological replicate was a pool of tissue taken from at least seven individuals. Actin (GenBank accession number AF111812.1) was used as the internal control to normalize the expression of the target gene. Levels of gene expression were normalized relative to that in the Westar (0–200 µm)

control. One-way ANOVA with Ducan's multiple range test ($P < 0.05$) was performed on each gene over the three distances to test for significant fold changes between treatments ($P < 0.05$).

2.3.7 Arabidopsis susceptibility screening:

We screened 49 loss-of-function Col-0 background Arabidopsis mutants for susceptibility to *L. maculans* (Table S3). PCR was performed to confirm homozygous insertion of the mutants. Col-0 plants were used as a resistant control line and mock water-inoculated controls were performed for all lines. Plant growth and fungal inoculation procedures were similar to that described for *B. napus* plant growth and fungal inoculation, with some modifications. Seeds were plated in MS medium in sterile conditions, then cold-treated for 3 days at 4°C, incubated in a controlled environment for 14 days and transplanted into a growth tray with growth mix. Inoculation of two similarly sized young leaves per plant was performed at the four to six leaf stage, and after inoculation a transparent plastic cover was placed over the plants to maintain high humidity. At least 30 plants from each treatment group were evaluated for blackleg resistance at 18–24 dpi and scored for disease severity.

Leaf tissue was collected in a 96-well plate from five biological replicates of Arabidopsis wild-type plants and mutants that displayed susceptibility at 20 dpi. DNA extraction buffer [1 M KCl, 100 mM 2-amino-2-(hydroxymethyl)-1,3-propanediol (TRIS)-HCl pH 7.5, 10 mM EDTA pH 8] and glass beads were added to each well and tissue was homogenized on a GenoGrinder 2000. DNA was precipitated in isopropanol, washed with 70% ethanol and suspended in TRIS-HCl pH 7.5. To properly normalize input for qPCR DNA was quantified with the Nanodrop 2000c and Quant-iT picogreen high-sensitivity dsDNA assay (ThermoFisher Scientific) on the fluorescent Nanodrop 3300. To measure 18s rDNA levels in foliar tissue, qPCR was performed with SYBR® SSO Fast Evagreen Supermix (Bio-Rad) in a 10 µl reaction volume. For each

reaction, 100 pg of extracted DNA was used. Conditions for the reaction were as follows: 98°C for 3 min, 40 cycles of 98°C for 5 sec, 60°C for 10 sec. Melt curves (0.5°C increments in a 55–95°C range) for each gene were performed to assess for non-specific targets and primer dimers.

2.4 Results:

2.4.1 The *LepR1–AvrLepR1* gene interaction is responsible for resistance in DF78 cotyledons:

To better understand the host–pathogen relationship between *B. napus* and *L. maculans*, we performed cotyledon inoculation assays based on the gene-for-gene model developed by Flor (1971) and frequently applied in the characterization of *R*-genes (Rouxel et al. 2003, Marcroft et al. 2012). A total of 34 characterized *L. maculans* isolates were tested against 104 *B. napus* varieties/lines (Zhang et al., 2016). We selected resistant line DF78 (*LepR1*) for further analysis because of its strong defense response against *L. maculans* (*AvrLepR1*) and our interest in the poorly characterized *R*-gene *LepR1*. Our results show that DF78 is resistant to all isolates carrying *AvrLepR1* or *AvrLm3*. As the *L. maculans* isolate D3 used for this study does not carry *AvrLm3* (Appendix I; Zhang et al., 2016), the response of DF78 cotyledons to the D3 *L. maculans* isolate must be the result of a *LepR1–AvrLepR1* gene interaction. To confirm this, *B. napus* variety Q2 (*Rlm3*; Van de Wouw et al. 2010) and *B. napus* line 1065 (*LepR1*; Zhang et al., 2016) were used as controls. When the Westar cultivar was challenged with all 34 isolates, no resistance was observed, confirming previous reports that Westar is universally susceptible to *L. maculans* (Appendix I).

2.4.2 Phenotypic and cellular characterization of *B. napus* cotyledons in response to *L. maculans* infection:

Next, we examined the phenotypic characteristics of resistant (DF78; *LepR1*) and susceptible (Westar) *B. napus* hosts infected with *L. maculans* (Fig. 2.1a). Lesions spread rapidly in susceptible cotyledons at 7 days post-inoculation (dpi), while in resistant hosts lesion size only slightly increased towards the end of the 14-day infection period (Fig. 2.1b). Scanning electron and light microscopy of resistant cotyledons showed minimal cellular breakdown adjacent to the infection site at 3 and 7 dpi (Fig. 2.1c,d,i,j), as is characteristic of ETD responses, despite the presence of fungal hyphae within the infection site (Fig. 2.1e). At 11 dpi, resistant hosts show marginal cellular degradation (Fig. 2.1k). In susceptible hosts, cells adjacent to the infection site were intact at 3 dpi (Fig. 2.1f) and widespread cell death by 7 (Fig. 2.1m) and 11 dpi (Fig. 2.1g,n) with fungal fruiting bodies being clearly visible (Fig. 2.1h,m).

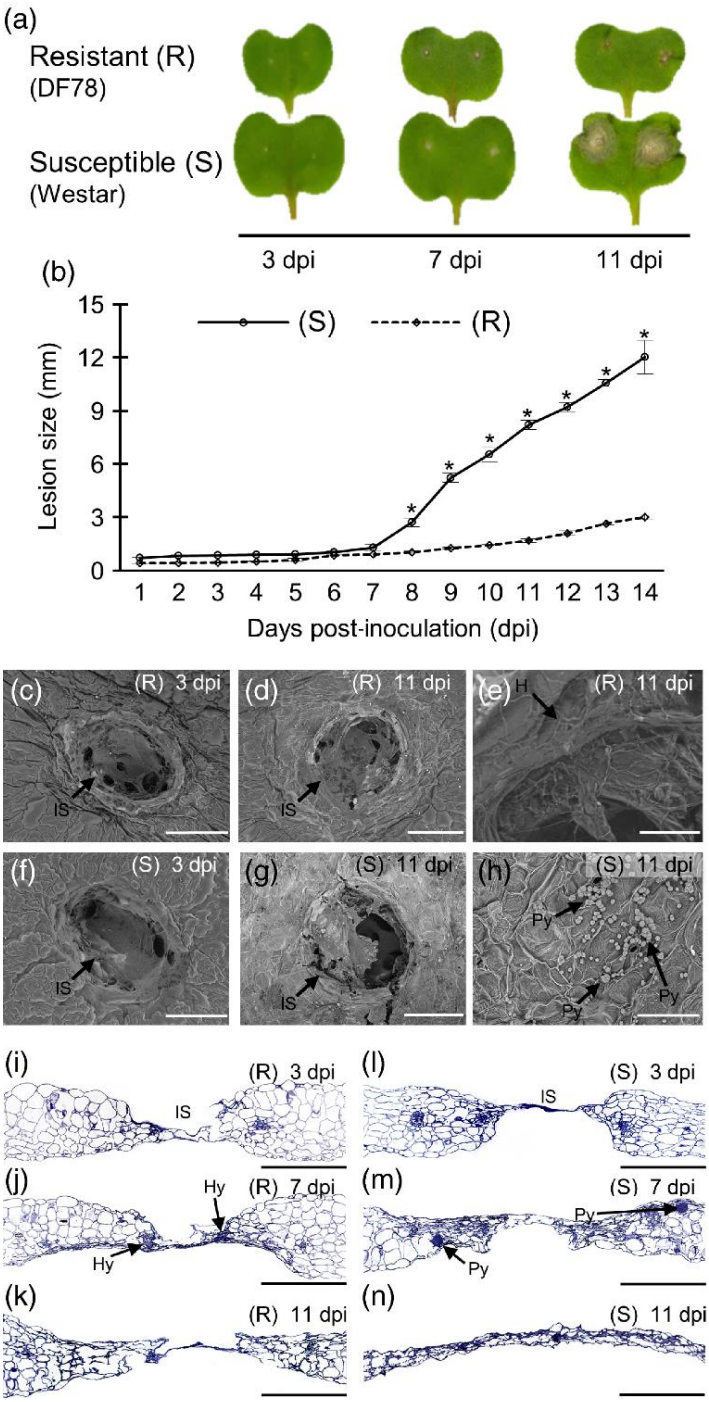

Fig. 2.1: Disease symptoms in *Brassica napus* cotyledons in response to *Leptosphaeria maculans* infection. (a) Disease symptoms in resistant (R) and susceptible (S) cotyledons at 3, 7 and 11 days post inoculation (dpi). (b) Lesion size over time. Asterisks ($P < 0.01$, Student's t-test). Scanning electron micrograph (SEM) of R at 3 dpi (c) and 11 dpi (d) at the infection site (black arrow): scale = 1 mm. (e) Fungal hyphae (H) at infection site: scale = 50 µm in R at 11 dpi. (f, g) SEM of S at 3 dpi (f) and 11 dpi (g) at the infection site (IS): scale = 1 mm. (h) SEM of pycnidia (Py) on S cotyledons at 11 dpi: scale = 200 µm. (i–n) Light micrographs of R at 3 dpi (i), 7 dpi (j), 11 dpi (k) and S at 3 dpi (l), 7 dpi (m) and 11 dpi (n): scale bars = 500 µm.

2.4.3 Global comparison of gene activity in the *B. napus–L. maculans* pathosystem:

To identify genes responsible for *B. napus* resistance to *L. maculans*, we profiled the transcriptomes of resistant and susceptible cotyledons using next-generation RNA sequencing across a 2-week infection period. First, hierarchical clustering analysis revealed relationships between genotypes and in response to *L. maculans* infection (Fig. 2.2a). Treatments generally grouped according to genotype at 0–3 dpi, apart from infected resistant cotyledons at 3 dpi that cluster with susceptible plants at 7 dpi, suggesting an accelerated defense response. Towards the latter stages of the infection process, treatments form a clade based largely on exposure to *L. maculans*, highlighting global shifts in gene expression in both genotypes following pathogen attack. Mock-inoculated resistant plants at 11 dpi were also placed within this clade, which may be related to its developmental profile and shared activation of senescence-associated genes.

Fig. 2.2(b) summarizes transcript populations in both genotypes and across treatments. Transcript abundance was measured as fragments per kilobase of gene per million mapped reads (FPKM) where a gene was scored as 'expressed' when FPKM ≥1 (Mortazavi et al. 2008, Trapnell et al. 2012). Regardless of genotype or treatment, the number of active genes was similar, with an average of 41,110 expressed genes (41% of the *B. napus* gene models). Transcript abundance was scored as low (FPKM ≥1 to <5), moderate (FPKM ≥5 to <25) or high (FPKM ≥25), with most transcripts detected at low (53%) or moderate (36%) levels. Cumulatively 57,654 transcripts were detected across all 12 treatments with an FPKM ≥1. The full annotation and all gene expression levels can be found in Data S1.

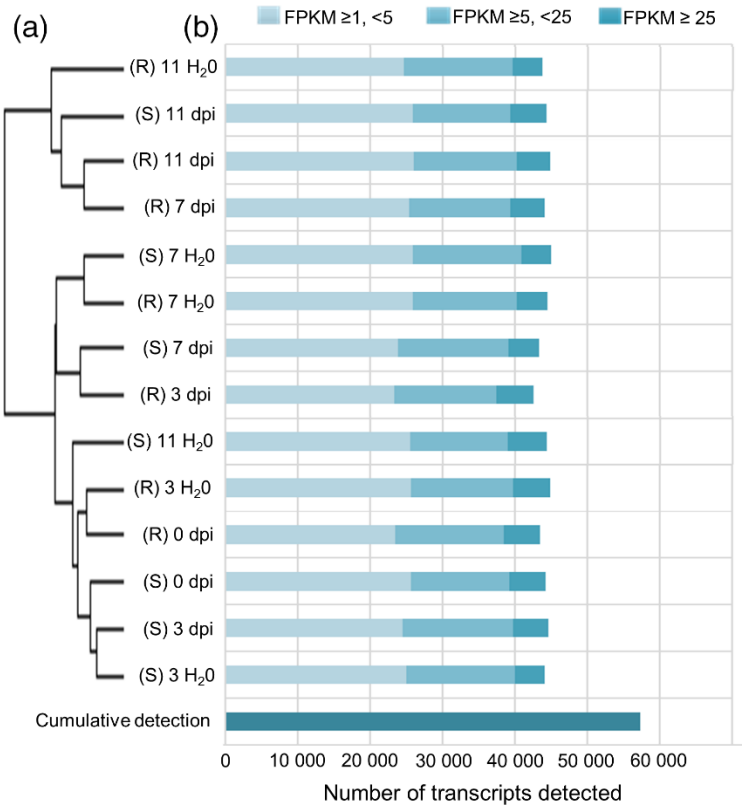

Fig. 2.2: Hierarchical clustering and global gene activity in the *Brassica napus*–*Leptosphaeria maculans* pathosystem. (a) Hierarchical clustering of all differentially expressed genes detected in the dataset. (b) Number of transcripts detected in both genotypes across all treatments. Transcripts with an FPKM (fragments per kilobase of gene per million mapped reads) >1 are considered to be detected. Detected transcripts are subdivided into low (FPKM ≥1 to <5), moderate (FPKM ≥5 to <25) or high (FPKM ≥25) detection levels.

2.4.4 Thousands of genes are activated in *B. napus* in response to *L. maculans:*

To identify the genes that contribute to plant resistance, differential gene expression analysis was performed at all stages of the 11-day infection process in both resistant and susceptible hosts and data were compared with their respective mock, water-inoculated controls. At 3, 7 and 11 dpi, we detected a total of 1992, 3234 and 4173 upregulated differentially expressed genes (DEGs; $P < 0.05$) in resistant hosts and 571, 3873 and 8489 upregulated DEGs in susceptible hosts, respectively (Fig. 2.3a–c). The number of DEGs shared between resistant and susceptible host cotyledons also increased over time, probably due to the total number of

DEGs between treatments. A complete summary of all DEGs, both up- and down-regulated, can be found in Data S2.

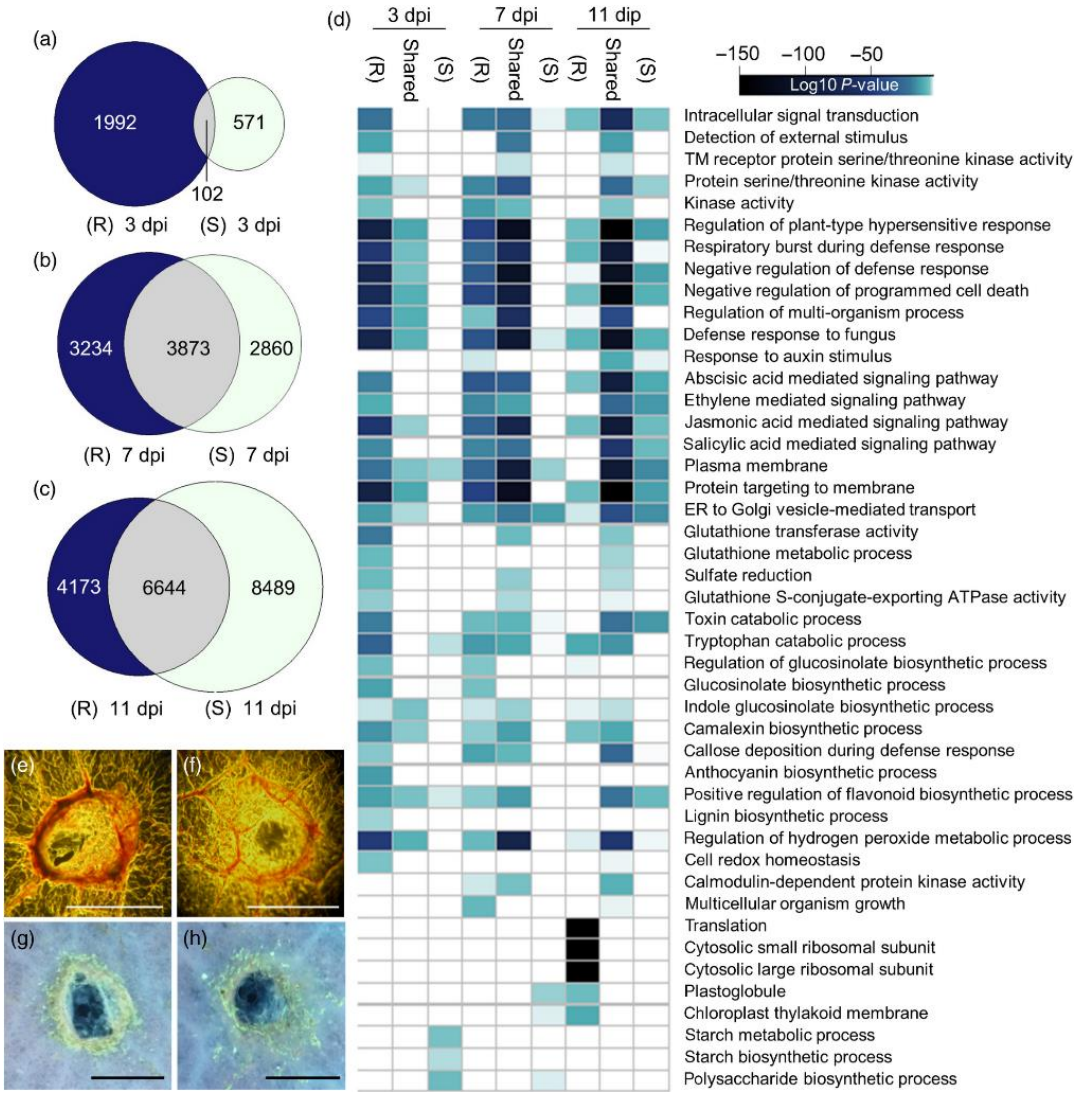

Fig. 2.3: Upregulated differentially expressed genes in resistant (R) and susceptible (S) *Brassica napus* cotyledons inoculated with *Leptosphaeria maculans* as compared with mock inoculated controls. (a–c) Venn diagram showing activated genes at (a) 3, (b) 7 and (c) 11 days post- inoculation (dpi) in response to *L. maculans* in R (left), S (right) or shared between both genotypes (intersect). (d) Heatmap of enriched Gene Ontology terms identified from upregulated genes. Terms are considered enriched at $P < 0.001$. A darker blue color represents a greater statistical enrichment. (e, f) Deposition of lignified plant materials at the site of infection in R (e) and S (f) hosts at 7 dpi. Lignified plant materials appear dark orange/red. (g, h) Aniline blue callose staining of R (g) and S (h) B. napus cotyledons inoculated with *L. maculans* at 7 dpi. Scale bars = 1 mm.

2.4.5 Host resistance is associated with pathogen recognition, cell signaling and vesicular trafficking in resistant plants:

To identify the biological processes, molecular functions and cellular components contributing to host resistance against *L. maculans*, we performed Gene Ontology (GO) term enrichment on all upregulated DEG sets (Fig. 2.3d, Data S3). The DEGs identified in resistant cotyledons at 3 dpi are enriched with kinase activity ($P = 1.05 \times 10^{-13}$), signal transduction ($P = 1.5 \times 10^{-4}$) and plasma membrane ($P = 2.85 \times 10^{-30}$), and code for wall-associated kinases (WAKs), RLKs, RLPs, LRR-NBS receptors, and transducers of signaling such as MAPKs and MAPK kinases (MKK). Specifically, we identified two putative homologs of *RLP30* (*BnaA06g12200D*, *BnaA06g12220D*), receptor complex regulator *SUPPRESSOR OF BIR1 1* (*SOBIR1*, *BnaA03g14760D*, *BnaCnng39490D*) and homologs of signal transducer *MKK9* (*BnaA02g35860D*, *BnaC02g22230D*) that were upregulated specifically in resistant cotyledons at 3 dpi (Table 1).

Table 2.1: Accumulation of transcripts during *Leptosphaeria maculans* infection in resistant (R) and susceptible (S) *Brassica napus* cotyledons. Significant ($P < 0.05$) decreases or increases in transcript abundance compared with mock controls are in bold.

		Fold change versus mock control					
Brassica napus locus	Putative annotation	R 3 dpi	R 7 dpi	R 11 dpi	S 3 dpi	S 7 dpi	S 11 dpi
BnaA03g46200D	*PUTATIVE NBS-LRR RECEPTOR*	2.16	6.03	3.02	**0.85**	10.46	26.07
BnaC04g12970D	*PUTATIVE NBS-LRR RECEPTOR*	2.12	3.55	**1.40**	**0.54**	2.40	12.61
BnaA03g14760D	*SUPRESSOR OF BIR1 1*	2.10	5.12	2.13	**1.43**	2.80	21.13
BnaCnng39490D	*SUPRESSOR OF BIR1 1*	2.99	3.86	3.19	**1.36**	3.74	7.21
BnaC04g43230D	*RECEPTOR-LIKE PROTEIN 30*	4.60	12.75	3.12	**0.70**	4.92	37.27
BnaA06g12200D	*RECEPTOR-LIKE PROTEIN 30*	2.97	5.90	**1.28**	**1.41**	1.54	12.65
BnaA04g06980D	*CRK10*	5.12	3.29	14.21	**0.42**	0.82	17.56
BnaA02g21140D	*CRK39*	5.20	41.07	10.07	**1.12**	27.26	205.9
BnaA02g35860D	*MAP KINASE KINASE 9*	2.00	2.86	2.30	**0.64**	1.72	12.94
BnaC02g22230D	*MAP KINASE KINASE 9*	5.39	5.27	2.41	0.40	4.90	25.43
BnaA08g17130D	*SEC23/24 TRANSPORT GENE*	**0.99**	2.40	**0.80**	**1.41**	0.82	2.20
BnaC03g73490D	*SYNTAXIN OF PLANTS 121*	**1.03**	1.71	1.86	**1.85**	1.05	7.90
BnaA07g30760D	*KUNITZ TRYPSIN INHIBITOR 1*	2.69	3.51	9.31	**0.59**	0.03	0.14
BnaC09g20030D	*BAX INHIBITOR 1*	1.82	3.08	4.53	**1.39**	11.54	38.20
BnaC03g58590D	*NECROTIC SPOTTED LESIONS 1*	1.70	1.98	1.70	**1.31**	1.70	19.29
BnaC03g22580D	*NUDIX HYDROXYLASE H7*	5.53	17.96	11.44	**1.54**	39.82	27.34
BnaC01g41070D	*BOTRYTIS SUSCEPTIBLE 1 INTERACTOR*	1.66	1.08	**1.18**	**0.64**	0.69	6.87
BnaC06g13910D	*DEFENDER AGAINST DEATH 1*	1.81	1.83	1.74	**1.28**	0.55	45.89
BnaA07g15670D	*DEVELOPMENT AND CELL DEATH 1*	2.73	1.30	2.20	**0.99**	1.00	28.99
BnaC09g50680D	*SULFITE REDUCTASE 1*	1.77	2.62	**0.97**	**0.69**	1.29	1.05
BnaA03g38670D	*APK1*	2.65	5.89	6.69	**1.27**	0.81	3.16
BnaA01g34620D	*APK1*	3.37	4.87	25.01	**0.59**	0.83	2.15
BnaA09g20370D	*APS REDUCTASE 1*	2.85	2.40	1.79	**1.14**	5.60	6.53
BnaC09g22760D	*APS REDUCTASE 1*	2.27	1.19	**1.32**	**1.24**	12.51	5.02
BnaA06g28850D	*GLUTATHIONE SYNTHETASE 2*	1.55	2.01	1.94	**0.99**	1.64	1.87
BnaC07g27830D	*GLUTATHIONE SYNTHETASE 2*	1.87	1.81	1.85	**1.03**	0.84	1.78
BnaC09g40740D	*GLUTATHIONE S-TRANSFERASE PHI 12*	10.46	0.44	0.25	0.20	10.13	0.09
BnaA07g24870D	*LIPOXYGENASE 2*	**1.00**	19.09	13.06	0.00	0.00	0.05
BnaA07g24880D	*LIPOXYGENASE 2*	1.89	18.74	23.19	0.21	0.00	0.04
BnaA04g17560D	*CINNAMATE-4-HYDROXYLASE*	27.64	15.61	**1.48**	**1.50**	1.61	90.95
BnaC04g41120D	*CINNAMATE-4-HYDROXYLASE*	18.56	3.00	**1.61**	**0.77**	1.53	40.45
BnaA07g32800D	*CINNAMOYL-COA REDUCTASE*	21.61	45.49	32.21	**1.29**	116.69	206.3
BnaA08g16100D	*CYP79B2*	1.68	13.03	9.54	**1.38**	1.70	1.99
BnaA08g04520D	*CYP83B1*	1.78	2.07	3.70	**0.86**	0.64	0.78
BnaC04g01210D	*WRKY46*	2.43	3.07	2.18	**1.07**	11.31	11.3
BnaA04g23480D	*WRKY54*	2.49	6.85	3.24	**1.17**	4.65	8.72
BnaA09g35840D	*WRKY70*	3.32	12.87	23.49	**1.47**	27.31	24.71
BnaC06g05910D	*ANAC019*	3.09	2.76	1.95	0.29	0.20	191.8
BnaA07g28000D	*ANAC019*	4.11	5.69	2.33	0.16	1.36	1369.3
BnaC08g18090D	*MYB51*	1.55	6.58	5.16	**1.03**	8.40	13.42

dpi, days post-inoculation.

2.4.6 SA and JA signaling are strongly affected by the *LepR1–AvrLepR1* gene interaction:

RNA sequencing and GO term enrichment identified DEGs in resistant cotyledons at 3 dpi associated with the SA-mediated signaling pathway ($P = 6.70 \times 10^{-18}$), ET-mediated signaling pathway ($P = 6.57 \times 10^{-12}$), and JA-mediated signaling pathway ($P = 2.48 \times 10^{-65}$; Fig.

2.3d). To further characterize the temporal regulation of hormone production and signaling in response to *L. maculans*, we examined transcript levels of hormone biosynthetic genes and markers for SA, ET, JA, ABA and auxin across the infection process in both genotypes (Appendix II).

Expression of SA biosynthetic gene *ISOCHORISMATE SYNTHASE 1* homologs, in addition to SA marker *PATHOGENESIS-RELATED GENE 1* (*PR1*), increased an average of 5.01-fold against the mock at 3 dpi in resistant plants, compared with an increase of 1.26-fold in their susceptible counterparts. Data show an increased abundance of transcripts related to ET/JA biosynthesis and signaling by 3 dpi in resistant cotyledons, including *ACC OXIDASE 2* (*BnaA09g13300D, BnaC09g13570D*) and the ET-JA marker *PDF1.2* (*BnaA07g32130D, BnaC02g23620D*), that continued to accumulate across the infection process. Remarkably, in susceptible hosts, expression levels of several JA-biosynthetic genes decreased. For example, the expression of *LIPOXEGENASE 2* (*LOX2*; *BnaA07g24870D, BnaA07g24880D*), *ALLENE OXIDE SYNTHASE* (*AOS*; *BnaC02g29610D*) and *ALLENE OXIDE CYCLASE 3* (*AOC3*; *BnaC09g52550D*) decreased an average of 4.01-fold compared with mock controls at 7 and 11 dpi (Appendix II). Finally, expression of auxin (*NITRILASE 2, BnaA06g38980D, BnaC02g07040D, BnaC03g54910D, BnaCnng75490D*) and ABA (*NINE-CIS-EPOXYCAROTENOID DIOXYGENASE 3, BnaA01g29390D, BnaC01g36910D, BnaC05g39200D*) markers increased in susceptible cotyledons at 11 dpi and may be the result of widespread cell death late in the infection process (Fig. 2.1n).

2.4.7 Regulation of cell death is associated with ETD against *L. maculans*:

We identified DEGs associated with negative regulation of programmed cell death ($P = 4.76 \times 10^{-76}$) upregulated specifically in resistant hosts at 3 dpi (Table 1), including putative

homologs of *BAX INHIBITOR 1* (*BnaC09g20030D*), *BOTRYTIS SUSCEPTIBLE 1 INTERACTOR* (*BnaC01g 41070D*), *DEVELOPMENT AND CELL DEATH 1* (*BnaA07g 15670D*), *NUDIX HYDROXYLASE HOMOLOG 7* (*BnaC03g22580D*), *METACASPASE 2* (*BnaA01g14460D*) and *NECROTIC SPOTTED LESIONS 1* (*BnaC03g58590D*). Activation of cell death regulators early during ETD may limit lesion spread following the biotrophic–necrotrophic transition of *L. maculans*.

2.4.8 Rapid activation of genes associated with sulfur metabolism:

DEGs associated with sulfate reduction ($P = 1.51 \times 10^{-7}$), sulfate assimilation ($P = 1.14 \times 10^{-11}$) and glutathione metabolic process ($P = 8.64 \times 10^{-8}$) were identified specifically in resistant cotyledons at 3 dpi (Fig. 2.3d), including sulfur assimilators *APS REDUCTASE* (*APR1*, *BnaA09g20370D, BnaC09g22760D*), *APR2* (*BnaC04g 19270D*), *APR3* (*BnaC01g13420D, BnaC07g37060D*) and *SULFITE REDUCTASE* (*BnaC09g50680D*), as well as sulfate activators *ADENOSINE 5'-PHOSPHOSULFATE KINASE 1* (*APK1*, *BnaA03g38670D*) and *APK2* (*BnaA01g34620D, BnaC01g00790D, BnaC07g51290D*). Additionally, homologs of *GLUTATHIONE SYNTHETASE 2* (*BnaA06g28850D, BnaC07g27830D*) were upregulated specifically in resistant hosts at 3 dpi (Appendix III, Table 1). In addition to its role as a redox regulator, glutathione is a key intermediary in sulfur metabolism and the largest reservoir of non-protein reduced sulfur in the cell. It also directly serves a role in toxin neutralization through the activity of glutathione-S-transferases (GST). DEGs enriched for GST activity ($P = 2.77 \times 10^{-21}$) were also identified in resistant hosts at 3 dpi, including *GST PHI 2* (*GSTF2*; *BnaA03g26140D*), *GSTF6* (*BnaC05g01540D*), *GSTF12* (*BnaC09g40740D*), *EARLY RESPONSE TO DEHYDRATION 9* (*ERD9, BnaA06g06160D*), *ERD13* (*BnaA03g14150D*) and 26 other GSTs (Data S2).

2.4.9 Coordinated lignin deposition is observed in resistant cotyledons following infection with *L. maculans*:

Genes coding for the formation of monolignols, *CINNAMATE-4-HYDROXYLASE* (*BnaA04g17560D, BnaC04g41120D*), *CINNAMOYL-ALCOHOL DEHEHYDROGENASE 8*/ *ELICITOR-ACTIVATED GENE 3* (*BnaC03g61120D*) and *CINNAMOYL-COA REDUCTASE* (*BnaA07g32800D*), had a combined average 17.6-fold increase in expression following *L. maculans* infection in resistant hosts at 3 dpi with no appreciable increase in the susceptible genotype (Table 1). Sequencing data are supported by histochemical analyses of lignin deposition at the inoculation sites of both genotypes (Fig. 2.3e,f and Appendix III) . Resistant hosts showed prominent and coordinated deposition of lignin proximal to the site of pathogen infection and surrounding vasculature. In susceptible hosts, lignin deposition appeared uncoordinated and diffuse.

2.4.10 Activation of IGS biosynthetic genes and callose deposition:

We identified DEGs specific to resistant cotyledons at 3 dpi that are associated with IGS biosynthetic process ($P = 5.38 \times 10^{-5}$). In resistant hosts, every gene of the IGS biosynthetic pathway was upregulated following *L. maculans* infection, whereas in the susceptible genotype several genes required for IGS production, such as *CYP79B2* and *CYP83B1* (Table 1), were downregulated during infection (Appendix IV). DEGs associated with callose deposition during the defense response ($P = 1.98 \times 10^{-5}$) were also identified in resistant cotyledons at 3 dpi, and largely overlapped with the IGS biosynthetic genes and regulators described above. To visualize callose deposition, we stained infected and non-infected cotyledons with aniline blue. Callose accumulated directly adjacent to infection site of resistant cotyledons (Fig. 2.3g) and was comparatively thin and discontinuous in susceptible hosts (Fig. 2.3h).

2.4.11 The transcription factors NAC and WRKY are associated with the accelerated defense response in resistant hosts:

To identify the transcription factors (TFs) associated with the accelerated defense response of resistant hosts we extracted differentially expressed TF-coding genes from the enriched GO terms: regulation of plant-type hypersensitive response ($P = 1.05 \times 10^{-95}$), intracellular signal transduction ($P = 1.54 \times 10^{-23}$) and defense response to fungus ($P = 3.03 \times 10^{-93}$) at 3 dpi. Of the 36 TF-coding transcripts (Appendix V), 19.4 and 30.5% coded for members of the NAC and WRKY TF families, respectively. We also identified IGS-promoting *MYB51*, JA-responsive JAZ TFs and *BZIP60* and *HSF-A4A* associated with the cellular heat-shock response. Although specifically activated in resistant hosts early at 3 dpi, 94.6% of these transcripts accumulated in susceptible cotyledons to levels exceeding all other treatments by 11 dpi (Appendix V). These data suggest that the timely expression of TFs may be essential for cellular reprogramming early in the defense response against *L. maculans*.

2.4.12 Identification of genes specifically activated by the *LepR1-AvrLepR1* gene interaction:

To identify genes that specifically contribute to resistance in the *LepR1–AvrLepR1* interaction, we compared both the susceptible and resistant host transcriptomes across the infection process. We found 1221 upregulated DEGs shared at 3, 7 and 11 dpi in resistant host cotyledons (Fig. 2.4a). We then compared the 1221 shared DEGs in resistant host cotyledons with upregulated DEGs at 3, 7 and 11 dpi in the susceptible host counterpart (Fig. 2.4b). Of these 1221 DEGs, only 54 were exclusive to resistant host cotyledons. These 54 resistant-specific transcripts included genes involved in signal transduction and gene regulation, such as *RLP30* (*BnaA06g12220D*), *CYSTEINE-RICH RECEPTOR-LIKE PROTEIN KINASE 11* (*CRK11*, *BnaA01g12650D*), *CRK21* (*BnaAnng25570D*), *NON-INDUCIBLE IMMUNITY-INTERACTING*

GENE 2 (*BnaC07g23070D*) and *ETHYLENE RESPONSIVE ELEMENT BINDING FACTOR 1* (*BnaAnng21280D*). Further, this list contains two genes associated with sulfur assimilation, *SULFATE TRANSPORTER 4.1* (*BnaA03g04410D*) and *APS-KINASE 2* (*APK2*; *BnaC07g51290D*), and multiple IGS biosynthetic genes (Fig. 2.4c). The complete list of 54 resistant-specific genes can be found in Appendix VI.

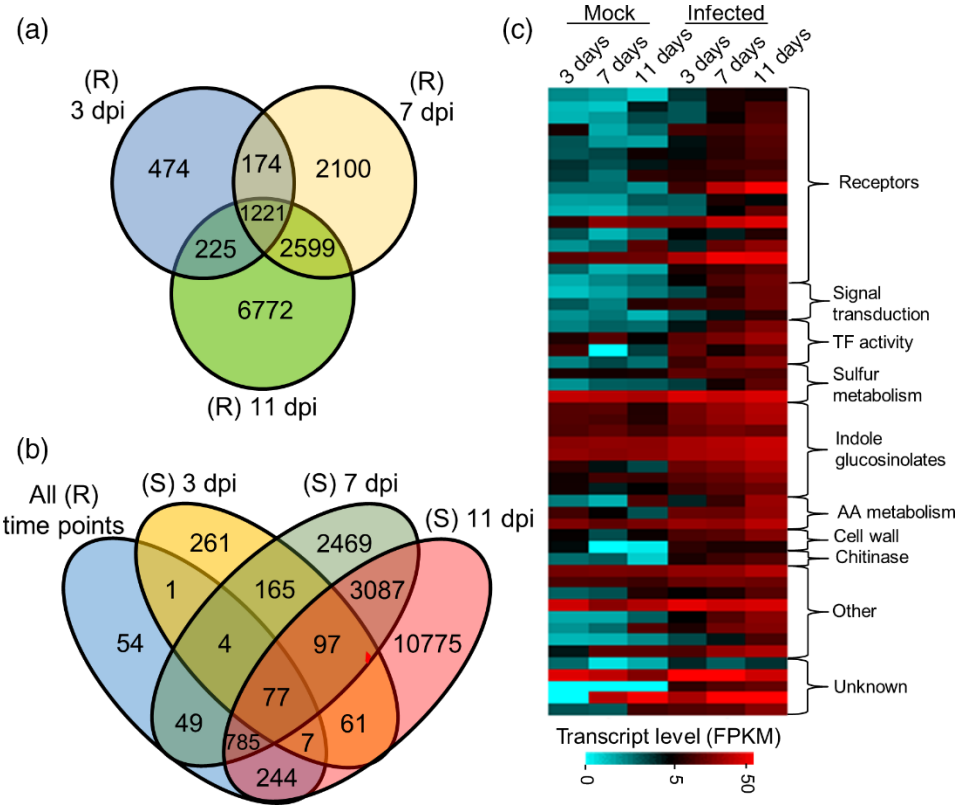

Fig. 2.4: Identification of differentially expressed genes (DEGs) specific to resistant (R) cotyledons inoculated with *Leptosphaeria maculans*. (a) Venn diagram showing all genes upregulated in R hosts at 3, 7 and 11 days post inoculation (dpi). (b) Identification of DEGs specific to R hosts. (c) Expression profiles of 54 DEGs specific to R hosts. Expression levels are measured in FPKM (fragments per kilobase of gene per million mapped reads).

While not a host to *L. maculans*, Arabidopsis plants become susceptible to this pathogen if they are compromised in their ability to detect and/or respond appropriately (Bohman et al. 2004). To functionally characterize the resistant-specific genes identified in our analyses, we challenged 49 corresponding Arabidopsis T-DNA mutants with *L. maculans* (Appendix VII).

Seven gene disruptions resulted in a breakdown of Arabidopsis non-host resistance by 20 dpi (Fig. 2.5b–i): *apk2-1* and *apk2-2*, deficient in production of activated sulfur required for biosynthesis of sulfur-containing secondary compounds including IGS and camalexin (Mugford et al. 2009); *kunitz trypsin inhibitor 1* (*kti1*), a negative regulator of phytopathogen-induced cell death; receptors *at4g18250-1*, *at4g18250–2* and *at3g53490*; and the receptor partner *lysm-interacting kinase 1* (*lik1*). LIK1, a phosphorylation target of the chitin receptor CERK1, is associated with activation of JA-ET signaling and the repression of SA immune responses (Le et al. 2014). T-DNA mutants of *PENTRATION 1* (*PEN1*), a proven regulator of non-host resistance (Nakao et al. 2011), were used as a positive control and were susceptible to *L. maculans*. Wild-type Col-0 plants inoculated with *L. maculans* (Fig. 2.5a) or water (Fig. 2.5j) did not show any symptoms associated with infection.

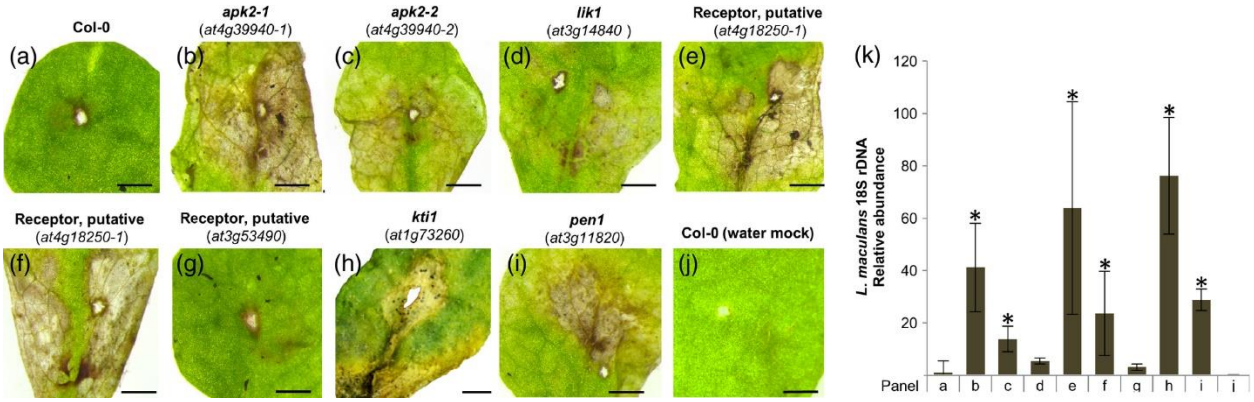

Fig. 2.5: Disease symptoms in Arabidopsis following *Leptosphaeria maculans* infection. (a) Wild- type Col- 0, (b, c) *at4g39940.1*, *aps kinase 2*, (d) *at3g14840.1*, *lysm interacting kinase 1*, (e, f) *at4g18250.1*, putative receptor, (g) *at3g53490.1*, putative receptor, (h) *at1g73260.1*, *kunitz trypsin inhibitor 1*, (i) *at3g11820*, *penetration 1*, (j) Col- 0 water inoculated mock control. Scale bar = 1 mm. (j) Relative abundance of *L. maculans* 18s rDNA in each mutant. Asterisk (*) denotes significant difference ($P < 0.05$, Student's t- test) in fungal load compared with Col- 0.

Next, we measured fungal load by qPCR to confirm that lesion progression observed in the T-DNA insertion mutants was a result of *L. maculans* growth and development (Fig. 2.5k). Fungal load was significantly greater ($P < 0.05$) in all mutants except *lik1* ($P = 0.309$) and

at3g53490 (P = 0.462), suggesting that the extent of lesion spread is correlated to fungal load. Other T-DNA alleles of *LIK1* and *AT3G53490* showed no susceptibility to *L. maculans* (Appendix VII). This is not surprising, as the effects of T-DNA insertions on gene expression are variable (Wang 2008) and these two mutants already display a weak phenotype. A complete list of screened mutants can be found in Appendix VII.

2.4.13 Laser microdissection and spatial distribution of gene activity underlying plant resistance:

We then hypothesized that the resistant-specific genes identified through our transcriptome and mutant analysis would also be operative directly at the infection site to restrict spread of the pathogen into host tissues. To test this hypothesis, we used laser microdissection (LMD) coupled with quantitative PCR (qPCR) to identify how resistant-specific genes and other important defense regulators are spatially partitioned within the cotyledon directly at and distal to the infection site (Fig. 2.6). We focused our attention on cotyledons at 7 dpi – a critical time point observed between the two genotypes in response to *L. maculans* (Fig. 2.1b). All genes (*LIK1*, *PR1*, *WRKY25*, *PDF1.2*, *APK2*, *RBOHF*, *CYP79B2*, *BnaA03g43720D* and *BnaC04g27200D*) were highly expressed in resistant host cotyledons infected with *L. maculans* compared with the susceptible line or mock controls and further validate our sequencing data.

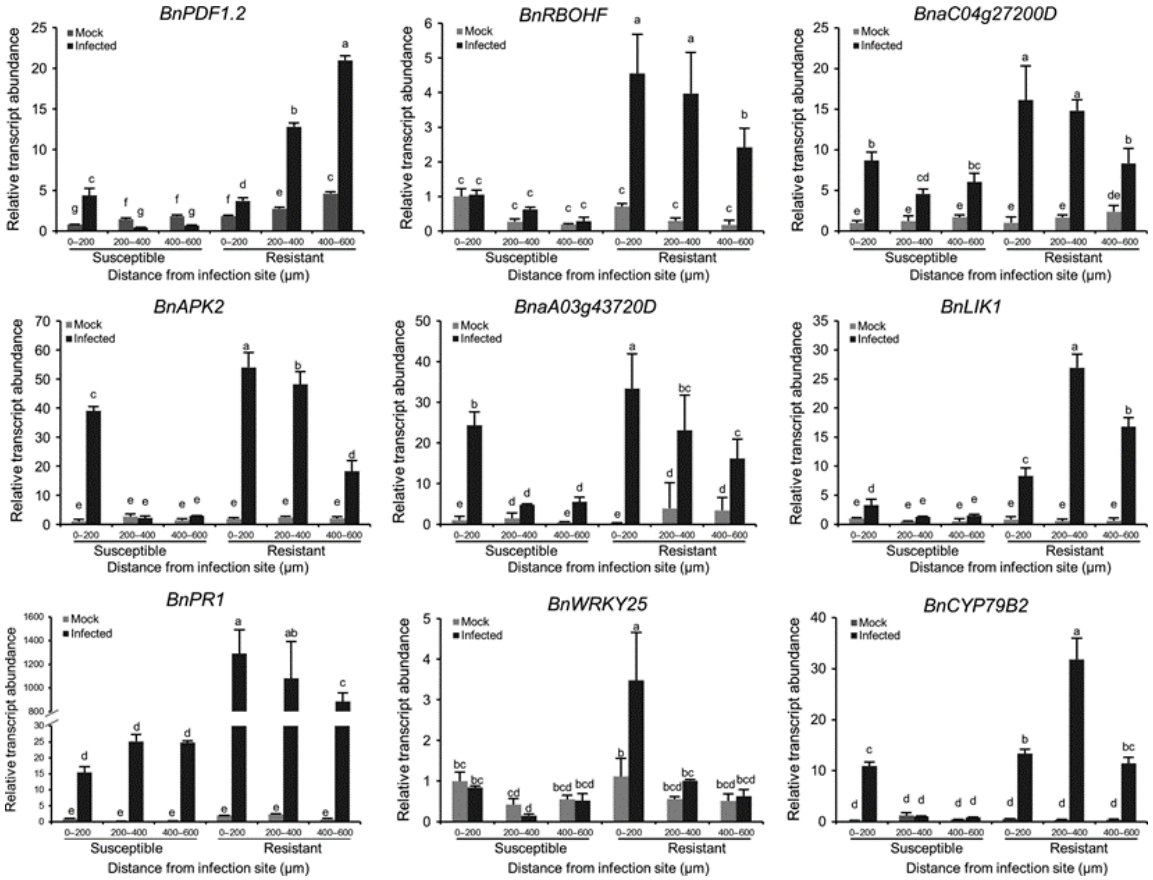

Fig. 2.6: *Brassica napus* gene expression following inoculation with *Leptosphaeria maculans.* Relative transcript abundance of *BnPDF1.2*, *BnRBOHF*, *BnaC04g27200D*, *BnAPK2*, *BnaA03g43720D*, *BnLIK1*, *BnPR1*, *BnWRKY25* and *BnCYP79B2* in susceptible (S) and resistant (R) cotyledons as measured 0–200, 200–400 and 400–600 µm from the inoculation site. Actin (GenBank accession number AF111812.1) was used as the internal control and to normalize expression data. Relative transcript abundance is normalized relative to S mock (0–200 µm) treatment. Error bars represent standard deviation of the mean. For each gene, different lowercase letters indicate significant differences among mean values (one- way anova with Ducan's multiple range test; $P < 0.05$). The results are based on three replicates in three independent experiments.

When resistant host cotyledons were challenged with *L. maculans*, *APK2*, *RBOHF*, *WRKY25*, *BnaA03g43720D*, *BnaC04g27200D* and the SA signaling marker *PR1* accumulated at greater levels within tissues 0–200 µm from the infection site. Levels of *LIK1* and *CYP79B2* were greatest 200–400 µm from the infection site. A marker of JA-ET signaling, *PDF1.2*, was the only transcript to accumulate highest in tissues taken distally (400–600 µm) from the

infection site of resistant hosts. These data provide evidence of the spatial coordination of defense gene activity in tissues directly at the infection site in response to *L. maculans* attack.

2.5 Discussion:

We profiled gene expression in susceptible and resistant cotyledons of *B. napus* before, during and after infection with the hemibiotrophic fungus *L. maculans* to uncover key components of the ETD pathway. Our experiments showed an accelerated defense response in resistant host tissues coinciding with the deposition of lignin and callose that probably prevents colonization and reproduction by *L. maculans* in apoplastic spaces in canola cotyledons. Transcripts associated with resistance accumulated in gradients away from the infection site, providing unprecedented spatial resolution of the *B. napus–L. maculans* pathosystem.

Arabidopsis mutants of two uncharacterized receptors (*at4g18250* and *at3g53490*) were susceptible to *L. maculans*, suggesting a conserved defensive role in the Brassicaceae. Globally, accelerated defense during ETD is associated with rapid activation of RLPs, RLKs, TIR-NBS receptors and receptor partner proteins by 3 dpi involved in perception of PAMPs and observed late in the infection process in susceptible cultivars (Haddadi et al., 2016). Of the receptors, 17 were specific to the resistant line and 12 were uncharacterized with no previously described host– pathogen annotation in *B. napus*, Arabidopsis or any other plant pathosystem (Table S2). As ETD pathways are mediated through extracellular RLPs and their associated partner proteins (Stotz et al., 2014), upregulation of these receptors may produce a positive feedback loop amplifying the plant immune response and improving pathogen detection. Furthermore, if ETD and non-host resistance pathways are similar in their architecture, Arabidopsis presents a putative source of effective *R*-genes with the potential to bolster blackleg resistance in canola.

R-gene efficacy is often independent of the host cell death response (Schiffer et al. 1997, Cawly et al. 2005), suggesting that cell death may not always be responsible for host resistance but rather a by-product of runaway immune response or cell damage due to infection. Indeed, many necrotrophic or facultatively necrotrophic pathogens will induce host cell death mechanisms to facilitate infection (Lorang et al. 2007, Kabbage et al. 2013), and *L. maculans* has been shown to produce a necrosis- and ET-inducing peptide upon its biotrophic–necrotrophic transition (Haddadi et al., 2016). The phytopathogen-induced cell death repressor *KTI1* was induced specifically in resistant hosts. When challenged with *L. maculans*, lesions spread rapidly in *kti* Arabidopsis plants like the phenotype of *accelerated cell death 2* plants described by Bohman et al. (2004). Although hemibiotrophic, *L. maculans* has been defined as primarily necrotrophic (Staal and Dixelius 2008) and can survive within dead or dying plant tissues. Thus, the recognition of *L. maculans* and activation of cell death regulators early in the infection process are likely to contribute to delayed onset of cell death observed during ETD. The comparative lack of these regulators early in susceptible hosts may explain its rapid lesion formation following the biotrophic–necrotrophic transition of *L. maculans*.

JA signaling has been shown to repress hypersensitive-like cell death in Arabidopsis (Rao et al. 2000) and may be an overarching regulator of the genes described above. Susceptible cotyledons show a notable lag in JA response through diminished expression of integral JA biosynthetic genes *LOX2, AOS* and *AOC* at the time of rapid lesion spread. The expression of NAC TFs early in resistant host cotyledons may directly promote production of JA (Appendix V). For example, NAC019 and NAC055 promote JA-induced transcription of *LOX2* (Bu et al. 2008), and a*nac019anac055* double mutants are susceptible to fungal necrotrophic pathogens (Bu et al., 2008).

Resistance to *L. maculans* may also involve the production of IGS. Production of IGS is required for resistance against some hemibiotrophic fungi (Hiruma et al. 2013), and in vitro studies have shown S-glycosides from *B. napus*, predominantly those derived from sinigrin, are toxic to *L. maculans* (Mithen et al. 1986). Our data show activation of the complete IGS biosynthetic pathway in resistant cotyledons. The production of IGS is linked to sulfur metabolism as all indole-derived phytoalexins in the brassicas contain sulfur (Pedras et al. 2011). Thus, activation of genes associated with sulfur assimilation during the *LepR1–AvrLepR1* interaction supports the production of IGS. Mugford et al. (2009) directly linked the sulfur activator APK2 to IGS production in Arabidopsis. Although we have shown that *apk2* Arabidopsis plants are susceptible to *L. maculans*, the mechanism by which susceptibility in conferred is unclear. Other members of the IGS biosynthetic pathway that were challenged, including *cyp79b2*, *cyp79b3*, *cyp83b1* and *cypb5c*, had no discernible phenotype. The lack of a phenotype in IGS-compromised Arabidopsis plants may be due to complementation by the antifungal indole alkaloid camalexin, effective against *L. maculans* (Bohman et al. 2004). As *B. napus* is unable to produce camalexin, IGS-derived phytoalexins may play an important role in defense.

We suspected that key components of the ETD pathway are likely to be spatially controlled directly at the infection site. Coordination of the ETD pathway, as revealed by LMD and qPCR, increased the spatial resolution of the dataset and demonstrated targeted activity of receptors and downstream signal transduction pathways in tissues directly in contact with and those adjacent to *L. maculans*. While hormone levels are known to flux over time during plant defense, our data show an antagonistic spatial relationship between SA and JA-ET signaling

pathways established specifically in resistant host cotyledons, as indicated by the distribution of hormone markers *PR1* and *PDF1.2*.

The IGS-marker *CYP79B2* was highly expressed adjacent to the infection site in an area of combined SA and JA-ET signaling. Consistent with our dataset, Frerigmann and Gigolashvili (2014) found that expression of the main IGS-inducing TF, *MYB51*, was greatest with joint application of SA and JA. Thus, deposition of antifungal IGS-derived phytoalexins most likely does not occur in areas of direct pathogen contact but rather upstream of invading *L. maculans*, and is potentially guided by hormone gradients formed during defense.

Rapid activation of defense regulators, including TFs, in resistant hosts can contribute to the deposition of lignin, callose and other anti-fungal metabolites preceding fungal invasion. This is complemented by the ability of resistant plants to direct defense activity to the host–pathogen interface by coordinating gene expression to areas of direct fungal contact or to areas adjacent to the infection site. For example, expression of *WRKY25* in resistant host cotyledons is concentrated around 400 µm from the infection site. As a negative regulator of SA-mediated defense responses (Zheng et al. 2007) and a positive regulator of ET biosynthesis (Li et al. 2011), activity of WRKY25 would prevent runaway SA signaling and cell death, thus mitigating disease progression and the likelihood of colonization by *L. maculans*.

Our data represent a valuable resource that captures gene activity following activation of ETD pathways in the *B. napus–L. maculans* pathosystem. The identification and characterization of genes responsible for mitigating plant disease demonstrates the utility of our dataset. Further, our data provide a preliminary framework in support of spatial transcriptional gradients responsible for plant resistance. Temporal and spatial regulation of gene expression both contribute to disease resistance, as expression of all tested genes was tightly controlled at the

infection site. While many of the underlying molecular mechanisms responsible for host resistance remain unresolved, access to technologies that can dissect cells and tissues immediately at and distal to the infection site should provide clues for directed crop improvement.

2.6 Acknowledgements:

This work was supported through a Manitoba Agriculture Rural Development Initiatives Growing Forward 2 grant to MFB and WGDF as well as a Canola Agronomic Research Program (CARP) grant through the Canola Council of Canada to WGDF. XZ was supported by a China Council Scholarship, MGB was supported by National Science and Engineering Research Council Vanier Scholarship, and JLM by a CGS-M Scholarship.

3 SeqEnrich: A tool to predict transcription factor networks from co-expressed Arabidopsis and *Brassica napus* gene sets

Michael G. Becker[1], Philip L. Walker[1], Nadège C. Pulgar-Vidal[2], Mark F. Belmonte[1,*]

[1]Department of Biological Sciences, University of Manitoba, Winnipeg, Manitoba, Canada

[2]Department of Computer Science, University of Manitoba, Winnipeg, Manitoba, Canada

[*]Corresponding author

Email: Mark.Belmonte@umanitoba.ca

Author contributions:

Michael Becker conceptualized the experiment, contributed to data curation, contributed to computational analysis, built databases, and contributed to coding, prepared figures and wrote the manuscript. Philip Walker contributed to data curation, contributed to computational analysis, and prepared Fig. 3.1. Nadège Pulgar-Vidal contributed to coding and designed the IUPAC converter. Mark Belmonte conceptualized the experiment and edited the manuscript.

3.1 Abstract:

Transcription factors and their associated DNA binding sites are key regulatory elements of cellular differentiation, development, and environmental response. New tools that predict transcriptional regulation of biological processes are valuable to researchers studying both model and emerging-model plant systems. SeqEnrich predicts transcription factor networks from co-expressed Arabidopsis or *Brassica napus* gene sets. The networks produced by SeqEnrich are supported by existing literature and predicted transcription factor – DNA interactions that can be functionally validated at the laboratory bench. The program functions with gene sets of varying sizes and derived from diverse tissues and environmental treatments. SeqEnrich presents as a powerful predictive framework for the analysis of Arabidopsis and *Brassica napus* co-expression data, and is designed so that researchers at all levels can easily access and interpret predicted transcriptional circuits. The program outperformed its ancestral program ChipEnrich, and produced detailed transcription factor networks from Arabidopsis and *Brassica napus* gene expression data. The SeqEnrich program is ideal for generating new hypotheses and distilling biological information from large-scale expression data.

3.2 Introduction:

Advances in next generation RNA sequencing (RNA-Seq) technologies to investigate biological processes is becoming commonplace in research laboratories. Despite these advances, the analyses of large scale RNA-Seq datasets are time consuming and publicly available tools able to analyze this information are often difficult to navigate for researchers with limited bioinformatics experience. Deriving relevant biological information from large-scale datasets represents a significant bottleneck in sequencing experiments. Thus, new user-friendly tools that facilitate analyses of large datasets are in demand from scientists studying both model and emerging-model plant systems.

A major objective in gene expression analyses is the identification of transcription factors (TFs) and cis-regulatory elements that direct cellular bioprocesses at the cellular, tissue, or whole plant level or in response to biotic or abiotic stresses. Many of the currently available tools, including Grassius Regulatory Grid Explorer hosted by the Arabidopsis Gene Regulatory Information Server (AGRIS; Yilmaz et al. 2011) and HRGRN (Dai et al. 2016), are ideal for individual gene lookups but are not conducive to large datasets. Additionally, several tools can effectively identify enriched promoter motifs from Arabidopsis datasets, such as the motif analysis tool hosted by The Arabidopsis Information Server (TAIR; Rhee 2003), the Cistome tool at the Toronto Bio-Analytic Resource (BAR; Austin et al. 2016), and Arabidopsis Motif Scanner (Mele 2016); however, these programs are not designed to identify enriched biological processes or generate TF networks. The Arabidopsis Interactions Viewer hosted by the Toronto BAR identifies experimentally validated protein-DNA interactions and generates a transcription network from an input query list (Geisler-Lee et al. 2007). This tool can build on this network by adding predicted or validated protein-protein interactions. Ultimately, this provides detailed and

accurate information on direct interactions between genes within a dataset, but reliance on experimentally validated protein-DNA interactions limits discovery. Further, the Arabidopsis Interactions Viewer does not identify enriched cis-regulatory elements or relate networks back to biological function. Further, none of the programs above take input data derived from the emerging model species *Brassica napus* (canola).

ChipEnrich was developed to perform promoter analysis, TF-DNA binding prediction, and functional enrichment in a single Java-based tool (Orlando et al. 2009, Belmonte et al. 2013). Developed to analyze large-scale co-expressed gene sets from the Arabidopsis ATH1 microarray, ChipEnrich takes a list of genes identified through clustering or differential gene expression analyses and identifies enriched Gene Ontology (GO) terms, TF families, and TF binding site motifs. The program also offers an analysis function that associates these terms into a TF network thus providing a predictive framework into the transcriptional programs of co-expressed gene sets. While this program has been used successfully in the analysis of large-scale microarray data (Belmonte et al. 2013, Khan et al. 2015, Silva et al. 2016), it is limited to ATH1 GeneChip sequences of the model plant Arabidopsis and publicly available information on i) gene function ii) nucleotide sequence of DNA binding sites and iii) TF-DNA sequence motif interactions.

Here, we developed SeqEnrich (Data S6) based on the ChipEnrich platform to predict TF networks from next generation RNA-Seq datasets. The SeqEnrich program contains the most extensive database of TFs, TF-DNA sequence motif interactions, and gene function(s) for the efficient interrogation of Arabidopsis or *B. napus* gene sets. SeqEnrich was able to successfully predict TF networks supported by existing experimental data in addition to providing new insights into the underlying transcriptional circuitry controlling biological process in space and

time. This program demonstrates a substantial improvement when compared to its ancestor ChipEnrich. SeqEnrich complements existing tools available for Arabidopsis, merging the functions of multiple tools into a single user-friendly program. Additionally, this serves as the first resource able to produce transcription factor networks from *B. napus* datasets.

3.3 Materials and Methods:

3.3.1Program execution:

The SeqEnrich software was developed using Java language and designed to be fully compatible with Windows and Linux operating systems. SeqEnrich is a user-friendly application that takes an input text format (.txt) query list of Arabidopsis Genome Initiative (AGI; The Arabidopsis Genome Initiative 2000) identifiers or *B. napus* annotation v5 identifiers (Chalhoub et al. 2014). Input gene lists are developed through differential gene expression or clustering analyses performed following next generation RNA-Seq experiments.

The SeqEnrich jar file (Data S6) and SeqEnrich source code (Data S7) are freely available. Updated versions of the SeqEnrich program will be deposited as they become available at http://www.belmontelab.com and updated source code deposited at the SourceForge open-source repository (https://sourceforge.net/).

3.3.2 GO term enrichment:

GO term enrichment was defined as the ratio between (a) the number of genes in the query list belonging to the GO term and (b) the total number of genes belonging to the GO term within the genome compared to the ratio of (c) the total number of genes within the query list to (d) the total number of genes within the genome. Significantly enriched GO terms are reported as

p-values calculated from the hypergeometric distribution using the Apache Commons Math Library (http://jakarta.apache.org/commons/math). SeqEnrich reports all GO term enrichment data and produces a summary file containing significantly enriched data with a p-value of < 0.001.

3.3.3 DNA sequence motif enrichment:

For each gene within the input query list, known TF binding sites are called from a lookup array within the program database. This array was created by identifying known TF binding sites within all gene promoters in the *B. napus* and Arabidopsis genomes. Here, we focus on motif enrichment within the 1 kb upstream region from the transcription start site, capturing the majority of Arabidopsis TF binding sites (Yu et al. 2016). Background motif distributions are determined from the TF binding sites identified within all promoters across the genome. Statistical enrichment for each DNA sequence motif within the query list was determined using the hypergeometric distribution. In addition, a subanalysis identifies DNA sequence motifs enriched within promoters of query genes associated with each enriched GO term. SeqEnrich reports all motif enrichment data and produces a summary file containing significantly enriched motifs with a p-value of < 0.001.

3.3.4 Prediction of transcription factor networks:

Fig. 3.1 shows a conceptual TF network generated using the SeqEnrich program. To produce TF networks, the SeqEnrich program performs an analysis and subanalysis of the input query list. In the analysis, DNA sequence motifs significantly ($p < 0.001$) enriched in promoters of query genes are associated with TFs within the same query gene list capable of binding to that DNA sequence motif. In the subanalysis, DNA sequence motifs significantly ($p < 0.001$)

enriched in promoters of query genes of individual significantly enriched GO terms ($p < 0.001$) are associated with TFs within the query gene list capable of binding to that sequence motif.

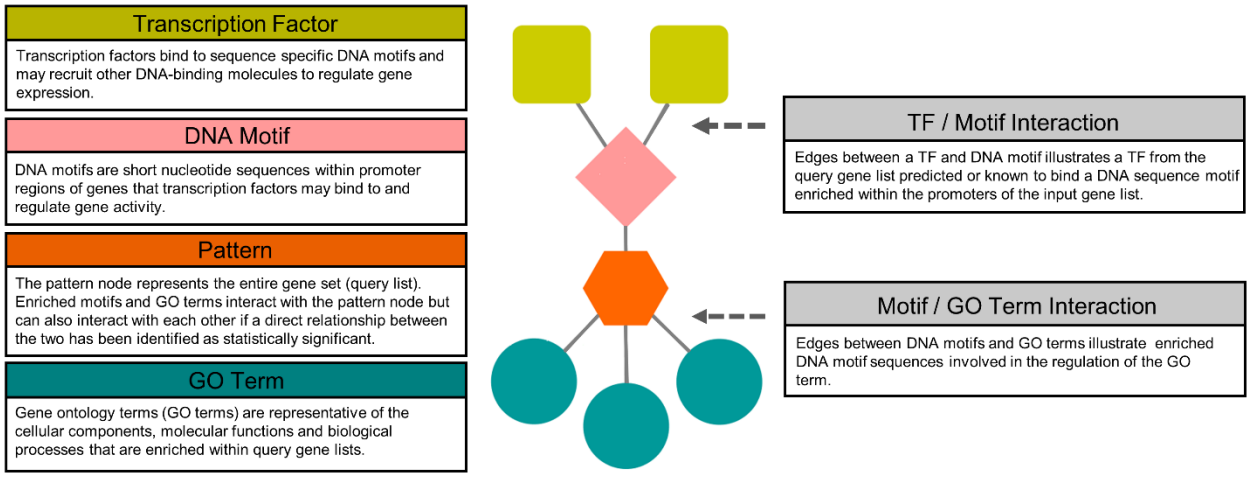

Fig. 3.1: Conceptual description of a transcription factor network. TFs are represented as green rounded squares, DNA motifs as pink diamonds, gene patterns as orange hexagons, and gene ontology (GO) terms as blue circles. Connections between TFs and motifs, and between motifs and patterns/GO terms are represented by a grey connecting line.

Together, these analyses produce connections between TFs, enriched DNA motifs, query genes (gene pattern), and GO terms and is presented in output network files. SeqEnrich produces two network files: i) TF networks from the analysis identifying DNA sequence motifs and GO terms enriched within the entire query list, and the associated TFs (extension .analysis.networks.txt) and ii) TF networks from the subanalysis identifying motifs enriched within each individual enriched GO term, and associated TFs (extension .subanalysis.networks.txt). Output network files are compatible with the Cytoscape visualization tool (http://www.cytoscape.org/), and p-values imported as edge attributes. A separate attributes file is produced and labels each node presented in the network file as a "pattern", "GO term", "motif", or "TF".

3.3.5 Database construction:

The database for the SeqEnrich program was built using information from publicly available sources (Fig. 3.2). The GO term database and genome annotations were derived from data curated by the TAIR consortium (TAIR10, https://www.arabidopsis.org) and *B. napus* annotation v5 (Chalhoub et al. 2014). Arabidopsis and *B. napus* TFs were identified using information from several databases to ensure inclusion of all TFs: i) JASPAR (http://jaspar.genereg.net/) ii) Plant TFDB (http://planttfdb.cbi.pku.edu.cn/) iii) Plant Transcription Factor Database (http://plntfdb.bio.uni-potsdam.de/) and iv) Database of Arabidopsis Transcription Factors (http://datf.cbi.pku.edu.cn/). A database of experimentally validated TF binding sites was built using information from the following sources: i) JASPAR ii) CIS-BP (http://cisbp.ccbr.utoronto.ca/) iii) Arabidopsis protein binding microarray (Franco-Zorrilla et al. 2014) iv) Yeast-one hybrid experiments (Kelemen et al. 2015) and v) Arabidopsis DAP-sequencing experiments (O'Malley et al. 2016).

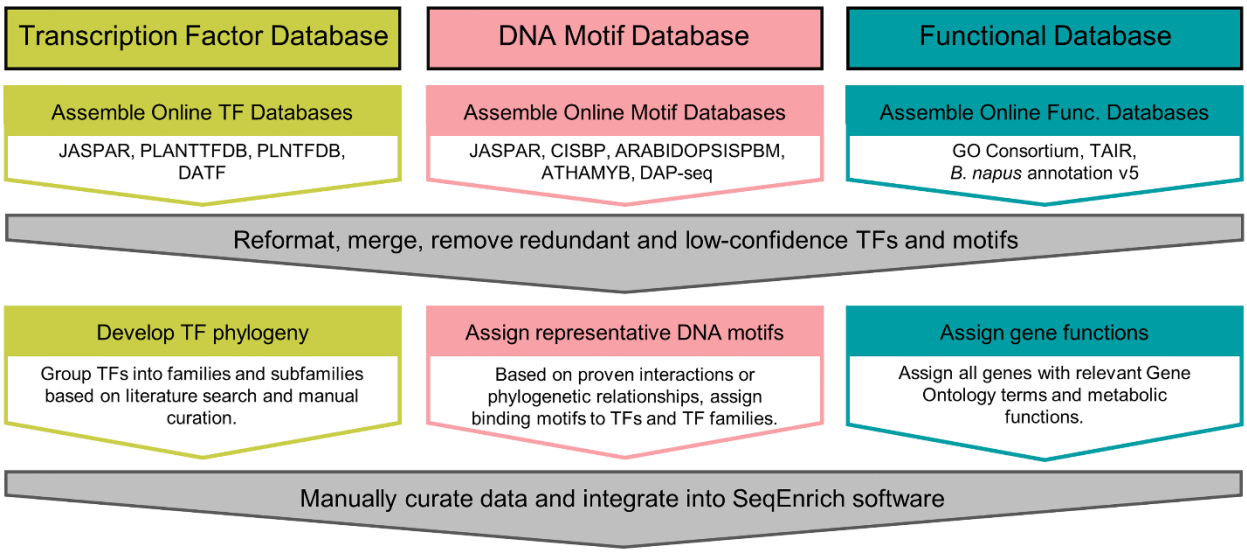

Fig. 3.2: Design and assembly of the SeqEnrich database. Information on transcription factors, DNA binding site motifs, and gene functions were collected from publicly available sources and integrated into the SeqEnrich program.

All motif databases presenting motifs in MEME format were converted into degenerate IUPAC codes using a custom Java script (Data S8) to ensure consistency and clarity amongst motifs. If the probability of any given nucleotide at each position within a motif is <0.10, it is not recorded at that position during generation of the IUPAC code (Table 1). This probability cut-off provided an ideal balance between specificity and sensitivity. Lower thresholds that were tested generated overly general motifs, and higher thresholds eliminated putative binding sites.

Table 3.1: IUPAC codes used for representation of nucleotides in motifs and corresponding likelihood of each nucleotide at position.

IUPAC	IUPAC	Nucleotide probabilities
A	Adenine	$[p(A) \geq 0.1, p(T) < 0.1, p(C) < 0.1, p(G) < 0.1]$
C	Cytosine	$[p(A) < 0.1, p(T) < 0.1, p(C) \geq 0.1, p(G) < 0.1]$
G	Guanine	$[p(A) < 0.1, p(T) < 0.1, p(C) < 0.1, p(G) \geq 0.1]$
T	Thymine	$[p(A) < 0.1, p(T) \geq 0.1, p(C) < 0.1, p(G) < 0.1]$
R	A or G	$[p(A) \geq 0.1, p(T) < 0.1, p(C) < 0.1, p(G) \geq 0.1]$
Y	C or T	$[p(A) < 0.1, p(T) \geq 0.1, p(C) \geq 0.1, p(G) < 0.1]$
S	G or C	$[p(A) < 0.1, p(T) < 0.1, p(C) \geq 0.1, p(G) \geq 0.1]$
W	A or T	$[p(A) \geq 0.1, p(T) \geq 0.1, p(C) < 0.1, p(G) < 0.1]$
K	G or T	$[p(A) < 0.1, p(T) \geq 0.1, p(C) < 0.1, p(G) \geq 0.1]$
M	A or C	$[p(A) \geq 0.1, p(T) < 0.1, p(C) \geq 0.1, p(G) < 0.1]$
B	C or G or T	$[p(A) < 0.1, p(T) \geq 0.1, p(C) \geq 0.1, p(G) \geq 0.1]$
D	A or G or T	$[p(A) \geq 0.1, p(T) \geq 0.1, p(C) < 0.1, p(G) \geq 0.1]$
H	A or C or T	$[p(A) \geq 0.1, p(T) \geq 0.1, p(C) \geq 0.1, p(G) < 0.1]$
V	A or C or G	$[p(A) \geq 0.1, p(T) < 0.1, p(C) \geq 0.1, p(G) \geq 0.1]$

Following amalgamation of motif databases, data filtering was used to remove duplicate entries and non-informative motifs. A non-informative motif was defined as a motif that lacked sequence specificity and had a $p < 0.02$ of occurring at any individual locus within a promoter by chance. To improve the resolution and accuracy of SeqEnrich, TF phylogenetic relationships were used to predict TF-DNA sequence motif interactions. For example, TFs with no experimentally validated binding information or TFs with conflicting experimental data could be

assigned putative DNA binding site motifs based on information from closely related TFs. These TF phylogenetic relationships were determined by combining existing TFF phylogenetic footprinting data (Ferrari et al. 2003, Parenicova 2003, Englbrecht et al. 2004, Reyes et al. 2004, Nakano et al. 2006, Wang et al. 2008, Guo et al. 2008, Kaplan-Levy et al. 2012, Du et al. 2013, Kelemen et al. 2015, Stender et al. 2015) and protein clustering performed with MUSCLE v3.8.31 (http://www.drive5.com/muscle/muscle.html). Using TF phylogenetic relationships to predict TF binding sites represents a new feature of SeqEnrich and dramatically improves the number of TFs with known or predicted binding sites, with 902 new predicted TF-DNA sequence motif interactions as compared to the original ChipEnrich program.

3.4 Results and Discussion:

3.4.1 The SeqEnrich database:

The SeqEnrich database contains a total of 2,263 Arabidopsis TFs and 240 Arabidopsis degenerate DNA binding site motifs, representing a 44.8% and 135% increase respectively, as compared to the original ChipEnrich software. As an additional comparison, the AGRIS databases (Yilmaz et al. 2011) currently contain 1,773 TFs and 99 DNA binding site motifs (http://arabidopsis.med.ohio-state.edu). The majority (85.4%) of TFs in the AGRIS transcription factor database overlapped with SeqEnrich. For the remaining ~15%, many were incorrectly classified as C3H family TFs due to their zinc finger, RING-type domains. Experimental evidence has suggested that they are more likely involved in ubiquitination (Lechner et al. 2002, Pan et al. 2016). The newly developed *B. napus* database contains 8,306 TFs and 228 degenerate motifs. The greater number of TFs in *B. napus* can be explained by a genome duplication event

since its divergence from Arabidopsis and its large allotetraploid genome of ~90,000 genes (Chalhoub et al. 2014). The decline in the number of binding site motifs identified in *B. napus* is likely due to its comparative lack of experimental TF binding data.

Since little information about *B. napus* TF binding sites are available, the majority of *B. napus* binding site motifs are predicted from closely related Arabidopsis homologs. Using homology to predict TF binding sites is common in mammalian systems (Cartharius et al. 2005, Hemberg and Kreiman 2011), and is supported by multiple independent experiments that identify conserved TF target sequences between plant species as distally related as Arabidopsis and rice (Nakano et al. 2006, Yanhui et al. 2006, Guo et al. 2008). Our SeqEnrich program represents the largest database for *B. napus* TFs and motifs currently available and is accessible within the program source code (Data S7) and as a separate download at http://www.belmontelab.com.

3.4.2 Validation of the SeqEnrich program:

To demonstrate how the SeqEnrich program improves detection of TF-DNA sequence motif interactions, we compared its output to previously published Arabidopsis TF networks from publicly available datasets (Belmonte et al. 2013, Taylor-Teeples et al. 2014). A total of 661 genes co-expressed in the chalazal endosperm of the mature seed (Data S9) were used as input into both the ChipEnrich (Fig. 3.3A) and SeqEnrich programs (Fig. 3.3B). This comparison identified 2.6-fold more TFs, 7.1-fold more enriched GO terms, and 9.3-fold more enriched motifs using the SeqEnrich program with the same gene query list. As the SeqEnrich database contains only 44.8% more motifs than ChipEnrich, the observed increase in motif detection is likely due to the improved accuracy of new databases and not solely a result of increase in

database size. Similarly, the larger number of enriched GO terms in SeqEnrich can be attributed to the improvements in TAIR curated GO annotations.

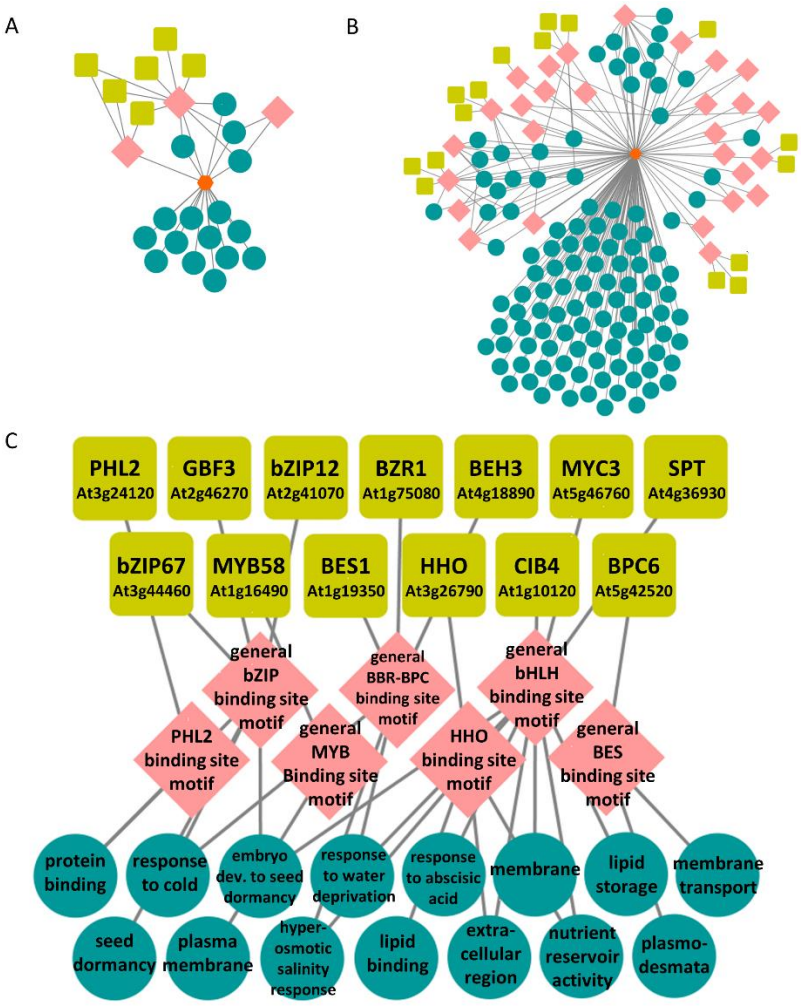

Fig. 3.3: Predicted transcription factor networks from the chalazal endosperm of Arabidopsis. A) Predicted transcriptional module developed from the ChipEnrich program; B) predicted transcriptional module using the SeqEnrich program; C) subset of the transcriptional module produced from the subanalysis function of the SeqEnrich program. A predicted bZIP, bHLH, MYB, and BES transcriptional module controlling biological processes within the mature endosperm of Arabidopsis.

We also identified predictive TF networks in mature chalazal endosperm using the subanalysis function of SeqEnrich (Fig. 3.3C). This transcriptional circuit predicts the regulation

of a number of seed-related bioprocesses, including “nutrient reservoir activity”, “embryo development to seed dormancy”, “lipid storage”, “response to abscisic acid”, and “seed dormancy” by TFs binding to the BZIP, MYB, BES, and BHLH binding sites. As the subanalysis function is a new function in the program a direct comparison between subanalyses is not possible; however, several of the DNA binding sites identified, including PHL2, BBR-BPC, BES, HHO are found exclusively within the SeqEnrich database. Several of these TFs identified in this circuit, including SPATULA and BZR1, are already associated with seed maturation and have delayed development phenotypes (Vaistij et al. 2013, Li and He 2016). Other TFs identified in the subanalysis, including PHL2, CIB4, and BPC6, have no known biological function. Based on the late timing of their expression, they may serve as transcriptional regulators of seed maturation active in tissue-specific subregions of the seed.

To confirm that the SeqEnrich output is reflective of *in vivo* gene regulation, we tested the program on a dataset containing TFs and DNA targets with proven interactions. We used the Taylor-Teeples et al. (2015) dataset of coexpressed genes involved in secondary cell wall biosynthesis of the Arabidopsis steele, which includes TF-motif interactions confirmed with yeast one hybrid experiments (Taylor-Teeples et al. 2014). We produced a network with these data containing 58 TFs targeting genes associated with cell wall, xylem, lignin, cellulose and hemicellulose, root development, and regulation of transcription (Appendix X). Our analysis identified enriched bZIP, homeobox domain (HD), and zinc-finger HD transcription factor families, which agrees with the findings in Taylor-Teeples et al. (2015). We also identified TFs PHABULOSA and REVOLUTA in our networks, which were a center of focus in Taylor-Teeples et al. (2015) and proven central regulators of xylem cell specification and secondary cell

wall biosynthesis. Together, these data support the ability of SeqEnrich to report meaningful biological predictions.

3.4.3 SeqEnrich predicts transcription factor networks in *Brassica napus*:

We used two different datasets (Data S9) to test the efficacy of the SeqEnrich program on large-scale *B. napus* RNA-Seq co-expressed gene lists: i) a tissue-specific dataset of 684 genes activated within the vasculature of the *B. napus* funiculus (Chan et al. 2016; Fig. 3.4A); and ii) a defense response dataset of 3,234 genes activated specifically in cotyledons resistant to the fungal pathogen *Leptosphaeria maculans* (Becker et al. 2017b; Fig. 3.4B-C). These datasets were selected because of i) the differences in the size of the query list, ii) the tissue type from where RNA sequencing was performed, and iii) the environmental conditions in which the plants were reared based on their cellular response.

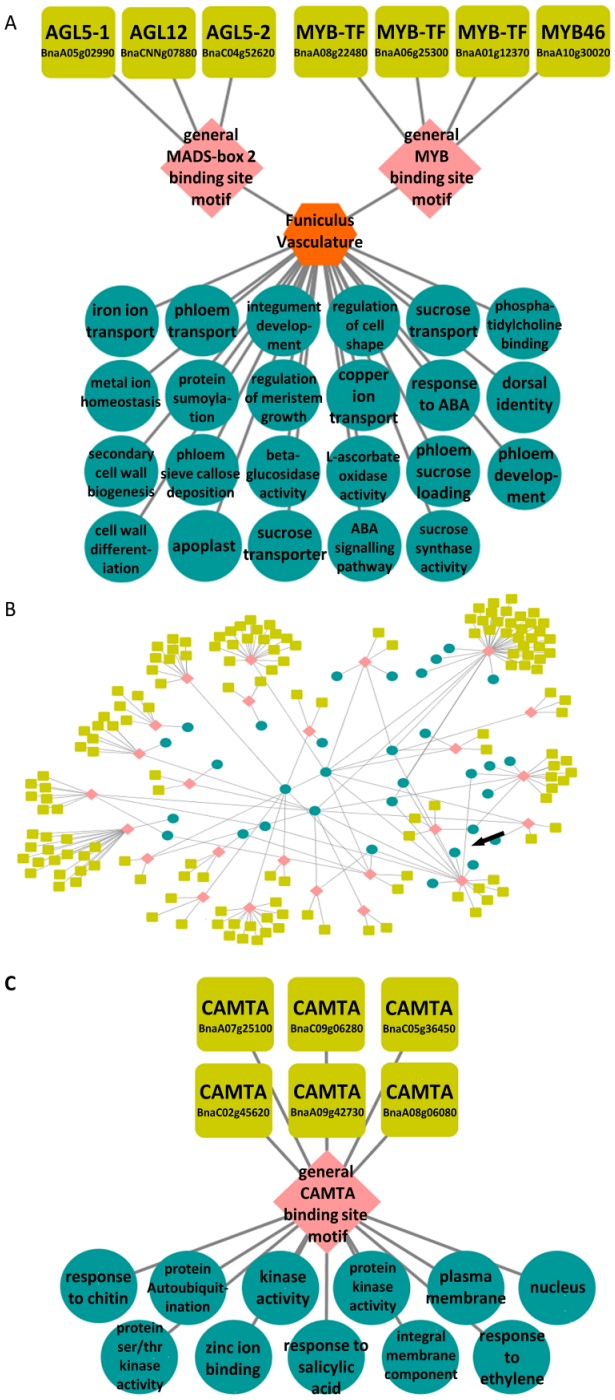

Fig. 3.4: Predicted transcription factor networks from *Brassica napus* gene sets. A) Subset of transcription factor network identified from funiculus vasculature dataset. MYB and MADS-box TFs are predicted to regulate genes associated with transport, metal ion homeostasis, and cell wall modification; B) subset of transcriptional module identified from the SeqEnrich subanalysis function predicted to be operative in *B. napus* seedlings infected with fungal pathogen *Leptosphaeria maculans*; C) transcriptional module depicted by arrow in (B), showing regulation of genes associated with defense bioprocesses by a family of calmodulin-binding transcriptional activators (CAMTAs).

The newly developed SeqEnrich program identified TFs binding to the MYB and MADS-box binding site motifs enriched within the promoters of genes specific to funiculus vasculature, and are associated with “phloem sieve callose deposition”, “secondary cell wall biogenesis”, “phloem sucrose loading”, “integument development”, and “metal ion homeostasis” (Fig. 3.4A). As the only connection between maternal tissue and the growing seed, the funiculus is responsible for nutrient transfer during seed filling (Chan et al. 2016). Two of the TFs identified in this transcriptional circuit have proven roles in plant root tissue (Tapia-López et al. 2008, Kim et al. 2014), which may be due to the similar functions of root and funicular tissues in nutrient transport (Chan and Belmonte 2013). For example, MYB46 is concentrated within the xylem of growing roots and a master regulator of secondary cell wall formation (Kim et al. 2014). The identification of MYB46 in funicular vasculature (Fig. 3.4A) clearly demonstrates the ability of SeqEnrich to generate new scientific hypotheses that can be functionally validated at the bench.

The SeqEnrich subanalysis predicted a large transcriptional network active in resistant *B. napus* cotyledons, suggesting that coordination of the defense response is complex and involves large numbers of TFs to control expression of genes responsible for plant defense and highlights the sensitivity of the program (Fig. 3.4B). Most TFs identified converged on similar binding site motifs. For example, 30 WRKY TFs were identified in a transcriptional module and are predicted to bind to a similar WRKY binding site motif. The large number of cognate TFs is likely due to gene duplication in the *B. napus* genome and redundant TF functions. A subsection of this network is presented in Fig. 3.4C and predicts a family of calmodulin binding transcriptional activators (CAMTAs) binding to the CAMTA binding site motif enriched in gene promoters associated with “response to chitin”, “kinase activity”, “response to salicylic acid”,

and “response to ethylene” during defense. As calmodulin has been shown to accumulate in resistant plants upon pathogen exposure (Kawai-Yamada et al. 2009), the activity of calmodulin-binding TFs is logical and provides additional evidence into the predictive framework of the SeqEnrich analysis using *B. napus* data. As the binding sites of these CAMTAs were unknown until recent DAP-seq experiments (O’Malley et al. 2016) this clearly demonstrates the sensitivity of our newly developed program afforded by its carefully constructed DNA sequence motif databases.

3.4.4 Program utility:

Tools to identify enriched GO terms (Du et al. 2010) or DNA sequence motifs (Yan et al. 2005, Blatti and Sinha 2014, Medina-Rivera et al. 2015, Mele 2016) from Arabidopsis gene sets are available, however, none exist that combine these functions into a complete analysis that identifies TF-DNA sequence interactions within biological processes encoded by gene sets of RNA-Seq data. Here, SeqEnrich identifies enriched DNA sequence motifs within the promoters of query gene sets or a smaller subset of genes belonging to a biological process with predicted or known TF-DNA sequence motif interactions. Further, the SeqEnrich program interrogates current databases of GO terms, DNA sequence motifs, and TFs thus reducing manual data curation by the user. Current user-friendly programs that facilitate rapid analysis of RNA-Seq data and elucidation of regulatory networks are limited to humans and other mammalian systems (Roider et al. 2007, Kwon et al. 2012, Haynes et al. 2013, Babur et al. 2014). Our SeqEnrich program serves the plant biology community and is designed for the model organism Arabidopsis and economically important *B. napus*. Given the utility and applications of the program and the continued generation of large scale RNA-Seq datasets from model and emerging model plant systems, we are currently developing similar data analysis platforms for

globally-important monocot crop systems such as rice and corn. The hypotheses generated from this program can then be transferred to the laboratory bench to functionally characterize the underlying molecular mechanisms of the plant.

3.5 Conclusion:

The SeqEnrich program represents a powerful user-friendly platform for the analyses of large scale RNA-Seq datasets and the prediction of TF networks from differential gene expression or co-expression analyses. We show the program can be applied broadly across query gene lists of different sizes, tissue types, and experimental treatments. The program's ease of use allows researchers without a background in computational biology to perform comprehensive analysis of RNA-Seq data and identify TF-DNA motif interactions orchestrating complex biological processes.

3.6 Acknowledgements:

This work was supported by Discovery and Accelerator Supplement grants from the National Science and Engineering Research Council of Canada to MFB, a Vanier Scholarship to MGB and USRA to PLW and NCPV.

4 Transcriptome analysis of *Rlm2*-mediated host immunity in the *Brassica napus-Leptosphaeria maculans* pathosystem

Department of Biological Sciences, University of Manitoba, Winnipeg, MB Canada, R3T 2N2

Author contributions:

Michael Becker conceptualized the experiment, performed laser microdissection, prepared libraries, analyzed and visualized data, performed functional experiments, and wrote the manuscript.

4.1 Abstract:

Our study captured gene activity directly at the *B. napus* - *L. maculans* host pathogen interface in susceptible and resistant (*Rlm2*) cotyledons using laser microdissection and dual RNA sequencing. The use of laser microdissection improved pathogen detection and identified putative *L. maculans* effectors and lytic enzymes operative during host colonization. Within 24 hours of inoculation we detected global shifts in gene activity in resistant cotyledons associated with jasmonic acid and calcium signaling pathways that bolster defense. Quantification of jasmonic acid confirmed higher concentrations of this phytohormone during incompatible immune responses. Furthermore, resistance against *L. maculans* was abolished when the calcium chelator EGTA was applied to the inoculation site despite active SA signaling as indicated by the reporter *PR1*, highlighting the importance of calcium in initiating *B. napus* immunity against *L. maculans*. We integrated gene expression data with all available information on cis-regulatory elements and transcription factor binding. These *in silico* analyses suggest early cellular reprogramming during immunity is coordinated by CAMTA, BZIP, and bHLH transcription factors. Together, this is the first transcriptomic investigation of the *Rlm2-AvrLm2* incompatible interaction and provides high-resolution data that serves as a resource for researchers studying defense against hemibiotrophic fungi.

4.2 Introduction:

Blackleg disease, caused by the hemibiotrophic fungus *Leptosphaeria maculans*, is a major cause of yield loss in the *Brassicaceae* (Fitt et al. 2008). Following spore germination on the cotyledon or leaf surface, pathogen hyphae bypass the epidermis through stomata or surface wounding (Hammond et al. 1985) and move into the apoplast where the fungus grows biotrophically. Activation of host immune receptors in response to *L. maculans* triggers cell signaling systems that initiate defense (Ma and Borhan 2015). These receptors include race-specific *R*-genes effective at juvenile stages of the plant lifecycle (Raman *et al.*, 2013). When plant *R*-gene products and corresponding pathogen *Avr* gene products interact, an incompatible interaction occurs leading to pathogen arrest. There are currently 16 individual *R*-genes that have been identified in Brassica germplasm (*LepR1 – R4*, *RlmS*, *Rlm1 – 11*) and their corresponding effectors have been identified (Raman *et al.*, 2013). Many of the *L. maculans Avr*-genes have been cloned, however only two of the *R*-genes, *Rlm2* (Larkan et al. 2015) and *LepR3* (Larkan et al. 2013), have been cloned and identified as membrane surface receptor-like proteins (RLP).

L. maculans is assumed to remain undetected in the apoplast for several days while adapting to host antimicrobial compounds (Stotz et al. 2014). While the genetics of the *L. maculans – B. napus* interaction is fairly well explained, the interplay between *L. maculans* and its host during establishment is largely unresolved. Several recent reports indicate the complexity of *L. maculans* effector-mediated suppression of host defense. For example, AvrLm4-7 affects the host immune responses associated with salicylic acid (SA) and ethylene (ET) signaling, and reactive oxygen species (ROS) production (Nováková et al. 2015); however, the observed effects of AvrLm4-7 may be indirect as it prevents host detection of AvrLm3 and AvrLm5-9 (Plissonneau et al. 2016, Ghanbarnia et al. 2018). The production of cytokinins by *L. maculans*

(Trdá et al. 2017) or the activation of additional, yet to be identified fungal effectors, may also affect immune signaling and colonization of the host plant. Despite the growing body of evidence dissecting this pathosystem little is known about early host immune signaling during pathogen establishment and certainly nothing about fungal gene activity early in the infection process directly at the infection site.

The receptor-like R-protein Rlm2 interacts with membrane receptor kinase SOBIR1 (Larkan et al. 2015) and likely partners with BRI1-ASSOCIATED RECEPTOR KINASE 1 (BAK1) to form a fungal receptor complex (Ma and Borhan 2015). Pathogen detection through this receptor complex triggers host phosphorylation cascades that integrate with signals from pathogen-associated molecular pattern (PAMP) immune receptors including Chitin-Elicited Receptor Kinase 1 (CERK1; Ma et al. 2016, Yamada et al. 2017, Peng et al. 2018). These cascades function synergistically with signals from calcium decoders, such as calcium dependent protein kinases (CPKs/CDPKs; Boudsocq et al. 2010). In Arabidopsis, these signals, in concert with cues from intracellular oxidation states, lead to widespread transcriptional reprogramming (Yuan et al. 2017) that involves CAMTA, WRKY, BZIP, ERF, and BES transcription factors (TFs; Seybold et al. 2014, Li et al. 2016). Additionally, a SOBIR1 homolog in cotton was recently shown to directly activate bHLH TFs (Zhou et al. 2018) emphasizing the need to characterize transcriptional reprogramming during RLP-mediated immunity. In *B. napus* and other members of the Brassica family global transcriptional regulation of defense remains largely unexplored. Rather, research has focused on individual TFs or TF families (He et al. 2016, Zhou et al. 2017).

Widespread transcriptional changes during defense lead to specific hormone responses that modulate cellular signaling and propagate defense signals across the cotyledon. Previously,

salicylic acid (SA) signaling has been generally associated with defense against biotrophic fungal pathogens, whereas ethylene and jasmonic acid (JA) have been associated with defense against necrotrophs (Glazebrook 2005). However, this paradigm is heavily scrutinized as an increasing number of studies show essential roles for JA signaling in biotrophic and hemibiotrophic interactions, especially at early infection stages, and exceptions suggest more complex interactions of defense hormones (Derksen et al. 2013). In the grapevine – *Plasmopara viticola* (powdery mildew) pathosystem, JA accumulates specifically in incompatible lines in the first 24 hours of infection (Guerreiro et al. 2016). Both JA and abscisic acid (ABA) play important roles in early defense signaling in the wheat – *Fusarium graminearum* pathosystem (Qi et al. 2016), and both SA and JA are associated with potato defense against hemibiotroph *Verticillium dahliae* (Zhu et al. 2017). Additionally, symbiotic fungi such as *Laccaria biocolor* rely on effectors that repress JA signaling to facilitate initial colonization (Plett et al. 2014). Previous RNA-Seq studies have shown increased JA-associated gene activity in RLP-SOBIR1 mediated immunity (Zuluaga et al. 2016b, Becker et al. 2017b); however, JA concentrations have never been directly measured and the signaling mechanisms upstream of JA activation are unclear.

Signaling molecules responsible for immunity, such as receptors, kinases, TFs, and regulators of hormone production are cell-specific and mainly targeted at the host pathogen interface (Chandran et al. 2010, Lenzi et al. 2016). Because available transcriptome data for the *B. napus-L. maculans* pathosystem is derived from the response of whole- or hand-dissected cotyledons (Lowe et al. 2014, Haddadi et al. 2016, Sonah et al. 2016, Becker et al. 2017b), these signals are often too weak to be detected. The combination of laser microdissection (LMD) and transcriptome profiling can monitor gene activity within the first host cells responding to pathogen. This technique has improved our understanding of the soybean response to *Heterodera*

glycines, identifying specific activation of heat-shock and *LOX* genes during host incompatibility (Klink et al. 2005). Roux et al. (2014) used a similar strategy to identify tissue-specific gene sets associated with nodule formation in *Medicago truncatula*, capturing known and novel symbiotic genes validated by *in-situ* mRNA hybridizations. Although LMD has been used to investigate host pathogen interactions previously (Klink et al. 2005, Tang et al. 2006, Chandran et al. 2010, Hacquard et al. 2010, Roux et al. 2014, Becker et al. 2017b), these studies generally performed downstream analysis with qPCR or arrays. To our knowledge this is the first study to combine the resolution of LMD with the depth of next generation RNA-Seq in the study of a plant host-microbe interactions.

This study captures gene activity in *B. napus* and *L. maculans* directly at the host pathogen interface in a susceptible (Topas) and resistant Topas transgenic line (T-*Rlm2*; Larkan *et al.*, 2015). Our predictive TF networks suggest bHLH, CAMTA, and bZIP TFs are active by 1 day post-inoculation (dpi) and are likely involved in cellular reprogramming during host pathogen incompatibility. TF activity was associated with rapid JA and calcium signaling responses unique to the resistant line. Application of calcium chelators at the inoculation site prevented host defense activation and completely abolished resistance providing physiological evidence that calcium influx is required for *Rlm2*-mediated immunity. Additionally, this research suggests prolific pathogen-induced repression of host defenses at the inoculation site coincides with activation of known *L. maculans* effectors. Taken together, our research provides a high-resolution analysis of gene activity guiding plant immune responses during the earliest stages of host pathogen interactions. Further, the data produced by this study serves as a valuable resource for researchers studying plant defense strategies against apoplastic hemibiotrophs.

4.3 Materials and Methods:

4.3.1 Plant growth and inoculation:

Susceptible Topas DH16516 and the *Rlm2* transgenic line NLA51-1 (Larkan et al. 2015) were grown in Sunshine mix #4 soil (SunGro Horticulture) in controlled environments with a 16-h photoperiod (21 ºC light, 16ºC dark). Seven-day old cotyledons were point inoculated with 10 µL of a *L. maculans* isolate 00-100 (*AvrLm2;* Ghanbarnia et al. 2015) pycnidia suspension (10^6) or sterile water (mock). All inoculations and tissue collections were performed between 11:00AM-2:00PM to minimize time of day effects. To explore the role of calcium in resistance, 10 µL of 5 mM EGTA was added to the inoculation site as an additional treatment and allowed to dry before inoculation.

4.3.2 Tissue Processing:

Inoculated cotyledons were processed for LMD at 1 and 3 dpi per the methods of Becker et al. (2017b). Inoculation sites were excised by making two cuts parallel to the cotyledon petiole-like structure. A minimum of 30 inoculation sites per biological replicate (3 biological replicates per treatment) were collected and fixed overnight in 3:1 (v:v) ethanol : acetic acid at 4°C. Tissues were then dehydrated in a graded ethanol series (30 min each: 75%, 85%, 95%, 100%, 100%) followed by xylenes infiltration (1 hour each: 3:1, 1:1, 1:3 ethanol : xylenes (v:v), 100% xylenes) at 4°C. Ten paraffin chips were added to the xylenes and kept at 4°C overnight. Following, samples were brought to room temperature before incubating at 42°C for 30 min and then at 58°C for 1 hour. The mixture was replaced with 100% melted paraffin every hour for 4 hours before embedding.

4.3.3 Sectioning and Laser Microdissection:

Embedded tissues were sectioned at 10 µm using a Leica RM2125 rotary microtome in RNase-free conditions and mounted on PEN membrane slides as per Millar et al. (2015). Slides were washed for 1 minute in xylenes to deparaffinize before proceeding to LMD on a Leica LMD6000. Sections of 100 µm proximal to the inoculation site were collected in 60 µl of lysis buffer. RNA was isolated from at least 20,000,000 μm^2 of collected tissue per biological replicate. RNA extractions were performed exactly as reported in Belmonte et al. (2013). Following, RNA quality was assessed using the Agilent 2100 Bioanalyzer, and were of sufficient quality for qRT-PCR and RNA-Seq as described in Millar et al. (2015) and Chan et al. (2016).

4.3.4 Library construction:

First and second strand cDNA synthesis was performed per the alternative HTR (C2) described in Kumar et al. (2012), with the following modifications: Input RNA decreased to 50-75 ng; no Poly(A) bead isolation was performed; anchored oligo(dT_{20}) primers were used during first stand synthesis instead of random hexamers; half reaction volumes for all steps; cDNA sheared via sonication instead of enzymatic digestion. Libraries were prepared using the NEBNext Ultra II kit per the manufacturer's instructions. Quality and distribution of libraries was assessed with the Agilent 2100 Bioanalyzer, and libraries were quantified with the NEBNext Library Quant Kit for Illumina and the NanoDrop 3300 fluorospectrometer. Library size selection of the 300-500 bp region was performed with the E-gel size select system. Sequencing was performed on the HiSeq 2500 at Genome Prairie, SK, Canada.

4.3.5 Data Analyses:

RNA sequencing of libraries produced ~423 million paired end reads, with an average of 17.6 million reads per sample (PRJNA477556). Adapter sequences, low-quality bases (Q<25), and low-quality reads (avg Q<30) were removed using the Trimmomatic v0.36 software (Bolger et al., 2014). Paired-end reads passing quality control were aligned to the *B. napus* genome (v4.1, Chalhoub et al., 2014) with HISAT2 in cufflinks compatability mode, allowing no more than two mismatches. Output SAM files were converted to BAM and sorted with Samtools. Raw counts were obtained from BAM files using the HTSeq Python Framework (Anders et al. 2015). Dendrograms and similarity matrices were generated from raw counts using DESeq (Love et al. 2014). From BAM files, Cuffquant, Cuffnorm, and Cuffdiff (Trapnell et al. 2012) were used to generate normalized counts in FPKM and to identify significantly differentially expressed genes (DEGs; $p<0.05$; false discovery rate = 0.05). Differentially expressed gene sets were input into SeqEnrich (Becker et al. 2017a) to identify enriched metabolic pathways, GO terms, promoter TF binding motifs, and predictive transcription factor networks. Networks were visualized in Cytoscape 3.6.0 (www.cytoscape.org).

L. maculans transcriptome analyses were performed per Haddadi et al. (2016). All reads were trimmed as above and mapped to the *L. maculans* isolate v23.1.3 genome (Rouxel et al., 2011). Transcript abundance was measured as Log2 RPKM (Reads Per Kilobase of exon per Million mapped reads). DEGs ($p<0.05$; false discovery rate = 0.05) were identified with DESeq2 (Love et al. 2014). Identification of secretory protein signals was performed according to Haddadi et al. (2016).

4.3.6 Real-time qPCR experiments:

RNA was converted to cDNA with the qScript cDNA Supermix (Quantabio). Following, qPCR was performed using the CFX Connect Real-Time System (Bio-Rad) and PerfeCTa SYBR-Green Supermix (Quantabio) as per manufacturer's instructions in a 15 µl reaction volume. A list of primer sequences is supplied in Appendix XI. The ΔΔCt method (Rieu and Powers, 2009) was used to compare relative mRNA abundance, normalized to the endogenous housekeeping gene *Actin* (GenBank AF111812.1). Statistics were performed as described in McLoughlin et al. (2018).

4.3.7 Jasmonic Acid Measurements:

Inoculation sites (30 per bioreplicate, and five bioreplicates per treatment) were hand-dissected, and immediately flash-frozen and pulverized in liquid nitrogen. Following, 5 mL of extraction solvent (2-propanol:H_20:HCl, 2:1:0.002, pH 2.4) and 25 ng of dihydrojasmonic acid internal standard (Toronto Research Chemicals, #D454265) were added to each sample, which were then shaken at 4°C for 30 min. Next, 7 mL of dichloromethane was added, and samples shaken again at 4°C for 30 min. After centrifugation at 5300 RPM for 5 min, the lower organic phase was transferred and dried on ice in a nitrogen evaporator system. Dried sample was then dissolved in methanol, mixed aggressively, and filtered through 0.2µM PTFE before ultra performance liquid chromatography (UPLC). JA standards were prepared with internal standards to generate calibration curves and response factors. Samples were analyzed on a Waters Acquity UPLC/MS with Micromass Quattromicro API, as described in Henriquez et al. (2016).

4.4 Results:

4.4.1 Overview of plant responses to *L. maculans* (*Avrlm2*)

First, we examined the phenotype of susceptible Topas DH16516 and the transgenic line NLA51-1 containing *Rlm2* (Topas:*Rlm2*) to characterize disease progression over time. At 1 and 3 dpi, no difference in lesion colour or size was visible between genotypes (Fig. 4.1A). By 10 dpi, lesion spread was significant in susceptible plants, encompassing the entire leaf by 14 days. In transgenic plants containing *Rlm2*, cotyledons remained healthy and green at 14 dpi, with a necrotic ring observed around the inoculation site.

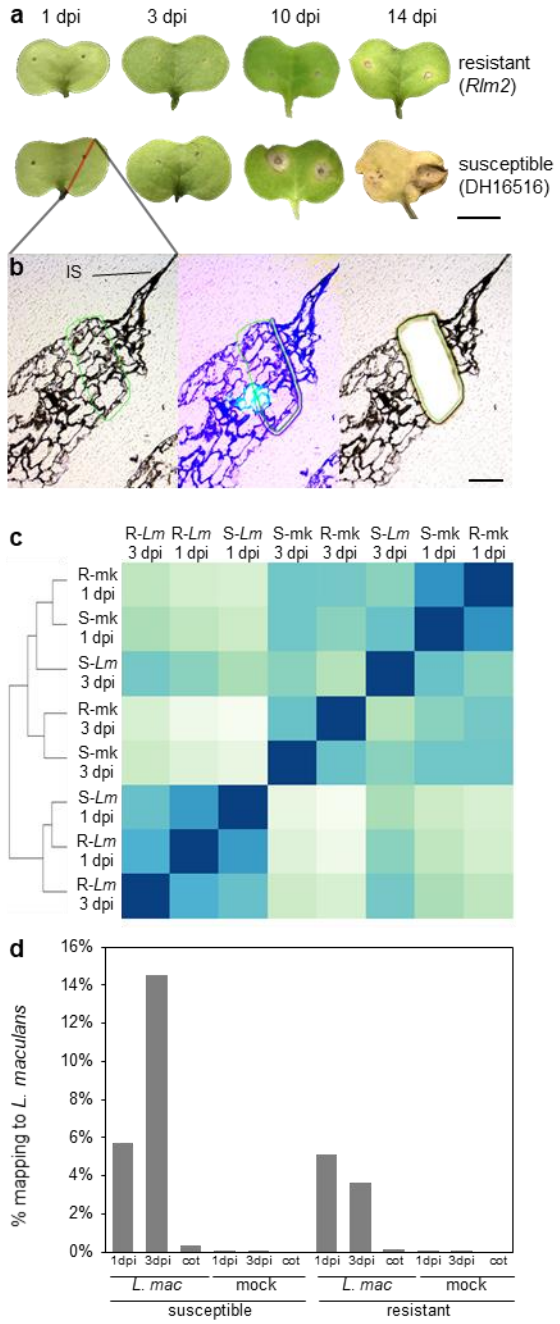

Fig. 4.1: Phenotypic response of resistant and susceptible hosts and preliminary data analysis. A) Disease progression in resistant Topas *Rlm2* (top) and susceptible Topas DH16516. Lesion spread is observed in susceptible hosts by 10 days post inoculation (dpi). Scale = 1 cm. B) Cross section of histologically processed cotyledon showing excision of plant tissue by laser microdissection. Collected fragments were used to generate sequencing libraries. C) Dissimilarity matrix, showing relationships between treatments and genotypes; R = resistant, S = susceptible, *Lm* = *L. maculans*, mk = mock. D) Average mapping rates of all treatments to the *L. maculans* genome. Data show highest mapping rates in susceptible hosts at 3 dpi, and lowest in hand-dissection cotyledons (cot) and mock controls.

4.4.2 Combined LMD and RNA sequencing improves pathogen detection at the earliest stages of infection

To capture gene activity at the host pathogen interface we used LMD-RNA-Seq, targeting the first 100 microns of healthy plant tissue adjacent to the inoculation site, equal to approximately two plant cell layers (Fig. 4.1B). Following histological processing, cellular structure was well-preserved in cross sections (Fig. 4.1B). To capture early signaling events during *L. maculans*' biotrophic phase, we focused our analysis on 1 and 3 dpi before visible lesion spread.

Following read quality control and alignments to the *B. napus* genome, hierarchical clustering was performed to identify relationships between genotypes and treatments (Fig. 4.1C). Samples clustered based on treatment and time point, apart from inoculated susceptible plants at 3 dpi that clustered with mock controls indicating a lack of a measurable defense response at this early stage in the susceptible line. Next, we plotted detection levels of *L. maculans* transcripts within each treatment (Fig. 4.1D). In all mock controls, few reads aligned to the *L. maculans* genome (<0.2%). At 1 dpi, pathogen alignment rates were similar in inoculated susceptible (5.7%) and resistant lines (5.2%). At 3 dpi, alignment rates were 14.6% and 3.6% in susceptible and resistant lines, respectively (Fig. 4.1D), suggesting that resistant plants may be effectively stopping the pathogen by 3 dpi. Additionally, we compared our alignment rates to those of RNA-Seq reads derived from hand-dissected inoculation sites at 3 dpi (Fig. 4.1D). Data show a marked increase in pathogen detection through the application of LMD, with an average 37-fold higher alignment rate in LMD-collected samples.

4.4.3 *L. maculans* gene expression profiles are different in resistant and susceptible *B. napus* lines

We next explored differences in the pathogen's gene activity during infection of susceptible and resistant lines. Principle component analysis (PCA) suggests similar mRNA profiles at 1 dpi regardless of host genotype but divergent responses at 3 dpi as indicated by independent clusters of samples (Fig. 4.2A). To elucidate the genes contributing to these responses, we investigated differential gene expression between *L. maculans* colonizing resistant and susceptible plants at both time points (Fig. 4.2B) and between time points (Fig. 4.2C). At 1 dpi, only 13 *L. maculans* genes, including hypothetical proteins and two putative pectate lyases (*LEMA_T033320; LEMA_T001630*; Data S10), were differentially expressed between the two interactions (Fig. 4.2B). At 3 dpi, this increased to 927 *L. maculans* DEGs (~8% of the *L. maculans* genome; Rouxel et al. 2011) that were influenced by host genotype. Differential gene expression analyses between time points identified 633 and 928 *L. maculans* DEGs that respond during infection of susceptible and resistant lines, respectively, and an additional 554 DEGs that were shared between interactions (Fig. 4.2C). Together, data revealed global shifts in *L. maculans* gene expression during infection -that are influenced by host genotype.

Expression of known *L. maculans Avr* genes during infection showed that *AvrLm2* and *AvrLm5-9* are the first *Avr*-genes expressed by the pathogen with detectable expression at 1 dpi and ~100-fold higher expression at 3 dpi (Fig. 4.2D). Expression of *AvrLm6* was first detected at 3 dpi, and *AvrLm1, 4-7,* and *11* were undetected (FPKM=0) in this dataset.

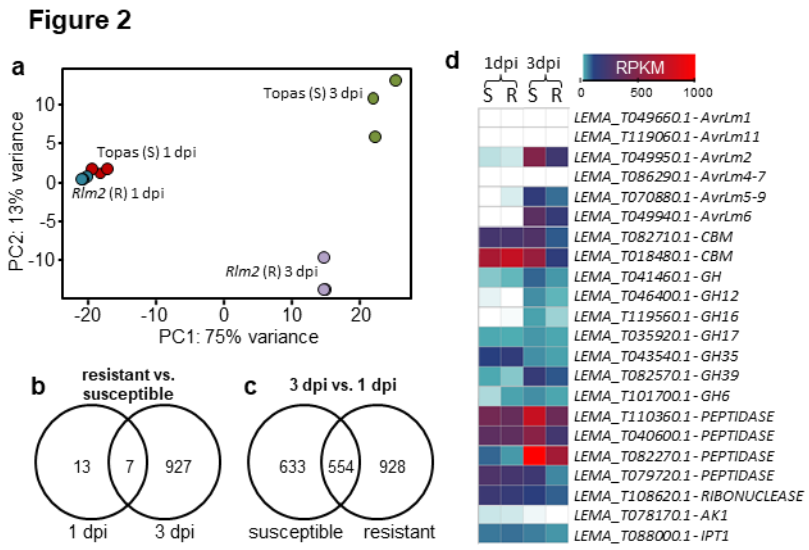

Fig. 4.2: *L. maculans* gene expression during its infection on susceptible and resistant hosts. A) PCA showing relationships between pathogen transcriptomes in infected treatments. Transcriptomes cluster together at 1 dpi and diverge by 3 dpi. B) Significantly ($p<0.05$) differentially expressed genes between *L. maculans* infection on resistant hosts vs. susceptible hosts. C) Significantly ($p<0.05$) differentially expressed genes between treatments at 3 dpi and 1 dpi. D) Selected gene set of virulence factors and known effectors, and their expression in reads per kilobase per million mapped (RPKM). A more intense red color denotes higher expression.

To determine putative *L. maculans* effectors involved in pathogen establishment we identified secretory signals within the N-terminal domain of translated DEGs (Data S11). The top five most upregulated genes (3 dpi vs. 1 dpi) within the predicted *L. maculans* secretome contained *AvrLm2* and *AvrLm6*, along with three hypothetical proteins of unknown function (*LEMA_T082980.1*, *LEMA_T054900.1*, *LEMA_T086540.1;* Data S11), highlighting the ability of our analysis to identify a combination of putative and characterized pathogen effectors.

Further analysis of the secretome identified *L. maculans* degradative enzymes and *Avr* genes with higher gene expression during colonization of susceptible plants at 3 dpi (Fig. 4.2D). This included *AvrLm2, 5-9, 6,* putative carbohydrate binding molecules (CBMs) with homology to starch hydrolyzing amylases (*LEMA_T082710.1*, *LEMA_T018480.1*), glucoside hydrolases

(*GH6, 12, 16, 17, 35, 39*), peptidases (*LEMA_T110360.1*; *LEMA_T040600.1*, *LEMA_T082270.1*, *LEMA_T079720.1*), and a ribonuclease (*LEMA_T108620.1*).

The production of cytokinins by *L. maculans* has been shown *in vitro*, and cytokinin biosynthetic enzyme AK1 activity increases disease severity (Trdá et al. 2017). Both *ADENOSINE KINASE 1* (*AK1*) and *ISOPENTENYLTRANSFERASE 1* (*IPT1*), involved in cytokinin production, were expressed at 1 dpi with decreasing expression by 3 dpi in both lines. In resistant plants, there was no detectable expression of *AK1* at 3 dpi.

4.4.4 Early differences in gene expression between resistant and susceptible plants

With notable differences in pathogen gene activity observed between compatible and incompatible interactions, we were next interested in examining host responses in plant cells directly adjacent to the inoculation site. At 1 dpi, 2572 (47%) upregulated DEGs (uDEGs) were shared between both genotypes, with an additional 541 (9.9%) uDEGs specific to susceptible plants and 778 (14.2%) specific to resistant plants. At 3 dpi, the number of shared uDEGs decreased to 2484 (31.0%), with 1193 (14.9%) and 2105 (26.3%) uDEGs specific to susceptible and resistant plants, respectively. Similar trends in the number and distribution of downregulated DEGs were observed in response to *L. maculans* inoculation (Fig. 4.3B). Together, data indicate a more conserved response between lines at 1 dpi and an overall stronger response to *L. maculans* in resistant plants at the mRNA level. All gene expression data are presented in Data S12.

Figure 3

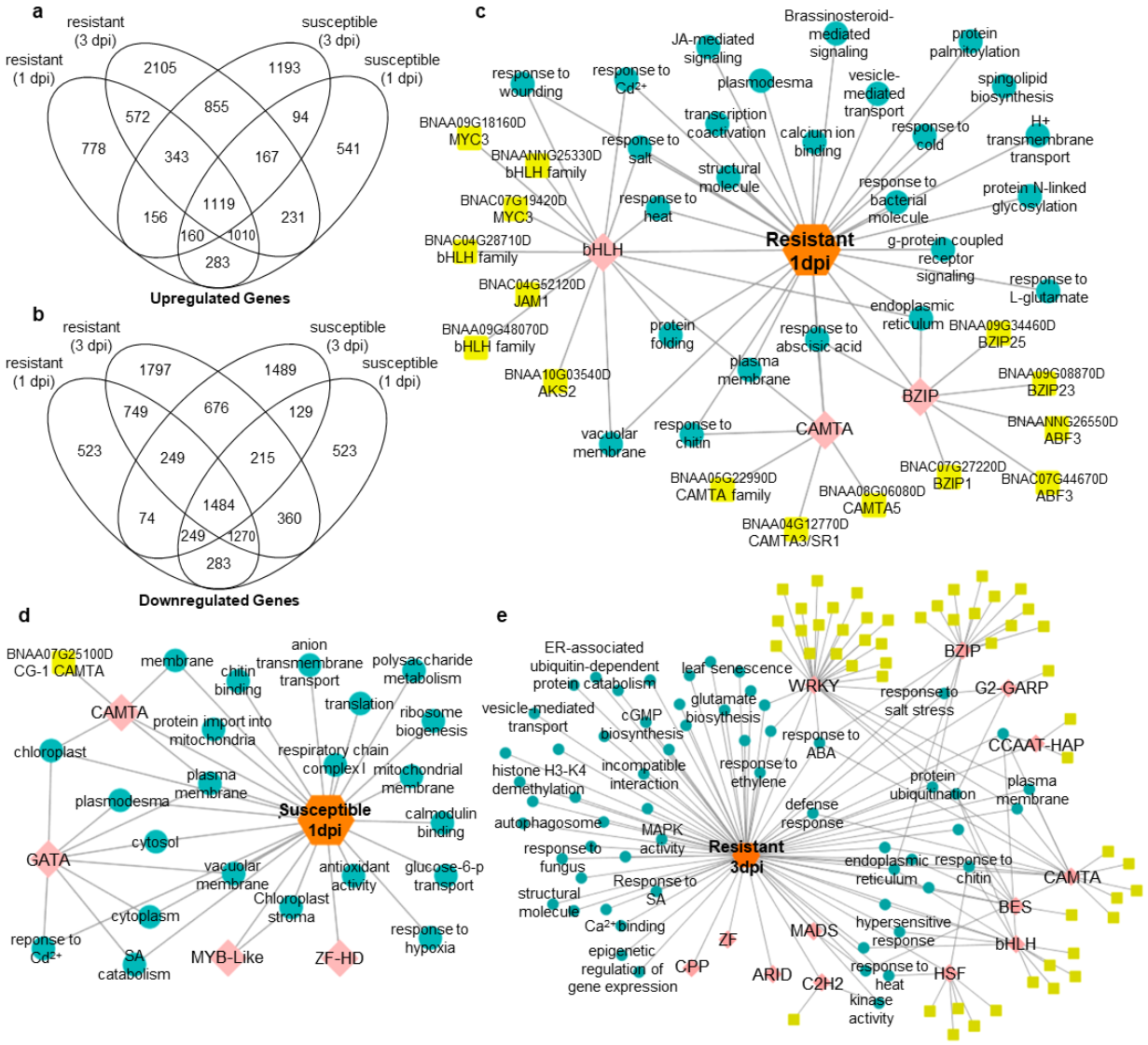

Fig. 4.3: Differential gene expression analyses and predictive transcription factor networks. A) Significantly ($p<0.05$) upregulated genes in each treatment as compared to their mock inoculated controls. Four-way VENN diagram shows number of unique or shared genes between treatments. B) Significantly ($p<0.05$) downregulated genes in each treatment as compared to their mock inoculated controls. Four-way VENN diagram shows number of unique or shared genes between treatments. C) Predicted network showing transcription factors (yellow squares), DNA binding motifs (pink diamonds), and gene ontology terms (teal circles) enriched in resistant-specific differentially expressed genes at 1 day post-inoculation (orange hexagon). Grey lines show predicted connections between transcription factors, motifs, gene ontology terms, or the resistant-specific gene set. D) Predicted network showing genes specifically upregulated in susceptible hosts at 1 day post-inoculation. E) Predicted network showing genes specifically upregulated in resistant hosts at 3 days post-inoculation.

4.4.5 JA and calcium-associated transcription factors influence the cellular response to *L. maculans* in resistant plants

Gene regulatory networks from our co-expressed gene sets were then studied using SeqEnrich. A putative gene regulatory network was identified in resistant plants early in the defense response (Fig. 4.3C). Data predict TF homologs canonically associated with JA (MYC3, JAM1), ABA (AKS2, ABF3) and calcium (CAMTA5, CAMTA3/SR1) signaling that regulate essential defense processes at the inoculation site in resistant plants. This includes overarching regulation of calcium ion binding, response to ABA, JA-mediated signaling, brassinosteriod-mediated signaling, response to chitin, and g-protein coupled receptor activity (Fig. 4.3C). The output from our network analyses can be found in Data S13.

To validate gene activity, we measured mRNA levels of *JAM1* and *MYC3* in all treatments using LMD-qPCR and found the expression of *JAM1* and *MYC3* was 8.8-fold and 1.8-fold higher in resistant plants compared to their susceptible counterparts respectively (Appendix XII). Both genes were upregulated in susceptible and resistant lines when compared to mock.

4.4.6 Genes associated with growth and development have contrasting expression profiles at the inoculation site of susceptible and resistant plants at 1 dpi

We were also interested in genes at the host pathogen interface that contribute to susceptibility. We discovered a putative regulatory network specific to susceptible plants at 1 dpi associated with development, energy production, and plastid maintenance (Fig. 4.3D). Specifically, four DNA sequence motifs (MYB-like, ZF, CAMTA, GATA) and one CG-1 CAMTA TF were predicted to coordinate bioprocesses associated with the chloroplast, mitochondrial membrane, respiratory chain complex I, polysaccharide metabolism, ribosome biogenesis, and glucose 6-p transport (Fig. 4.3D). In contrast, genes associated with

photosynthesis and primary metabolism were identified in a putative regulatory network downregulated in resistant plants (Appendix XIII). Downregulated DEGs were associated with response to cytokinin, photosynthesis, amino acid biosynthesis, metabolism, and unsaturated fatty acid biosynthesis (Appendix XIII), indicating these processes may be inhibited in resistant plants.

4.4.7 A heightened defense response in resistant hosts coincides with attenuated defense in susceptible cotyledons

We analyzed a complex predictive network active specifically in resistant plants at 3 dpi composed of WRKY, BZIP, bHLH, CAMTA, and heat-shock TFs (Fig. 4.3E). These TFs were predicted to regulate plant immune responses including protein ubiquitination, hypersensitivity, autophagosome, epigenetic regulation, MAP kinase activity, response to ethylene, SA, ABA, and calcium binding. We also identified a putative regulatory network active in all inoculated plants except susceptible plants at 3 dpi suggesting their expression may become attenuated in susceptible cotyledons. This network contains WRKY, heat-shock, DA 1, ABA INSENSITVE GROWTH 1, and CAMTA TFs that putatively regulate genes associated with kinase activity, JA-mediated signaling, PAMP-receptor signaling, and a diverse set of other plant defense responses (Appendix XIII).

4.4.8 Calcium signaling is required for resistance and basal defense against *L. maculans*

Because our network analyses associated resistance with CAMTAs and calcium-related biological functions, we investigated mRNA levels of calcium transporters, signal transducers, and binding proteins (Fig. 4.4A). Homologs of calcium sensors *CAM1*, *CAM5*, *CAM7*, and *CAM-LIKE 40* were 2.15-fold more expressed in resistant plants at 1 dpi. Similarly, calcium transporters (*CYCLIC NUCLETODIE GATED CALCIUM CHANNEL 3, 12, 19*; *CALCIUM*

ATPASE 2, 11) and calcium dependent signal transducers (*CALMODULIN-DOMAIN PROTEIN KINASE 5, 9*; *CALCIUM-DEPENDENT PROTEIN KINASE 6, 28*; and *CALCINEURIN B-LIKE GENE 1*) were an average of 1.41-fold higher in resistant plants at 1 dpi, increasing to 4.15-fold by 3 dpi.

Figure 4

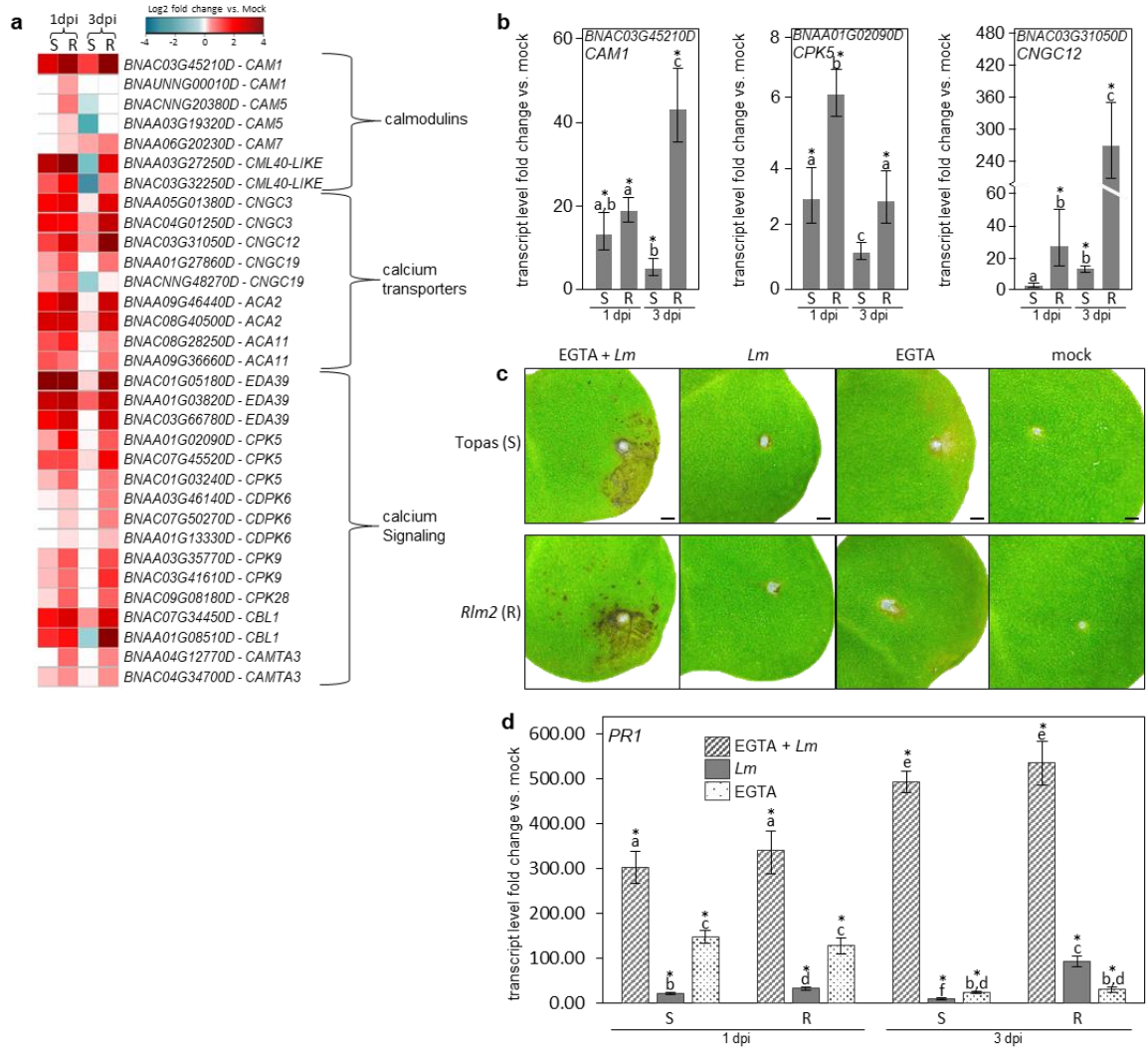

Fig. 4.4: Role of calcium signaling in resistance and inhibition of pathogen establishment. (A) Log2 FPKM fold change of calcium transporters and signal transducers. A more intense red colour denotes upregulation and blue downregulation vs. mock (B) Relative mRNA abundance of select genes from A as measured by qPCR. (C) Treatment of cotyledons with calcium chelator EGTA prior to infection at 3 dpi. EGTA + *Lm* = co-inoculation with calcium chelator and pathogen *L. maculans*; *Lm* = treatment with pathogen alone; EGTA = treatment with chelator alone; mock = inoculation with water. Scale = 1 mm. (D) relative mRNA abundance of *PR1* in

following EGTA application. Significance of qPCR results was determined with a one-way ANOVA ($p < 0.05$) between the different treatments, where significance is indicated by different letters. Significant deviation from mock controls is denoted by an (*), as determined by a Student's t-test ($p < 0.05$).

Previous studies have used the calcium chelator EGTA to explore the role of calcium in bioprocesses such as defense (Hu et al. 2007, Qiao et al. 2015, Lee and Back 2016, Ma et al. 2017). Here, we applied EGTA before inoculation with *L. maculans* to explore how the interaction would occur at a calcium-depleted interface. EGTA alone caused minor chlorosis around the inoculation site at 3 dpi (Fig. 4.4C). EGTA pre-treatment abolished resistance and caused rapid pathogen proliferation in both lines (Fig. 4.4C). By 3 dpi, fungal load was 19.5-fold higher in EGTA-pretreated resistant cotyledons versus *L. maculans* alone, and similar to pretreated susceptible cotyledons (Appendix XIV). Lesions continued to spread aggressively in EGTA-pretreated plants, with complete cotyledon coverage and visible pycnidia by 11 dpi (Appendix XIV).

We used *PR1* mRNA level as an indicator of SA-mediated defense activation in all treatments at 1 and 3 dpi (Fig. 4.4D). Inoculation without EGTA application induced *PR1* gene activity at both time points, with higher expression in resistant lines (1.48-fold higher at 1 dpi, 8.45-fold at 3 dpi). EGTA application without *L. maculans* inoculation transiently activated host defense, with a 149-fold increase *PR1* mRNA level in both treatments at 1 dpi that diminished by 3 dpi that may be related to observed chlorosis. EGTA pre-treatment preceding inoculation with *L. maculans* strongly increased *PR1* accumulation at both time points with no difference between genotypes, indicating SA signaling was not compromised by apoplastic calcium depletion (Fig. 4.4D).

4.4.9 JA production and signaling during *Rlm2*-mediated immunity to *L. maculans*

As hormone signaling is essential for host defense programming, we examined the expression of biosynthetic genes and markers for SA, JA, ET, auxin, and ABA directly at the inoculation site (Fig. 4.5A). Homologs of *ISOCHORISMATE SYNTHASE 1* (*ICS1*), critical to SA production, were an average of 1.6- and 3.1-fold higher in resistant cotyledons at 1 and 3 dpi, respectively, as compared to their susceptible counterpart. *ACC OXIDASE 2* (*ACO2*) and *ACC SYNTHASE 6* (*ACS6*), essential for ET production, were an average of 1.97- and 2.01-fold higher resistant cotyledons at 1 and 3 dpi, respectively. JA biosynthesis genes *ALLENE OXIDE SYNTHASE* (*AOS*) and *ALLENE OXIDE CYCLASE 3* (*AOC3*) had similar expression levels between lines at 1 dpi; however, at 3 dpi they were downregulated specifically in susceptible cotyledons. Additionally, a marker of JA/ET signaling, *PLANT DEFENSIN 1.2* (*PDF1.2*), was 3.2-fold downregulated in susceptible plants, in contrast to a 9.6-fold increase in resistant plants. Together, data indicate a robust JA response at the host pathogen interface at 3 dpi specifically in resistant plants.

Because of the higher expression of JA-related biosynthesis genes and markers in resistant plants, along with the abundance of JA-related TFs within regulatory networks, we measured JA concentration in all treatments (Fig. 4.5B). Interestingly, JA decreased in both susceptible and resistant cotyledons at 1 dpi as compared to mock controls (Fig. 4.5B). At 3 dpi, JA concentrations returned to near control levels in susceptible cotyledons and increased 1.8 times in resistant cotyledons.

Figure 5

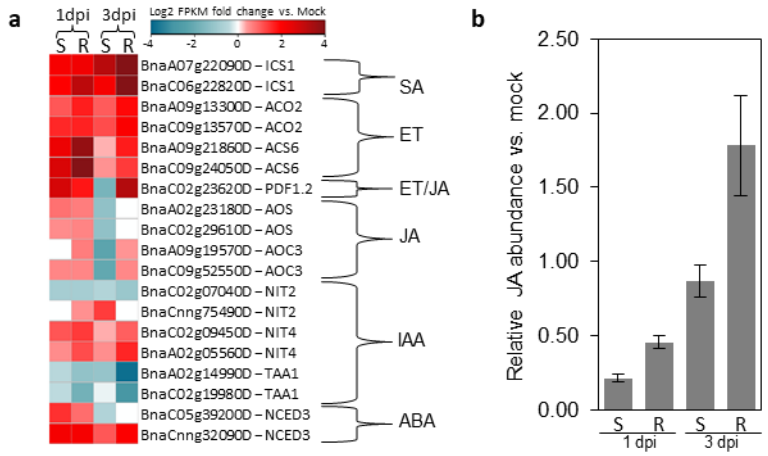

Fig. 4.5: Expression of hormone biosynthesis genes and signaling markers, and JA concentration in cotyledons, in response to *Leptosphaeria maculans*. (A) Log2 FPKM fold change of biosynthetic genes and signaling markers for salicylic acid (SA), ethylene (ET), combined ethylene and jasmonic acid (ET/JA), jasmonic acid (JA), auxin (IAA), and abscisic acid (ABA). (B) Concentration of JA in hand-dissected infection sites, as compared to mock controls. Error bars show standard error.

4.4.10 Pathogen detection and immune signaling is compromised in susceptible plants and maintained in *Rlm2*-mediated immunity

At the host pathogen interface, we identified cohorts of genes expressed specifically in resistant *Rlm2* plants at 3 dpi (Fig. 4.3E) or attenuated in susceptible plants at the same time point (Appendix XIII). These genes coded for core signaling machinery involved in fungal detection and defense elicitation through the receptors *SOBIR1* and *CERK1*. We plotted the mRNA levels of these receptors, along with their co-receptors and the downstream signal transduction machinery (Fig. 4.6A-B). With the exception of *MAPK KINASE 9* (*MKK9*), the entire pathway was more highly expressed in resistant plants at 3 dpi (Fig. 4.6B), although the majority of these genes were upregulated in both lines early (1 dpi) in the infection process. This includes homologs of *SOBIR1* and *CERK1*, along with functional partners *BAK1* and *LYK5*, and signal transducers *MAPK/ERK KINASE KINASE 1* (*MEKK1*), *MKK1*, *2*, *4*, and *MPK3*, *4*, *6* that

were an average of 4.0-fold higher at the host pathogen interface during *Rlm2*-mediated immunity.

Figure 6

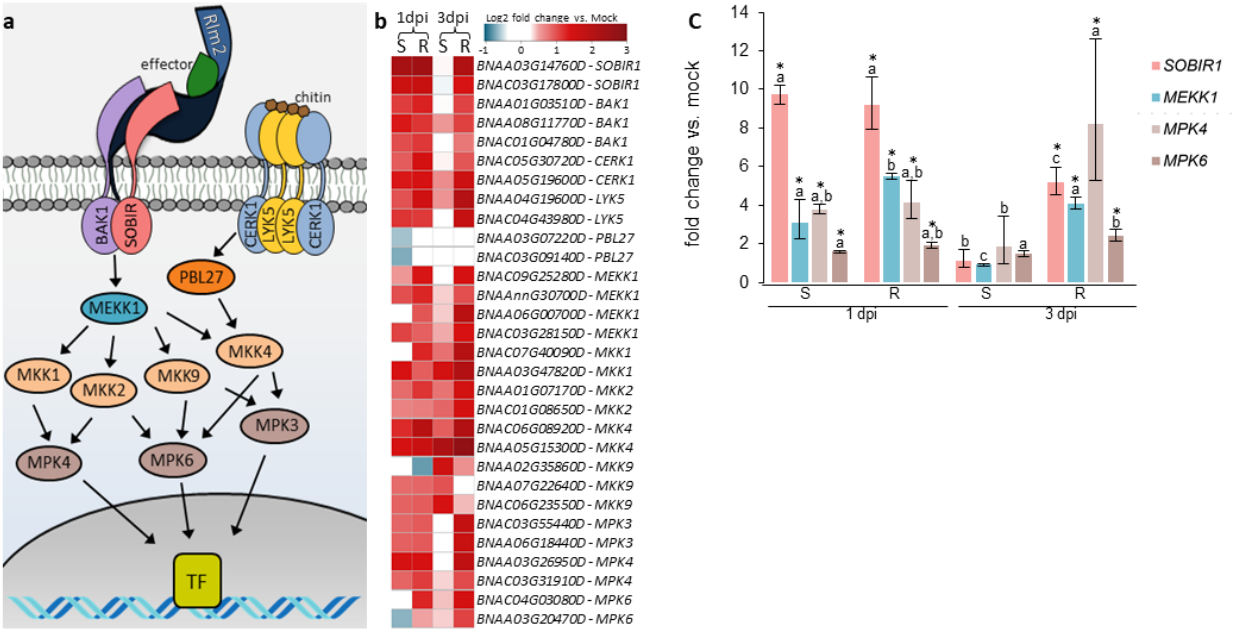

Fig. 4.6: Expression levels of cell-surface receptors and signal transduction machinery responsible for initiating host defense. (A) Partial model of signaling events following activation of cell-surface receptors SOBIR and CERK1. Activation of signal transduction cascades results in regulation of gene transcription. (B) Gene expression changes (Log2 fold change vs. mock) of signaling pathway components as measured by RNA-Seq. Genes associated with surface receptors and MAPK activity are upregulated in resistant hosts, but not susceptible, at 3 days post inoculation. (C) Gene expression of selected genes measured by qPCR. Significance of qPCR results for each target individually was determined with a one-way ANOVA ($p < 0.05$) between treatments, where significance is indicated by different letters. Significant deviation from mock controls is denoted by an (*), as determined by a Student's t-test ($p < 0.05$).

We then used targeted transcript profiling to measure mRNA abundance of *SOBIR1*, *MAPK/ERK KINASE KINASE 1* (*MEKK1*), *MPK4*, and *MPK6* directly at the inoculation site (Fig. 4.6C). At 1 dpi, all targets were upregulated during infection and showed similar expression profiles between genotypes (Fig. 4.6C). At 3 dpi, data show no difference between susceptible interactions and mock controls; however, all genes were significantly upregulated in resistant plants with mRNA levels 2.4- to 8.2-fold those observed in mock treatments (Fig. 4.6C).

4.5 Discussion:

We profiled *B. napus* and *L. maculans* gene activity directly at the host pathogen interface to better understand *Rlm2*-mediated immunity. A major challenge in dual transcriptome analysis of this pathosystem is overcoming low pathogen abundance at early infection stages. At 3 dpi, *L. maculans* mapping rates of <0.5% are commonly recorded, with researchers performing analyses with <1x coverage at these early disease stages (Haddadi et al. 2016, Sonah et al. 2016). Here, LMD markedly increased sensitivity with achieved *L. maculans* mapping rates up to 5.7% at 1 dpi and 14.5% at 3 dpi thus providing the necessary resolution to confidently monitor *L. maculans* gene activity during establishment on *B. napus* cotyledons.

Approximately 11.9% of the *L. maculans* genome responded during the first three days of infection, with major differences observed based on host genotype. Putative starch hydrolyzing CBMs, glucoside hydrolases, peptidases, and ribonucleases were strongly upregulated during infection of susceptible plants, suggesting *L. maculans* may be capable of mobilizing and utilizing host resources during establishment in susceptible cotyledons. The activation of bioprocesses related to plastid maintenance and photosynthesis in susceptible cotyledons at 24 hours post-inoculation may explain the elevated expression of *L. maculans* digestive enzymes in this line. In immune *Rlm2* cotyledons these photosynthetic processes are downregulated along with primary production and cytokinin responses, perhaps to restrict nutrient production that would support *L. maculans* progression into host tissues.

We observed rapid and widespread activation of calcium, JA, and ABA signaling during incompatible interactions directly at the host pathogen interface that is associated with the activity of bHLH, CAMTA, and BZIP TFs, including *CAMTA3*, *CAMTA5*, *BZIP1*, and *ABF3*. In Arabidopsis, CAMTA3 and CAMTA5 transcriptionally activate genes associated with ABA

signaling including the master regulator *DREB1* (Kidokoro et al. 2017). Our network analysis predicts BZIP1 and ABF3 coordinate with these CAMTAs to regulate immune responses in incompatible *B. napus* cotyledons. In Arabidopsis, *BZIP1* is transcriptionally activated by calcium signaling cascades and initiates ABA-mediated changes to glucose and amino acid metabolism (Hartmann et al. 2015) and ABF3 stimulates ABA-mediated chlorophyll degradation (Gao et al. 2016). Further, we predict MYC3 and JAM1, along with uncharacterized bHLHs, regulate genes canonically associated with wounding, heat-shock, salinity, and plasma membrane signaling in resistant (*Rlm2*) plants. In Arabidopsis, MYC3 is a positive regulator of JA (Cheng et al. 2011) and JAM1 a modulator of JA signaling (Sasaki-Sekimoto et al. 2013) that coordinate JA defense responses. The important role of bHLH TFs in RLP-SOBIR1 immunity is also supported by the recent discovery that bHLH TFs can be directly activated by SOBIR1 in cotton (Zhou et al. 2018). Together, this provides a putative regulatory framework activated during *Rlm2*-mediated immunity that reprograms cells to respond to the hemibiotrophic pathogen. As little information is available regarding transcriptional control of *B. napus* immunity, the uncharacterized BZIP and bHLH TFs identified through our analyses serve as targets for future functional studies.

Marked distinctions in the expression of JA biosynthesis genes and markers like *PDF1.2* suggest JA is repressed in susceptible cotyledons and is consistent with reports showing repression of JA markers during compatible *L. maculans – B. napus* interactions (Lowe et al. 2014, Becker et al. 2017b), despite endogenous JA levels never being assayed. Here, we confirm this important signaling hormone is present at lower concentrations in susceptible cotyledons as compared to *Rlm2* plants. JA signaling plays a central role in defense against necrotrophs by limiting cell death (Rossi et al. 2011) and favouring accumulation of antifungal compounds

(Antico et al. 2012). As *L. maculans* has been described as a primarily necrotrophic (Staal and Dixelius 2008) an effective response to the pathogen would likely involve extensive JA signaling. Accordingly, our data suggest *Rlm2*-mediated immune signaling at the inoculation site triggers production of JA that can modify gene expression before the necrotrophic transition of *L. maculans*. The ability of JA to antagonize cell death provides an explanation for the delayed onset of cell death commonly observed in *B. napus* cotyledons during the incompatible response to *L. maculans* (Stotz et al. 2014).

When the calcium chelator EGTA was applied to the inoculation site *Rlm2*-mediated immunity was abolished, and infection progressed rapidly in both lines suggesting calcium signaling is required to initiate resistance. The ability of EGTA to compromise calcium signaling during defense has been demonstrated previously. Pre-treatment of wheat leaves with EGTA prevented NO production and delayed the peak hypersensitive response to *Puccinia triticina* by 24 hours (Qiao et al. 2015), and also increased *Tobacco Mosaic Virus* load in Arabidopsis leaves by obstructing systemic acquired resistance and preventing *PR1* accumulation (Zhao et al. 2018). In our study accumulation of *PR1* suggests SA signaling was not compromised by EGTA treatment and occurs upstream or independent of calcium influx. Additionally, as calcium deficiency in cotyledons initiates abiotic stress responses (Simon 1978), SA production was likely stimulated by calcium chelation in combination with *L. maculans* inoculation. This runaway SA production may have induced cell death and contributed to observed susceptibility. Although EGTA was applied locally at the inoculation site, and its effect is transient, *L. maculans* colonized the entire cotyledon despite the presence of *Rlm2*. This suggests early signaling events that prevent fungal establishment are likely critical for determining host fate.

Gene regulatory network analyses identified a robust defense response in *Rlm2* cotyledons at 3 dpi uncovering a large gene set with attenuated expression at the inoculation site in susceptible cotyledons. Further investigation revealed these attenuated genes were largely involved in pathogen detection and MAPK signaling. This pathway is largely responsible for hormone balance and provides a plausible explanation for the observed repression of JA responses in susceptible plants. For example, MPK4 knockout plants constitutively activate SA-dependent defenses and have severely diminished JA signaling (Brodersen et al. 2006), and interference with MPK4 and MPK6 signaling decreases *PDF1.2* accumulation and causes hyper-susceptibility to *B. cinerea* (Schweighofer et al. 2007). Similarly, *BAK1* silencing reduces JA accumulation in response to herbivory in tobacco (Yang et al. 2011), and *mekk1*, *mkk1/mkk2*, and *mpk4* Arabidopsis have severe dwarfism caused by constitutive SA signaling and compromised JA signaling (Pitzschke et al. 2009). Activity of *Rlm2* and other *R*-genes likely protects the integrity of this MAPK signaling pathway, allowing the host to maintain normal JA signaling and respond appropriately.

Attenuation of defense signaling coincides with a sharp increase in *L. maculans* effector expression at 3 dpi that likely contributes to repression of immune signaling described above. Other pathogen effectors are known to target features of this signaling cascade including SOBIR1 (Wu et al. 2018), BAK1 (Zhou et al. 2014), CERK1 (Yamaguchi et al. 2013), and MAPK signaling (King et al. 2014, Zhang et al. 2017, Teper et al. 2018). This is consistent with the recent identification of MAPK9 as a target of *L. maculans* effector AvrLm1 (Ma et al., 2018). The ability of pathogens to interfere with defense signaling and stimulate nutrient production is not a new phenomenon. For example, *B. cinerea* knocks down host MAPK expression in tomato (Weiberg et al. 2014) and stimulates photosynthesis in tissues directly adjacent to inoculation

sites (Berger et al. 2004). This is the first time, however, that widespread gene expression attenuation has been described in the *B. napus – L. maculans* pathosystem. As these shifts in gene expression were not observed in previous RNA-Seq studies (Haddadi et al. 2016, Becker et al. 2017b) it suggests interference with plant signaling occurs primarily in cells at the host pathogen interface during establishment. This highlights the utility of LMD for capturing fine-scale interactions that occur primarily in cells directly interacting with pathogen.

Rlm2-mediated immunity may fortify defense and protect signaling pathways from pathogen interference through the production of calcium signals, such as those initiated through the *CPKs*/*CDPKs* upregulated in our dataset. For example, CPK5 stimulates hormone production in response to fungi (Gravino et al. 2015) and phosphorylates RBOHD to produce ROS (Dubiella et al. 2013). Additionally, core calcium sensors upregulated in resistant plants activate strong defensive cues; CAM1 increases nitric oxide (Choi et al. 2009, Zhou et al. 2016) and ROS (Choi et al. 2009) production, which is amplified in the presence of CBL1 (Drerup et al. 2013). Thus, calcium signaling likely works in concert with Rlm2/SOBIR1-mediated signaling to direct and amplify the immune response.

While the gene-for-gene resistance model has guided research on plant pathogen interactions in the past, it is becoming clear that plant immunity steps beyond a single gene and is orchestrated by diverse sets of receptors and downstream regulators. Currently, blackleg disease is primarily controlled through the effective application of *R*-genes that operate through yet to be uncovered mechanisms. In this manuscript, we described the earliest changes to gene expression that reprogram cells following *Rlm2* recognition of *L. maculans*. Understanding the processes that enable immunity in *B. napus* will provide the necessary information to tailor plant defense against biotic stress. Further, it is still unclear if all *R*-genes effective against *L.*

maculans converge on similar immune pathways to prevent pathogen attack or through distinct gene regulator networks. Answering this question may provide a ‘silver bullet’ to control this pathogen and help direct future research for crop improvement.

5 General Discussion and Future Directions

5.1 Overview

This work provides a detailed analysis of *B. napus* ETD across multiple stages of the *B. napus – L. maculans* interaction. We describe important differences in signaling between incompatible and compatible host-pathogen interactions related to calcium, plant phytohormones, biosynthesis of secondary metabolites, and transcriptional regulation. Importantly, this analysis has identified targets for ongoing functional characterization, including uncharacterized receptors and TFs that act as positive regulators of resistance. I have clearly shown that when several of these regulators are disrupted in the model plant Arabidopsis, non-host resistance to *L. maculans* is compromised. This suggests these regulators may be functionally conserved across plant species and have implications that span beyond the *B. napus*-*L. maculans* pathosystem. Future work investigating the mechanisms by which these genes contribute to plant resistance is ongoing. In this chapter I describe the possible next steps and future directions to improve our understanding of the *B. napus – L. maculans* pathosystem, and more broadly, plant defense mechanisms.

5.2 Comparison between *LepR1* and *Rlm2 R*-gene interactions:

In my thesis, I investigated *R*-gene interactions for both *LepR1* and *Rlm2* using either whole leaf- or LMD-RNA Seq analyses. While I observed several conserved features characteristic of plant defense in all lines, I also noted some differences at the RNA level observed only in resistant hosts. For example, resistant hosts appeared to have a stronger initial response to *L. maculans* with a greater number of genes differentially expressed at 1 and 3 dpi.

Data analysis suggests recognition of the pathogen through R proteins LepR1 or Rlm2 produces a strong cellular signal that transcriptionally activates thousands of genes.

Further, in both of our datasets ETD against *L. maculans* was associated with robust JA biosynthesis and signaling, which is consistent with ETD in other systems (Zuluaga et al. 2016). It would be of interest to explore how induction of JA signaling in susceptible hosts would affect disease severity. This could be accomplished through the application of exogenous JA at early disease stages, or by challenging mutants with *L. maculans* that display constitutive JA signaling, such as *cev1* (Ellis 2001). Understanding the appropriate hormone balance that coordinates *B. napus* ETD against *L. maculans* will be essential for our understanding of this pathosystem. This is important as we continue to develop efficient gene editing technologies, such as CRISPR, that make programming plant resistance possible and rely on an in-depth understanding of the host immune response.

5.3 Research Impact:

Plant resistance is a complex and nuanced process that involves dense layers of immune signaling to calibrate an appropriate response to a pathogen. Understanding the mechanisms involved is of significant interest to plant pathologists and has direct implications in food security. Specifically, this research focused on the plant immune response downstream of blackleg R protein activation and resolved missing links between detection of *L. maculans* and its elimination by the host. As our analyses only investigated two *R*-genes (*LepR1, Rlm2*) we cannot definitively conclude if all known *R*-genes offering protection against *L. maculans* operate through similar mechanisms. Future experiments elucidating the plant immune responses

activated by other *R*-genes may provide the information necessary to introduce robust resistance against *L. maculans* in *B. napus*.

My research has produced resources that will be of value to the scientific community. This includes large datasets that have been all been made publicly available. The utilization of my data into larger metanalyses should provide valuable information for plant pathologists studying ETD or general plant defense.

Plants coordinate complex biological processes such as plant defense by fine tuning gene expression through TF activity. Performing analyses outside of model systems can be challenging. In this thesis I introduced a new tool, SeqEnrich, for prediction of TF regulatory networks in the model Arabidopsis, and the important agricultural crop canola. We chose an open-source journal for publication to ensure the largest number of researchers would have access to the program. SeqEnrich was recently referenced by Dr. Nicolas Provart in a Report of the MASC Subcommittee demonstrating its establishment in the scientific community (Dijk and Velmurugan 2018). SeqEnrich is continuing to be updated as more genomic data becomes available, which includes support for additional plant species. Recently, we have adapted the program to support gene sets from maize. Additionally, using probability matrices instead of nucleotide strings in future SeqEnrich versions may improve sensitivity. This would adjust for the fact that TFs have variable affinities for different potential binding sites (Bailey et al. 2009).

TFs rarely function as a monomer *in vivo* and will generally modify transcription as a homodimer or heterodimer. SeqEnrich provides an efficient means to mine existing datasets to identify putative TF heterodimers that regulate transcription. By combining available information on protein-protein interactions with SeqEnrich analysis of co-expressed gene sets,

we can postulate what TFs work in combination to regulate important bioprocesses. This data will inform functional experiments investigating the cellular targets of these TFs.

My LMD transcriptome analysis used SeqEnrich to investigate cellular reprogramming at the earliest infection stages and identified *B. napus* TFs that may contribute to *L. maculans* resistance. Most of these TFs are uncharacterized in *B. napus*, and many have unknown functions in Arabidopsis. Like the screen performed following our first transcriptome analysis, testing corresponding mutants for susceptibility seems like a logical next step for these putative defense regulators. Further, if investigation identifies TFs with functional roles in defense, future experiments may include Chromatin-Immunoprecipitation (ChIP) sequencing that can positively identify TF binding sites (Aparicio et al. 2004, Yu et al. 2016).

5.4 Introduction of *PAD3* into *B. napus*:

Brassica napus lacks the ability to produce the phytoalexin camalexin, toxic to *L. maculans* in vitro (Pedras et al. 1998). In addition, Arabidopsis mutants deficient in camalexin production also have compromised resistance against *L. maculans* (Bohman et al. 2004). During our whole-cotyledon transcriptome investigation, we were able to track the expression for the entire camalexin biosynthetic pathway in *B. napus* except for the biosynthetic gene *PAD3*. Upon further investigation, no *PAD3* homologs were identified in the *B. napus* genome. Therefore, it seemed logical to transfer *PAD3* into *B. napus* to enable camalexin production. Despite our best efforts, we were unable to recover viable *B. napus* transformants overexpressing *AtPAD3*. In Arabidopsis, camalexin must be transported out of the cell through the exporter ABCG34 to prevent self-toxicity (Khare et al. 2017); however, no expressed *B. napus ABCG34* homologs were detected in our dataset. Therefore, future experiments should co-transform plants with

Arabidopsis *ABCG34*, or drive expression with native or inducible promoters to prevent accumulation of toxic camalexin within the cell. By doing so, it is possible that *B. napus* camalexin production could provide reasonable defense against *L. maculans* as is already observed in Arabidopsis.

5.5 Cloning of the putative immune receptor *AT4G18250*:

The uncharacterized gene, *AT4G18250*, was identified in our whole cotyledon transcriptome analysis and codes for a 686 amino acid putative transmembrane receptor-like protein kinase (RLK) with multiple pathogenesis-related domains. Alignments between AT4G18250 and known receptors reveal the highest similarity to a leaf rust disease resistance locus (Feuillet et al. 2003). Although our data indicate that *AT4G18250* may code for a R protein effective against *L. maculans*, little is known about its role in the immune response and certainly nothing about putative interacting partners in the presence or absence of fungal or bacterial effectors. Functional characterization of this receptor and its role in plant immunity should provide additional evidence into the molecular mechanisms underpinning plant host resistance against *L. maculans*.

During the last year of my PhD I cloned *AT4G18250* into plant expression vectors. This included generation of CaMV overexpression lines in Arabidopsis and *B. napus*, Arabidopsis complementation lines, and translational fusions with green fluorescent protein (GFP) to investigate cellular localization. Data show over a 93% reduction in mRNA levels in SALK T-DNA *at4g18250* mutants. In complementation assays using overexpression lines, data show a 3.01-fold increase in *AT4G18250* mRNA levels (Fig. 5.1).

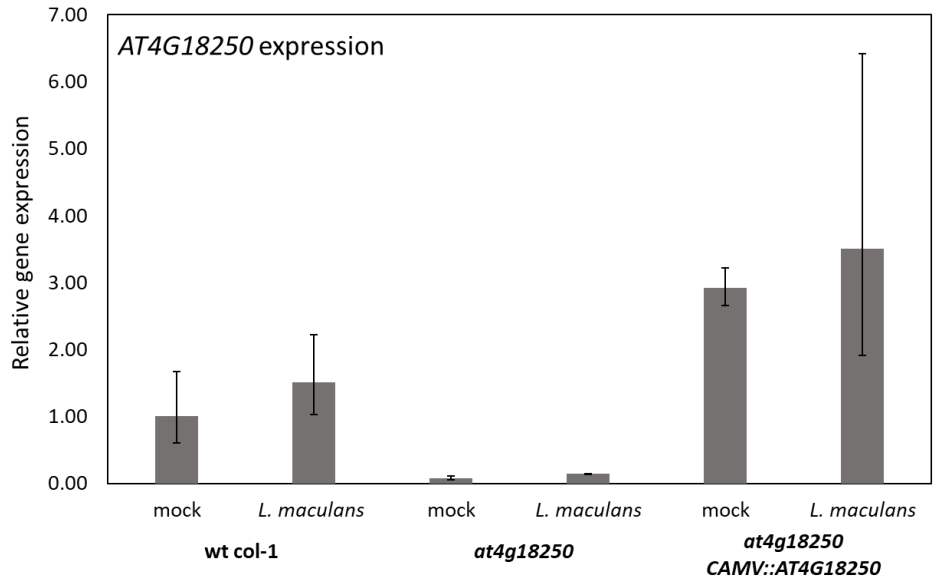

Fig. 5.1: Arabidopsis *AT4G18250* expression in SALK T-DNA insertion knockdown and complementation lines as measured with qPCR. In both mock and *L. maculans*-infected Arabidopsis, gene expression levels of *AT4G18250* were measured with qPCR.

Understanding timing of *AT4G18250* expression and localization within the cell should help elucidate its role in defense against fungal pathogens. Since we already have GFP overexpression lines, AT4G18250 and its associated partner proteins can be targeted using an anti-GFP antibody and interacting proteins identified through mass spectrometry (MS). With this strategy, we can elucidate signaling components that interact with AT4G18250 to coordinate immune signaling. In addition, RNA-Seq can be performed on *AT4G18250* knockout and overexpression lines to help identify downstream bioprocesses regulated by AT4G18250.

Taken together, AT4G18250 has the potential to provide a new source of resistance in *B. napus* that is effective against the devastating fungal pathogen *L. maculans.* Should this research progress, a logical next step would be to test *AT4G18250* overexpression lines in greenhouse trials and, if successful, testing in the field. Finally, this body of work clearly illustrates the progression of exploratory or discovery research that has the potential for translational applications to positively impact crop production on the Canadian prairies and beyond.

6 Literature Cited

Al-Daoud, F., Moran, M., Gossen, B., and Mcdonald, M.R. 2018. First report of clubroot (*Plasmodiophora brassicae*) on canola in Ontario. Can. J. Plant Pathol. **40**(1): 96–99.

Albert, I., Böhm, H., Albert, M., Feiler, C.E., Imkampe, J., Wallmeroth, N., Brancato, C., Raaymakers, T.M., Oome, S., Zhang, H., Krol, E., Grefen, C., Gust, A.A., Chai, J., Hedrich, R., Den, G. Van, and Nürnberger, T. 2015. An RLP23–SOBIR1–BAK1 complex mediates NLP-triggered immunity. Nat. Plants **1**(10): 1–9. Nature Publishing Group. doi:10.1038/nplants.2015.140.

Altschul, S.F.S.F., Gish, W., Miller, W., Myers, E.E.W.W.E.W., and Lipman, D.J.J. 1990. Basic local alignment search tool. *In* Journal of Molecular Biology **215**: 403–410. doi:10.1016/S0022-2836(05)80360-2.

Anders, S., Pyl, P.T., and Huber, W. 2015. HTSeq-A Python framework to work with high-throughput sequencing data. Bioinformatics **31**(2): 166–169. doi:10.1093/bioinformatics/btu638.

Ansan-Melayah, D. 1997. Phoma du colza: Des résistances spécifiques exploitables chez le colza. Phytoma-La Défense des végétaux **490**: 26–29.

Antico, C.J., Colon, C., Banks, T., and Ramonell, K.M. 2012. Insights into the role of jasmonic acid-mediated defenses against necrotrophic and biotrophic fungal pathogens. Front. Biol. (Beijing). **7**(1): 48–56. doi:10.1007/s11515-011-1171-1.

Aparicio, O., Geisberg, J. V., and Struhl, K. 2004. Chromatin Immunoprecipitation for Determining the Association of Proteins with Specific Genomic Sequences In Vivo. Curr. Protoc. Cell Biol **17**(7): 1–23. doi:10.1002/0471143030.cb1707s23.

Aubertot, J.-N., Salam, M.U., Diggle, A.J., Dakowska, S., and Jedryczka, M. 2006. SimMat, a new dynamic module of Blackleg Sporacle for the prediction of pseudothecial maturation of *L. maculans*/*L. biglobosa* species complex. Parameterisation and evaluation under Polish conditions. *In* Integrated Control in Oilseed Crops. pp. 277–285.

Austin, R.S., Hiu, S., Waese, J., Ierullo, M., Pasha, A., Wang, T.T., Fan, J., Foong, C., Breit, R., Desveaux, D., Moses, A., and Provart, N.J. 2016. New BAR tools for mining expression data and exploring Cis-elements in Arabidopsis thaliana. Plant J. **88**(3): 490–504. doi:10.1111/tpj.13261.

Axtell, M.J., and Staskawicz, B.J. 2003. Initiation of RPS2-specified disease resistance in Arabidopsis is coupled to the AvrRpt2-directed elimination of RIN4. Cell **112**(3): 369–377. doi:10.1016/S0092-8674(03)00036-9.

Babur, O., Dogrusoz, U., Cakır, M., Aksoy, B.A., Schultz, N., Sander, C., and Demir, E. 2014. Integrating biological pathways and genomic profiles with ChiBE 2. BMC Genomics **15**: 642. doi:10.1186/1471-2164-15-642.

Bahar, M.H., Wist, T.J., Bekkaoui, D.R., Hegedus, D.D., and Olivier, C.Y. 2018. Aster leafhopper survival and reproduction, and Aster yellows transmission under static and fluctuating temperatures, using ddPCR for phytoplasma quantification. Sci. Rep. **8**(1): 1–9. doi:10.1038/s41598-017-18437-0.

Bailey, T.L., Boden, M., Buske, F.A., Frith, M., Grant, C.E., Clementi, L., Ren, J., Li, W.W., and Noble, W.S. 2009. MEME Suite: Tools for motif discovery and searching. Nucleic Acids Res. **37**(S2): 202–208. doi:10.1093/nar/gkp335.

Baird, R.E., Philips, D. V, Mullinix, B.G., Alt, P.J., Baird, R.E., Phillips, D. V, Mullinix, B.G., and Alt, P.J. 2018. Relative longevity of *Leptosphaeria maculans* and associated mycobiota on canola débris. **80**: 1–11. doi:10.7202/706176ar.

Balestrini, R., Gómez-Ariza, J., Lanfranco, L., and Bonfante, P. 2007. Laser microdissection reveals that transcripts for five plant and one fungal phosphate transporter genes are contemporaneously present in arbusculated cells. Mol. Plant. Microbe. Interact. **20**(9): 1055–62. doi:10.1094/MPMI-20-9-1055.

Bargmann, B.O.R., and Birnbaum, K.D. 2010. Fluorescence Activated Cell Sorting of Plant Protoplasts. J. Vis. Exp. **36**(1): 2–5. doi:10.3791/1673.

Becker, M.G., Walker, P.L., Pulgar-Vidal, N.C., and Belmonte, M.F. 2017a. SeqEnrich: A tool to predict transcription factor networks from co-expressed Arabidopsis and *Brassica napus* gene sets. PLoS One **12**(6): 1–13. doi:10.1371/journal.pone.0178256.

Becker, M.G., Zhang, X., Walker, P.L., Wan, J.C., Millar, J.L., Khan, D., Granger, M.J., Cavers, J.D., Chan, A.C., Fernando, D.W., and Belmonte, M.F. 2017b. Transcriptome analysis of the *Brassica napus - Leptosphaeria maculans* pathosystem identifies receptor, signalling and structural genes underlying plant resistance. Plant J. **90**(3): 573–586. doi:10.1111/tpj.13514.

Belmonte, M.F., Kirkbride, R.C., Stone, S.L., Pelletier, J.M., Bui, A.Q., Yeung, E.C., Hashimoto, M., Fei, J., Harada, C.M., Munoz, M.D., Le, B.H., Drews, G.N., Brady, S.M., Goldberg, R.B., and Harada, J.J. 2013a. Comprehensive developmental profiles of gene activity in regions and subregions of the Arabidopsis seed. Proc. Natl. Acad. Sci. U. S. A. **110**(5): E435-44. doi:1222061110

Belmonte, M.F., Kirkbride, R.C., Stone, S.L., Pelletier, J.M., Bui, a. Q., Yeung, E.C., Hashimoto, M., Fei, J., Harada, C.M., Munoz, M.D., Le, B.H., Drews, G.N., Brady, S.M., Goldberg, R.B., and Harada, J.J. 2013b. Comprehensive developmental profiles of gene activity in regions and subregions of the Arabidopsis seed. Proc. Natl. Acad. Sci. **110**(5): E435–E444. doi:10.1073/pnas.1222061110.

Berger, S., Papadopoulos, M., Schreiber, U., Kaiser, W., and Roitsch, T. 2004. Complex regulation of gene expression, photosynthesis and sugar levels by pathogen infection in tomato. Physiol. Plant. **122**(4): 419–428. Wiley/Blackwell (10.1111). doi:10.1111/j.1399-3054.2004.00433.x.

Bhandari, S.R., Jo, J.S., and Lee, J.G. 2015. Comparison of glucosinolate profiles in different tissues of nine brassica crops. Molecules **20**(9): 15827–15841. doi:10.3390/molecules200915827.

Bigeard, J., Colcombet, J., and Hirt, H. 2015. Signaling mechanisms in pattern-triggered immunity (PTI). Mol. Plant **8**(4): 521–539. Elsevier Ltd. doi:10.1016/j.molp.2014.12.022.

Blatti, C., and Sinha, S. 2014. Motif enrichment tool. Nucleic Acids Res. **42**(W1): 1–6. doi:10.1093/nar/gku456.

Bohman, S., Staal, J., Thomma, B.P.H.J., Wang, M., and Dixelius, C. 2004. Characterisation of an Arabidopsis-*Leptosphaeria maculans* pathosystem: Resistance partially requires camalexin biosynthesis and is independent of salicylic acid, ethylene and jasmonic acid signalling. Plant J. **37**(1): 9–20. doi:10.1046/j.1365-313X.2003.01927.x.

Bolger, A.M., Lohse, M., and Usadel, B. 2014. Trimmomatic: A flexible trimmer for Illumina sequence data. Bioinformatics **30**(15): 2114–2120. doi:10.1093/bioinformatics/btu170.

Borhan, M.H., Holub, E.B., Kindrachuk, C., Omidi, M., Bozorgmanesh-frad, G., and Rimmer, S.R. 2010. WRR4, a broad-spectrum TIR-NB-LRR gene from Arabidopsis thaliana that confers white rust resistance in transgenic oilseed brassica crops: Short communication. Mol. Plant Pathol. **11**(2): 283–291. doi:10.1111/j.1364-3703.2009.00599.x.

Boudsocq, M., Willmann, M.R., McCormack, M., Lee, H., Shan, L., He, P., Bush, J., Cheng, S.-H., and Sheen, J. 2010. Differential innate immune signalling via Ca(2+) sensor protein kinases. Nature **464**(7287): 418–22. NIH Public Access. doi:10.1038/nature08794.

Bousset, L., Ermel, M., and Lebreton, L. 2018. The full life cycle of Leptosphaeria maculans completed on inoculated oilseed rape incubated under controlled conditions. Plant Pathol. **67**(6): 1321–1328.

Boys, E.F., Roques, S.E., Ashby, A.M., Evans, N., Latunde-Dada, A.O., Thomas, J.E., West, J.S., and Fitt, B.D.L.L. 2007. Resistance to infection by stealth: *Brassica napus* (winter oilseed rape) and *Pyrenopeziza brassicae* (light leaf spot). Eur. J. Plant Pathol. **118**(4): 307–321. doi:10.1007/s10658-007-9141-9.

Brodersen, P., Petersen, M., Bjørn Nielsen, H., Zhu, S., Newman, M.-A., Shokat, K.M., Rietz, S., Parker, J., and Mundy, J. 2006. Arabidopsis MAP kinase 4 regulates salicylic acid- and jasmonic acid/ethylene-dependent responses via EDS1 and PAD4. Plant J. **47**(4): 532–546. Wiley/Blackwell (10.1111). doi:10.1111/j.1365-313X.2006.02806.x.

Bu, Q., Jiang, H., Li, C.B., Zhai, Q., Zhang, J., Wu, X., Sun, J., Xie, Q., and Li, C. 2008. Role of the Arabidopsis thaliana NAC transcription factors ANAC019 and ANAC055 in regulating jasmonic acid-signaled defense responses. Cell Res. **18**(7): 756–767. doi:10.1038/cr.2008.53.

Bumee, S., Ingkasuwan, P., Kalapanulak, S., Meechai, A., Cheevadhanarak, S., and Saithong, T. 2013. Transcriptional regulatory network of Arabidopsis starch metabolism under extensive light condition: A potential model of transcription-modulated starch metabolism in roots of starchy crops. Procedia Comput. Sci. **23**: 113–121. Elsevier Masson SAS. doi:10.1016/j.procs.2013.10.015.

Cai, X., Huang, Y., and Jiang, D. 2018. Evaluation of oilseed rape seed yield losses caused by *Leptosphaeria biglobosa* in central China. **150**: 179–190. European Journal of Plant Pathology. doi:10.1007/s10658-017-1266-x.

Canadian Plant Disease Survey, 2017. Available from http://phytopath.ca/publication/cpds/. Accessed on August 17, 2018.

Carter, A.D., Bonyadi, R., and Gifford, M.L. 2013. The use of fluorescence-activated cell sorting in studying plant development and environmental responses. Int. J. Dev. Biol. **57**(6–8): 545–552. doi:10.1387/ijdb.130195mg.

Cartharius, K., Frech, K., Grote, K., Klocke, B., Haltmeier, M., Klingenhoff, A., Frisch, M., Bayerlein, M., and Werner, T. 2005. MatInspector and beyond: Promoter analysis based on transcription factor binding sites. Bioinformatics **21**(13): 2933–2942. doi:10.1093/bioinformatics/bti473.

Catanzariti, A.M., Do, H.T.T.T., Bru, P., Sain, M. De, Thatcher, L.F., Rep, M., de Sain, M., Thatcher, L.F., Rep, M., and Jones, D.A. 2017. The tomato I gene for Fusarium wilt resistance encodes an atypical leucine-rich repeat receptor-like protein whose function is nevertheless dependent on SOBIR1 and SERK3/BAK1. Plant J. **89**(6): 1195–1209. doi:10.1111/tpj.13458.

Cawly, J., Cole, A.B., Király, L., Qiu, W., and Schoelz, J.E. 2005. The plant gene CCD1 selectively blocks cell death during the hypersensitive response to Cauliflower mosaic virus infection. Mol. Plant. Microbe. Interact. **18**(3): 212–9. doi:10.1094/MPMI-18-0212.

Chalhoub, B., Denoeud, F., Liu, S., Parkin, I., et al. 2014. Early allopolyploid evolution in the post-Neolithic *Brassica napus* oilseed genome. Science **345**(6199): 950–953. doi:10.1126/science.1253435.

Chan, A., and Belmonte, M. 2013. Histological and ultrastructural changes in canola (*Brassica napus*) funicular anatomy during the seed lifecycle. Botany **91**(8): 671–679. doi:10.1139/cjb-2013-0141.

Chan, A.C., Khan, D., Girard, I.J., Becker, M.G., Millar, J.L., Sytnik, D., and Belmonte, M.F. 2016. Tissue-specific laser microdissection of the *Brassica napus* funiculus improves gene discovery and spatial identification of biological processes. J. Exp. Bot. **67**(11): erw179. doi:10.1093/jxb/erw179.

Chandran, D., Inada, N., Hather, G., Kleindt, C.K., and Wildermuth, M.C. 2010. Laser microdissection of Arabidopsis cells at the powdery mildew infection site reveals site-specific processes and regulators. Proc. Natl. Acad. Sci. U. S. A. **107**(1): 460–5. doi:10.1073/pnas.0912492107.

Chen, J., Tan, R., Guo, X., Fu, Z., Wang, Z., Zhang, Z.-Y., and Tan, X.-L. 2015. Transcriptome Analysis Comparison of Lipid Biosynthesis in the Leaves and Developing Seeds of *Brassica napus*. PLoS One **10**(5): e0126250. doi:10.1371/journal.pone.0126250.

Cheng, C.Y., Krishnakumar, V., Chan, A.P., Thibaud-Nissen, F., Schobel, S., and Town, C.D. 2017. Araport11: a complete reannotation of the Arabidopsis thaliana reference genome. Plant J. **89**(4): 789–804. doi:10.1111/tpj.13415.

Cheng, Z., Sun, L., Qi, T., Zhang, B., Peng, W., Liu, Y., and Xie, D. 2011. The bHLH transcription factor MYC3 interacts with the jasmonate ZIM-domain proteins to mediate jasmonate response in arabidopsis. Mol. Plant **4**(2): 279–288. doi:10.1093/mp/ssq073.

Chien, C.H., Chiang-Hsieh, Y.F., Chen, Y.A., Chow, C.N., Wu, N.Y., Hou, P.F., and Chang, W.C. 2015. AtmiRNET: A web-based resource for reconstructing regulatory networks of Arabidopsis microRNAs. Database **2015**(7): 1–11. doi:10.1093/database/bav042.

Choi, H.W., Lee, D.H., and Hwang, B.K. 2009. The pepper calmodulin gene CaCaM1 is involved in reactive oxygen species and nitric oxide generation required for cell death and the defense response. Mol. Plant. Microbe. Interact. **22**(11): 1389–400. The American Phytopathological Society . doi:10.1094/MPMI-22-11-1389.

Chow, C.N., Zheng, H.Q., Wu, N.Y., Chien, C.H., Huang, H. Da, Lee, T.Y., Chiang-Hsieh, Y.F., Hou, P.F., Yang, T.Y., and Chang, W.C. 2016. PlantPAN 2.0: An update of Plant Promoter Analysis Navigator for reconstructing transcriptional regulatory networks in plants. Nucleic Acids Res. **44**(1): D1154–D1164. doi:10.1093/nar/gkv1035.

Clay, N.K., Adio, A.M., Denoux, C., Jander, G., and Frederick, M. 2009. Glucosinolate Metabolites Required for an Arabidopsis Innate Immune Response. Science **323**(5910): 95–101. doi:10.1126/science.1164627.

Von Cruz, M. V., and Dierig, D.A. 2015. Industrial crops: Breeding for bioenergy and bioproducts. Ind. Crop. Breed. Bioenergy Bioprod. **2015**(10): 1–444. doi:10.1007/978-1-4939-1447-0.

Dai, X., Li, J., Liu, T., and Zhao, P.X. 2016. HRGRN: A graph search-empowered integrative database of arabidopsis signaling transduction, metabolism and gene regulation networks. Plant Cell Physiol. **57**(1): e12. doi:10.1093/pcp/pcv200.

Dangl, J.L., Horvath, D.M., and Staskawicz, B.J. 2013. Pivoting the Plant Immune System from Dissection to Deployment. Science **341**(6147): 1–14. doi:10.1126/science.1236011.

Delourme, R., Archipiano, M., Horvais, R., Tanguy, X., Rouxel, T., Brun, H., Renard, M., and Balesdent, M.H. 2004. A Cluster of Major Specific Resistance Genes to *Leptosphaeria maculans* in *Brassica napus*. Phytopathology **94**(6): 578–583.

Denancé, N., Sánchez-Vallet, A., Goffner, D., and Molina, A. 2013. Disease resistance or growth: the role of plant hormones in balancing immune responses and fitness costs. Front. Plant Sci. **4**: 155. doi:10.3389/fpls.2013.00155.

Deng, W., Yan, F., Zhang, X., Tang, Y., and Yuan, Y. 2015. Transcriptional profiling of canola developing embryo and identification of the important roles of BnDof5.6 in embryo development and fatty acids synthesis. Plant Cell Physiol. **56**(8): 1624–1640. doi:10.1093/pcp/pcv074.

Depotter, R.L.D., Deketelaere, S., Inderbitzin, P., von Tiedemann, A., Hofte, M., Subbarao, K., Wood, T.A., and Thomma, B.P.H.J. 2016. *Verticillium longisporum*, the invisible threat to oilseed rape and other brassicaceous plant hosts. Mol. Plant Pathol. **17**(7): 1004–1016.

Derksen, H., Rampitsch, C., and Daayf, F. 2013. Signaling cross-talk in plant disease resistance. Plant Sci. **207**: 79–87. Elsevier Ireland Ltd. doi:10.1016/j.plantsci.2013.03.004.

Desmazières, J.B. 1849. Dix-septième notice sur les plantes cryptogames récemment découvertes en France. Ann. Sci. Nat. Bot. **11**: 273–285.

Food and Agricultural Organization of the United States and The Organization for Economic Cooperation and Development. 2017. Oilseeds and Oilseed products in the OECD-FAO Agricultural Outlook 2017-2027.

Dijk, J. Van, and Velmurugan, R. 2018. Reports of the MASC Subcommittees. doi:10.1038/nmeth.4343.

Domínguez-Ferreras, A., Kiss-Papp, M., Jehle, A.K., Felix, G., and Chinchilla, D. 2015. An Overdose of the Arabidopsis Coreceptor BRASSINOSTEROID INSENSITIVE1-ASSOCIATED RECEPTOR KINASE1 or Its Ectodomain Causes Autoimmunity in a SUPPRESSOR OF BIR1-1-Dependent Manner. Plant Physiol. **168**(3): 1106–21. American Society of Plant Biologists. doi:10.1104/pp.15.00537.

Drerup, M.M., Schlücking, K., Hashimoto, K., Manishankar, P., Steinhorst, L., Kuchitsu, K., and Kudla, J. 2013. The Calcineurin B-Like Calcium Sensors CBL1 and CBL9 Together with Their Interacting Protein Kinase CIPK26 Regulate the Arabidopsis NADPH Oxidase RBOHF. Mol. Plant **6**(2): 559–569. doi:10.1093/mp/sst009.

Du, H.A.I., Wang, Y.O.N.G.I.N., Xie, Y.I., Liang, Z.H.E., Jiang, S.A.N.I.E., Zhang, S.H.H., and Huang, Y.U.I. 2013. Genome-Wide Identification and Evolutionary and Expression Analyses of MYB-Related Genes in Land Plants. DNA Res. **1**(5): 1–12.

Du, Z., Zhou, X., Ling, Y., Zhang, Z., and Su, Z. 2010. agriGO: A GO analysis toolkit for the agricultural community. Nucleic Acids Res. **38**(S2): 64–70. doi:10.1093/nar/gkq310.

Dubiella, U., Seybold, H., Durian, G., Komander, E., Lassig, R., Witte, C.-P., Schulze, W.X., and Romeis, T. 2013. Calcium-dependent protein kinase/NADPH oxidase activation circuit is required for rapid defense signal propagation. Proc. Natl. Acad. Sci. **110**(21): 8744–8749. doi:10.1073/pnas.1221294110.

Duke, K.A., Becker, M.G., Girard, I.J., Millar, J.L., Fernando, W.G.D., Belmonte, M.F., Kievit, T.R. De, Dilantha Fernando, W.G., Belmonte, M.F., and de Kievit, T.R. 2017. The biocontrol agent Pseudomonas chlororaphis PA23 primes Brassica napus defenses through distinct gene networks. BMC Genomics **18**(1): 1–16. doi:10.1186/s12864-017-3848-6.

Duvick, J., Fu, A., Muppirala, U., Sabharwal, M., Wilkerson, M.D., Lawrence, C.J., Lushbough, C., and Brendel, V. 2008. PlantGDB: A resource for comparative plant genomics. Nucleic Acids Res. **36**(S1): 959–965. doi:10.1093/nar/gkm1041.

Ellinger, D., Naumann, M., Falter, C., Zwikowics, C., Jamrow, T., Manisseri, C., Somerville, S.C.C., and Voigt, C.A.A. 2013. Elevated Early Callose Deposition Results in Complete Penetration Resistance to Powdery Mildew in Arabidopsis. Plant Physiol. **161**(3): 1433–1444. doi:10.1104/pp.112.211011.

Ellis, C. 2001. The Arabidopsis Mutant cev1 Has Constitutively Active Jasmonate and Ethylene Signal Pathways and Enhanced Resistance to Pathogens. Plant Cell Online **13**(5): 1025–1033. doi:10.1105/tpc.13.5.1025.

Englbrecht, C.C., Schoof, H., and Böhm, S. 2004. Conservation, diversification and expansion of C2H2 zinc finger proteins in the Arabidopsis thaliana genome. BMC Genomics **5**(1): 39. doi:10.1186/1471-2164-5-39.

Fernando, W.D., Zhang, X., Selin, C., Zou, Z., Liban, S.H., McLaren, D.L., Kubinec, A., Parks, P.S., Rashid, M.H., Padmathilake, K.R.E., and Rong, L. 2018. A six-year investigation of the dynamics of avirulence allele profiles, blackleg incidence, and mating type alleles of *Leptosphaeria maculans* populations associated with canola crops in Manitoba, Canada. Plant Dis. **102**(4): 790–798.

Fernando, W.G.D., Zhang, X., and Amarasinghe, C.C. 2016. Detection of *Leptosphaeria maculans* and *Leptosphaeria biglobosa* Causing Blackleg Disease in Canola from Canadian Canola Seed Lots and Dockage. Plants **5**(1): 12. doi:10.3390/plants5010012.

Ferrari, S., Plotnikova, J.M., De Lorenzo, G., and Ausubel, F.M. 2003. Arabidopsis local resistance to *Botrytis cinerea* involves salicylic acid and camalexin and requires EDS4 and PAD2, but not SID2, EDS5 or PAD4. Plant J. **35**(2): 193–205. doi:10.1046/j.1365-313X.2003.01794.x.

Fitt, B.D.L.L., Brun, H., Barbetti, M.J., and Rimmer, S.R. 2006. World-wide importance of phoma stem canker (*Leptosphaeria maculans* and *L. biglobosa*) on oilseed Rape (*Brassica napus*). Eur. J. Plant Pathol. **114**(1): 3–15. doi:10.1007/s10658-005-2233-5.

Fitt, B.D.L.L., Hu, B.C., Li, Z.Q., Liu, S.Y., Lange, R.M., Kharbanda, P.D., Butterworth, M.H., and White, R.P. 2008. Strategies to prevent spread of *Leptosphaeria maculans* (phoma stem canker) onto oilseed rape crops in China; costs and benefits. Plant Pathol. **57**(4): 652–664. doi:10.1111/j.1365-3059.2008.01841.x.

Flor, H.H. 1971. Current status of the gene-for-gene concept. Annual Review of Phytopathology **9**(1): 275–296.

Franco-Orozco, B., Berepiki, A., Ruiz, O., Gamble, L., Griffe, L.L., Wang, S., Birch, P.R.J.J., Kanyuka, K., and Avrova, A. 2017. A new proteinaceous pathogen-associated molecular pattern (PAMP) identified in Ascomycete fungi induces cell death in *Solanaceae*. New Phytol. **214**(4): 1657–1672. doi:10.1111/nph.14542.

Franco-Zorrilla, J.M., López-Vidriero, I., Carrasco, J.L., Godoy, M., Vera, P., and Solano, R. 2014. DNA-binding specificities of plant transcription factors and their potential to define target genes. Proc. Natl. Acad. Sci. U. S. A. **111**(6): 2367–72. doi:10.1073/pnas.1316278111.

Frerigmann, H., and Gigolashvili, T. 2014. Indolic Glucosinolate Biosynthesis in Arabidopsis thaliana. Mol. Plant **7**(5): 814–828. doi:10.1093/mp/ssu004.

Fudal, I., Ross, S., Gout, L., Blaise, F., Kuhn, M.L., Eckert, M.R., Cattolico, L., Balesdent, M.H., Rouxel, T., Versailles, F.-, Plantes, P., P-g, I.N.A., Bernard-Samain, S., Balesdent, M.H., and Rouxel, T. 2007. Heterochromatin-like regions as ecological niches for avirulence genes in the *Leptosphaeria maculans* genome: map-based cloning of AvrLm6. Mol. Plant. Microbe. Interact. **20**(4): 459–470. doi:10.1094/MPMI-20-4-0459.

Gaetán, S.A. 2005. Occurrence of Fusarium wilt on canola caused by *Fusarium oxysporum* f. sp. conglutinans in Argentina. Plant Dis. **89**(4): 432.

Gao, M., Wang, X., Wang, D., Xu, F., Ding, X., Zhang, Z., Bi, D., Cheng, Y.T., Chen, S., Li, X., and Zhang, Y. 2009. Regulation of Cell Death and Innate Immunity by Two Receptor-like Kinases in Arabidopsis. Cell Host Microbe **6**(1): 34–44. doi:10.1016/j.chom.2009.05.019.

Gao, S., Gao, J., Zhu, X., Song, Y., Li, Z., Ren, G., Zhou, X., and Kuai, B. 2016. ABF2, ABF3, and ABF4 Promote ABA-Mediated Chlorophyll Degradation and Leaf Senescence by Transcriptional Activation of Chlorophyll Catabolic Genes and Senescence-Associated Genes in Arabidopsis. Mol. Plant **9**(9): 1272–1285. doi:10.1016/j.molp.2016.06.006.

Gaude, N., Bortfeld, S., Duensing, N., Lohse, M., and Krajinski, F. 2012. Arbuscule-containing and non-colonized cortical cells of mycorrhizal roots undergo extensive and specific reprogramming during arbuscular mycorrhizal development. Plant J. **69**(3): 510–528. doi:10.1111/j.1365-313X.2011.04810.x.

Geisler-Lee, J., O'Toole, N., Ammar, R., Provart, N.J., Millar, a H., and Geisler, M. 2007. A Predicted Interactome for Arabidopsis. Plant Physiol. **145**(2): 317–329. doi:10.1104/pp.107.103465.

Ghanbarnia, K., Fernando, W.G.D., and Crow, G. 2011. Comparison of disease severity and incidence at different growth stages of naturally infected canola plants under field conditions by pycnidiospores of Phoma lingam as a main source of inoculum. Can. J. Plant Pathol. **33**(3): 355–363. doi:10.1080/07060661.2011.593189.

Ghanbarnia, K., Fudal, I., Larkan, N.J., Links, M.G., Balesdent, M.H., Profotova, B., Fernando, W.G.D.D., Rouxel, T., and Borhan, M.H. 2015. Rapid identification of the *Leptosphaeria maculans* avirulence gene *AvrLm2* using an intraspecific comparative genomics approach. Mol. Plant Pathol. **16**(7): 699–709. doi:10.1111/mpp.12228.

Ghanbarnia, K., Ma, L., Larkan, N.J., Haddadi, P., Fernando, W.G.D., and Borhan, M.H. 2018. *Leptosphaeria maculans* AvrLm9: A new player in the game of hide and seek with AvrLm4-7. Mol. Plant Pathol. **1**: 1–11. doi:10.1111/mpp.12658.

Gill, U.S., Lee, S., and Mysore, K.S. 2015. Host Versus Nonhost Resistance: Distinct Wars with Similar Arsenals. Phytopathology **105**(5): 580–587. doi:10.1094/PHYTO-11-14-0298-RVW.

Giovannetti, M., Balestrini, R., Volpe, V., Guether, M., Straub, D., Costa, A., Ludewig, U., and Bonfante, P. 2012. Two putative-aquaporin genes are differentially expressed during arbuscular mycorrhizal symbiosis in *Lotus japonicus*. BMC Plant Biol. **12**: 1–14. doi:10.1186/1471-2229-12-186.

Girard, I.J., Tong, C., Becker, M.G., Mao, X., Huang, J., Kievit, T. De, Fernando, W.G.D., Liu, S., and Belmonte, M.F. 2018. RESEARCH PAPER RNA sequencing of *Brassica napus* reveals cellular redox control of Sclerotinia infection. **68**(18): 5079–5091. doi:10.1093/jxb/erx338.

Glazebrook, J. 2005. Contrasting Mechanisms of Defense Against Biotrophic and Necrotrophic Pathogens. Annu. Rev. Phytopathol. **43**(1): 205–227. doi:10.1146/annurev.phyto.43.040204.135923.

Gomez, S.K., Javot, H., Deewatthanawong, P., Torres-Jerez, I., Tang, Y., Blancaflor, E.B., Udvardi, M.K., and Harrison, M.J. 2009. *Medicago truncatula* and *Glomus intraradices* gene expression in cortical cells harboring arbuscules in the arbuscular mycorrhizal symbiosis. BMC Plant Biol. **9**: 1–19. doi:10.1186/1471-2229-9-10.

Gout, L., Fudal, I., Kuhn, M.L., Blaise, F., Eckert, M., Cattolico, L., Balesdent, M.H., and Rouxel, T. 2006. Lost in the middle of nowhere: The *AvrLm1* avirulence gene of the Dothideomycete *Leptosphaeria maculans*. Mol. Microbiol. **60**(1): 67–80. doi:10.1111/j.1365-2958.2006.05076.x.

Gravino, M., Savatin, D.V., MacOne, A., and De Lorenzo, G. 2015. Ethylene production in *Botrytis cinerea*- and oligogalacturonide-induced immunity requires calcium-dependent protein kinases. Plant J. **84**(6): 1073–1086. doi:10.1111/tpj.13057.

Guerreiro, A., Figueiredo, J., Sousa Silva, M., and Figueiredo, A. 2016. Linking Jasmonic Acid to Grapevine Resistance against the Biotrophic Oomycete *Plasmopara viticola*. Front. Plant Sci. **7**: 565. Frontiers. doi:10.3389/fpls.2016.00565.

Gunasinghe, N., You, M.P., Banga, S., Banga, S.S.K.S.S., and Barbetti, M.J. 2017. Outstanding host resistance will resolve the threat from white leaf spot disease (*Pseudocercosporella capsellae*) to oilseed and vegetable Brassica spp. crops. Australas. Plant Pathol. **46**(2): 137–146. Australasian Plant Pathology. doi:10.1007/s13313-017-0470-7.

Guo, J., Wu, J., Ji, Q., Wang, C., Luo, L., Yuan, Y., Wang, Y., and Wang, J. 2008. Genome-wide analysis of heat shock transcription factor families in rice and Arabidopsis. J. Genet. Genomics **35**(2): 105–118. doi:10.1016/S1673-8527(08)60016-8.

Guo, X.W., and Fernando, W.G.D. 2005. Seasonal and Diurnal Patterns of Spore Dispersal by *Leptosphaeria maculans* from Canola Stubble in Relation to Environmental Conditions. Plant Dis. **89**(1): 97–104. doi:10.1094/PD-89-0097.

Haas, B.J., Delcher, A.L., Wortman, J.R., and Salzberg, S.L. 2004. DAGchainer: A tool for mining segmental genome duplications and synteny. Bioinformatics **20**(18): 3643–3646. doi:10.1093/bioinformatics/bth397.

Hacquard, S., Delaruelle, C., Legué, V., Tisserant, E., Kohler, A., Frey, P., Martin, F., and Duplessis, S. 2010. Laser capture microdissection of uredinia formed by *Melampsora larici-populina* revealed a transcriptional switch between biotrophy and sporulation. Mol. Plant. Microbe. Interact. **23**(10): 1275–86. doi:10.1094/MPMI-05-10-0111.

Hacquard, S., Tisserant, E., Brun, A., Legué, V., Martin, F., and Kohler, A. 2013. Laser microdissection and microarray analysis of Tuber melanosporum ectomycorrhizas reveal functional heterogeneity between mantle and Hartig net compartments. Environ. Microbiol. **15**(6): 1853–1869. doi:10.1111/1462-2920.12080.

Haddadi, P., Ma, L., Wang, H., and Borhan, M.H. 2016. Genome-wide transcriptomic analyses provide insights into the lifestyle transition and effector repertoire of *Leptosphaeria maculans* during the colonization of *Brassica napus* seedlings. Mol. Plant Pathol. **7**(2016): 1196–1210. doi:10.1111/mpp.12356.

Hammond, K.E., and Lewis, B.G. 1987. The establishment of systemic infection in leaves of oilseed rape by *Leptosphaeria maculans*. Plant Pathol. **36**(2): 135–147.

Hammond, K.E., Lewis, B.G., and Musa, T.M. 1985. A systemic pathway in the infection of oilseed rape plants by *Leptosphaeria maculans*. Plant Pathol. **34**(4): 557–565. doi:10.1111/j.1365-3059.1985.tb01407.x.

Hartmann, L., Pedrotti, L., Weiste, C., Fekete, A., Schierstaedt, J., Göttler, J., Kempa, S., Krischke, M., Dietrich, K., Mueller, M.J., Vicente-Carbajosa, J., Hanson, J., and Dröge-Laser, W. 2015. Crosstalk between Two bZIP Signaling Pathways Orchestrates Salt-Induced Metabolic Reprogramming in Arabidopsis Roots. Plant Cell **27**(8): 2244–60. American Society of Plant Biologists. doi:10.1105/tpc.15.00163.

Harvey, B.L., and Downey, R.K. 1964. The inheritence of erucic aid content in rapeseed (*Brassica napus*). Can. J. Plant Sci. **44**(8): 104–116.

Haynes, B., Maier, E., and Kramer, M. 2013. Mapping Functional Transcription Factor Networks from Gene Expression Data. Genome Res. **23**: 1319–1328. doi:10.1101/gr.150904.112.23.

He, Y., Mao, S., Gao, Y., Zhu, L., Wu, D., Cui, Y., Li, J., and Qian, W. 2016. Genome-wide identification and expression analysis of WRKY transcription factors under multiple stresses in *Brassica napus*. PLoS One **11**(6): 1–18. doi:10.1371/journal.pone.0157558.

He, Y., Zhou, J., Shan, L., and Meng, X. 2018. Plant cell surface receptor-mediated signaling - a common theme amid diversity. J. Cell Sci. **131**(2): jcs209353. doi:10.1242/jcs.209353.

Heese, A., Hann, D.R., Gimenez-Ibanez, S., Jones, A.M.E., He, K., Li, J., Schroeder, J.I., Peck, S.C., and Rathjen, J.P. 2007. The receptor-like kinase SERK3/BAK1 is a central regulator of innate immunity in plants. Proc. Natl. Acad. Sci. **104**(29): 12217–12222. doi:10.1073/pnas.0705306104.

Hegewald, H., Koblenz, B., and Wensch-dorendorf, M. 2017. Yield, yield formation, and blackleg disease of oilseed rape cultivated in high-intensity crop rotations. Arch. Agron. Soil Sci. **63**(13): 1785–1799. Taylor & Francis. doi:10.1080/03650340.2017.1307508.

Hemberg, M., and Kreiman, G. 2011. Conservation of transcription factor binding events predicts gene expression across species. Nucleic Acids Res. **39**(16): 7092–7102. doi:10.1093/nar/gkr404.

Henderson, M.P. 1918. The blackleg disease of cabbage caused by Phoma lingam (Tode). Desmaz. Univ. Wisconsin-Madison.

Henriquez, M.A., Soliman, A., Li, G., Hannoufa, A., Ayele, B.T., and Daayf, F. 2016. Molecular cloning, functional characterization and expression of potato (*Solanum tuberosum*) 1-deoxy-

d-xylulose 5-phosphate synthase 1 (StDXS1) in response to *Phytophthora infestans*. Plant Sci. **243**: 71–83. Elsevier Ireland Ltd. doi:10.1016/j.plantsci.2015.12.001.

Hiruma, K., Fukunaga, S., and Pi, M. 2013. Glutathione and tryptophan metabolism are required for Arabidopsis immunity during the hypersensitive response to hemibiotrophs. **1**(15): 2–7. doi:10.1073/pnas.1305745110.

Hogekamp, C., and Küster, H. 2013. A roadmap of cell-type specific gene expression during sequential stages of the arbuscular mycorrhiza symbiosis. BMC Genomics **14**(1). doi:10.1186/1471-2164-14-306.

Honaas, L.A., Wafula, E.K., Yang, Z., Der, J.P., Wickett, N.J., and Altman, N.S. 2013. Functional genomics of a generalist parasitic plant : Laser microdissection of host-parasite interface reveals host-specific patterns of parasite gene expression. BMC Plant Biol. **13**(9).

Hu, X., Jiang, M., Zhang, J., Zhang, A., Lin, F., and Tan, M. 2007. Calcium-calmodulin is required for abscisic acid-induced antioxidant defense and functions both upstream and downstream of H2O2 production in leaves of maize (*Zea mays*) plants. New Phytol. **173**(1): 27–38. doi:10.1111/j.1469-8137.2006.01888.x.

Hwang, S., Strelkov, S.E., Peng, G., Ahmed, H., Zhou, Q., and Turnbull, G. 2016. Blackleg (*Leptosphaeria maculans*) Severity and Yield. **5**(31): 1–11. doi:10.3390/plants5030031.

Jones, J.D.G., Vance, R.E., and Dangl, J.L. 2016. Intracellular innate immune surveillance devices in plants and animals. Science **354**(6316). doi:10.1126/science.aaf6395.

Kabbage, M., Williams, B., and Dickman, M.B. 2013. Cell Death Control: The Interplay of Apoptosis and Autophagy in the Pathogenicity of Sclerotinia sclerotiorum. PLoS Pathog. **9**(4). doi:10.1371/journal.ppat.1003287.

Kale, S.D., and Tyler, B.M. 2011. Entry of oomycete and fungal effectors into plant and animal host cells. Cell. Microbiol. **13**(12): 1839–1848. doi:10.1111/j.1462-5822.2011.01659.x.

Kaliff, M., Staal, J., Myrenås, M., and Dixelius, C. 2007. ABA is required for Leptosphaeria maculans resistance via ABI1- and ABI4-dependent signaling. Mol. Plant. Microbe. Interact. **20**(4): 335–45. doi:10.1094/MPMI-20-4-0335.

Kaplan-Levy, R.N., Brewer, P.B., Quon, T., and Smyth, D.R. 2012. The trihelix family of transcription factors - light, stress and development. Trends Plant Sci. **17**(3): 163–171. Elsevier Ltd. doi:10.1016/j.tplants.2011.12.002.

Kawai-Yamada, M., Hori, Z., Ogawa, T., Ihara-Ohori, Y., Tamura, K., Nagano, M., Ishikawa, T., and Uchimiya, H. 2009. Loss of calmodulin binding to bax inhibitor-1 affects pseudomonas-mediated hypersensitive response-associated cell death in Arabidopsis thaliana. J. Biol. Chem. **284**(41): 27998–28003. doi:10.1074/jbc.M109.037234.

Kelemen, Z., Sebastian, A., Xu, W., Grain, D., Salsac, F., Avon, A., Berger, N., Tran, J., Dubreucq, B., Lurin, C., Lepiniec, L., Contreras-Moreira, B., and Dubos, C. 2015. Analysis of the DNA-binding activities of the arabidopsis R2R3-MYB transcription factor family by one-hybrid experiments in yeast. PLoS One **10**(10): 1–22. doi:10.1371/journal.pone.0141044.

Keon, J., Antoniw, J., Carzaniga, R., Deller, S., Ward, J.L., Baker, J.M., Beale, M.H., Hammond-Kosack, K., and Rudd, J.J. 2007. Transcriptional adaptation of *Mycosphaerella graminicola* to programmed cell death (PCD) of its susceptible wheat host. Mol. Plant. Microbe. Interact. **20**(2): 178–193. doi:10.1094/MPMI-20-2-0178.

Khajali, F., and Slominski, B.A. 2012. Review Factors that affect the nutritive value of canola meal for poultry. Poultry Science **91**(10): 2564–2575.

Khan, D., Millar, J.L., Girard, I.J., Chan, A., Kirkbride, R.C., Pelletier, J.M., Kost, S., Becker, M.G., Yeung, E.C., Stasolla, C., Goldberg, R.B., Harada, J.J., and Belmonte, M.F. 2015. Transcriptome atlas of the Arabidopsis funiculus - a study of maternal seed subregions. Plant J. **82**(1): 41–53. doi:10.1111/tpj.12790.

Khan, M., Subramaniam, R., and Desveaux, D. 2016. Of guards, decoys, baits and traps: pathogen perception in plants by type III effector sensors. Curr. Opin. Microbiol. **29**: 49–55.

Kidokoro, S., Yoneda, K., Takasaki, H., Takahashi, F., Shinozaki, K., and Yamaguchi-Shinozaki, K. 2017. Different Cold-Signaling Pathways Function in the Responses to Rapid and Gradual Decreases in Temperature. Plant Cell **29**(4): 760–774. doi:10.1105/tpc.16.00669.

Kim, H.-S.H., Desveaux, D., Singer, A.U., Patel, P., Sondek, J., and Dangl, J.L. 2005. The *Pseudomonas syringae* effector AvrRpt2 cleaves its C-terminally acylated target, RIN4, from Arabidopsis membranes to block RPM1 activation. Proc. Natl. Acad. Sci. **102**(18): 6496–6501. doi:10.1073/pnas.0500792102.

Kim, W.C., Kim, J.Y., Ko, J.H., Kang, H., and Han, K.H. 2014. Identification of direct targets of transcription factor MYB46 provides insights into the transcriptional regulation of secondary wall biosynthesis. Plant Mol. Biol. **85**(6): 589–599. doi:10.1007/s11103-014-0205-x.

King, S.R., McLellan, H., Boevink, P.C., Armstrong, M.R., Bukharova, T., Sukarta, O., Win, J., Kamoun, S., Birch, P.R., and Banfield, M.J. 2014. *Phytophthora infestans* RXLR effector PexRD2 interacts with host MAPKKKs to suppress plant immune signaling. Plant Cell **26**(3): 1345–1359.

Klessig, D.F., Choi, H.W., Dempsey, D.M.A., Rd, T., and Dempsey, M.A. 2018. Systemic Acquired Resistance and Salicylic Acid: Past, Present and Future. Mol. Plant-Microbe Interact. **2018**: MPMI-03-18-0067-CR.

Kliebenstein, D.J., Rowe, H.C., Denby, K.J., Avenue, O.S., Biology, C., Bag, P., and Africa, S. 2005. Secondary metabolites influence Arabidopsis/Botrytis interactions: Variation in host production and pathogen sensitivity. Plant J. **44**(1): 25–36. doi:10.1111/j.1365-313X.2005.02508.x.

Klink, V.P., Alkharouf, N., MacDonald, M., and Matthews, B. 2005. Laser capture microdissection (LCM) and expression analyses of *Glycine max* (soybean) syncytium containing root regions formed by the plant pathogen *Heterodera glycines* (soybean cyst

nematode). Plant Mol. Biol. **59**(6): 965–79. doi:10.1007/s11103-005-2416-7.

Kooliyottil, R., Dandurand, L.-M., Kuhl, J.C., Caplan, A., and Xiao, F. 2017. Microaspiration of *Solanum tuberosum* root cells at early stages of infection by *Globodera pallida*. Plant Methods **13**(1): 68. BioMed Central. doi:10.1186/s13007-017-0219-x.

Kostik, V., Memeti, S., and Bauer, B. 2013. Fatty acid composition of edible oils and fats. J. Hyg. Eng. Des. **4**: 112–116.

Kulkarni, S.R., Vaneechoutte, D., Velde, J. Van De, and Vandepoele, K. 2018. TF2Network : predicting transcription factor regulators and gene regulatory networks in Arabidopsis using publicly available binding site information. **46**(6). Oxford University Press. doi:10.1093/nar/gkx1279.

Kumar, R., Ichihashi, Y., Kimura, S., Chitwood, D.H., Headland, L.R., Peng, J., Maloof, J.N., and Sinha, N.R. 2012. A High-Throughput Method for Illumina RNA-Seq Library Preparation. Front. Plant Sci. **3**(8): 202. doi:10.3389/fpls.2012.00202.

Kumar, R., Megha, S., Ha, M., Basu, U., and Kav, N.N. V. 2016. A global study of transcriptome dynamics in canola (*Brassica napus* L .) responsive to *Sclerotinia sclerotiorum* infection using RNA-Seq. **590**: 57–67. doi:10.1016/j.gene.2016.06.003.

Künstler, A., Bacsó, R., Gullner, G., Hafez, Y.M., and Király, L. 2016. Staying alive - is cell death dispensable for plant disease resistance during the hypersensitive response? Physiol. Mol. Plant Pathol. **93**(1): 75–84. doi:10.1016/j.pmpp.2016.01.003.

Kwon, A.T., Arenillas, D.J., Worsley Hunt, R., and Wasserman, W.W. 2012. oPOSSUM-3: advanced analysis of regulatory motif over-representation across genes or ChIP-Seq datasets. G3 (Bethesda). **2**(9): 987–1002. doi:10.1534/g3.112.003202.

Larkan, N.J., Lydiate, D.J., Parkin, I. a P., Nelson, M.N., Epp, D.J., Cowling, W. a, Rimmer, S.R., and Borhan, M.H. 2013. The *Brassica napus* blackleg resistance gene LepR3 encodes a receptor-like protein triggered by the *Leptosphaeria maculans* effector AVRLM1. New Phytol. **197**(2): 595–605. doi:10.1111/nph.12043.

Larkan, N.J., Ma, L., and Borhan, M.H. 2015. The *Brassica napus* receptor-like protein RLM2 is encoded by a second allele of the *LepR3/Rlm2* blackleg resistance locus. Plant Biotechnol. J. **13**(7): 983–992. doi:10.1111/pbi.12341.

Laxmi, A. 2015. Transcriptional regulation of drought response: a tortuous network of transcriptional factors. **6**(10): 1–11. doi:10.3389/fpls.2015.00895.

Le, M.H., Cao, Y., Zhang, X.C., and Stacey, G. 2014. LIK1, a CERK1-interacting kinase, regulates plant immune responses in arabidopsis. PLoS One **9**(7): 1–10. doi:10.1371/journal.pone.0102245.

Lechner, E., Goloubinoff, P., Genschik, P., and Shen, W.H. 2002. A gene trap Dissociation insertion line, associated with a RING-H2 finger gene, shows tissue specific and developmental regulated expression of the gene in Arabidopsis. Gene **290**(1–2): 63–71. doi:10.1016/S0378-1119(02)00556-5.

Lee, H.A., and Yeom, S.I. 2015. Plant NB-LRR proteins: Tightly regulated sensors in a complex manner. Brief. Funct. Genomics **14**(4): 233–242. doi:10.1093/bfgp/elv012.

Lee, H.Y., and Back, K. 2016. Mitogen-activated protein kinase pathways are required for melatonin-mediated defense responses in plants. J. Pineal Res. **60**(3): 327–335. doi:10.1111/jpi.12314.

Lenzi, L., Caruso, C., Bianchedi, P.L., Pertot, I., and Perazzolli, M. 2016. Laser microdissection of grapevine leaves reveals site-specific regulation of transcriptional response to *Plasmopara viticola*. Plant Cell Physiol. **57**(1): 69–81. doi:10.1093/pcp/pcv166.

Li, B., Meng, X., Shan, L., and He, P. 2016. Transcriptional Regulation of Pattern-Triggered Immunity in Plants. Cell Host Microbe **19**(5): 641–650. doi:10.1016/j.chom.2016.04.011.

Li, H., Sivasithamparam, K., and Barbetti, M. 2006. Blackleg disease (*Leptosphaeria maculans*) on oilseed rape– evidence for it being a polycyclic disease in Australia and implications for disease management. *In* Genetics and Breeding: Breeding for Stress Resistance.

Li, Q., Rong, S., Hu, B., Jiang, Y., Hou, S., Fei, W., Chen, F., Wu, X., Fan, Z., and Lei, W. 2013. Distribution of blackleg disease on oilseed rape in China and its pathogen identification. Chinese J. Oil Crop Sci. **35**: 415–423.

Li, Q.F., and He, J.X. 2016. BZR1 Interacts with HY5 to Mediate Brassinosteroid- and Light-Regulated Cotyledon Opening in Arabidopsis in Darkness. Mol. Plant **9**(1): 113–125. Elsevier. doi:10.1016/j.molp.2015.08.014.

Li, S., Fu, Q., Chen, L., Huang, W., and Yu, D. 2011. Arabidopsis thaliana WRKY25, WRKY26, and WRKY33 coordinate induction of plant thermotolerance. Planta **233**: 1237–1252. doi:10.1007/s00425-011-1375-2.

Liban, S.H., Cross, D.J., Kutcher, H.R., Peng, G., and Fernando, W.G.D.D. 2016. Race structure and frequency of avirulence genes in the western Canadian *Leptosphaeria maculans* pathogen population, the causal agent of blackleg in brassica species. Plant Pathol. **65**(7): 1161–1169. doi:10.1111/ppa.12489.

Liebrand, T.W.H., van den Berg, G.C.M., Zhang, Z., Smit, P., Cordewener, J.H.G., America, A.H.P., Sklenar, J., Jones, A.M.E., Tameling, W.I.L., Robatzek, S., Thomma, B.P.H.J., and Joosten, M.H.A.J. 2013. Receptor-like kinase SOBIR1/EVR interacts with receptor-like proteins in plant immunity against fungal infection. Proc. Natl. Acad. Sci. **110**(32): 13228–13228. doi:10.1073/pnas.1313401110.

Limpens, E., Moling, S., Hooiveld, G., Pereira, P.A., Bisseling, T., Becker, J.D., and Küster, H. 2013. Cell- and Tissue-Specific Transcriptome Analyses of *Medicago truncatula* Root Nodules. PLoS One **8**(5). doi:10.1371/journal.pone.0064377.

Lin, L., Allemekinders, H., Dansby, A., Campbell, L., Durance-Tod, S., Berger, A., and Jones, P.J. 2013. Evidence of health benefits of canola oil. Nutr. Rev. **71**(6): 370–385. doi:10.1111/nure.12033.

Long, W., Zou, X., and Zhang, X. 2015. Transcriptome Analysis of Canola (*Brassica napus*) under Salt Stress at the Germination. PLoS One **10**(2): e0116217.

Lorang, J.M., Sweat, T.A., and Wolpert, T.J. 2007. Plant disease susceptibility conferred by a "resistance" gene. Proc. Natl. Acad. Sci. **104**(37): 14861–14866.

Love, M.I., Huber, W., and Anders, S. 2014. Moderated estimation of fold change and dispersion for RNA-seq data with DESeq2. Genome Biol. **15**(12): 1–21. doi:10.1186/s13059-014-0550-8.

Lowe, R.G.T., Cassin, A., Grandaubert, J., Clark, B.L., Van De Wouw, A.P., Rouxel, T., and Howlett, B.J. 2014. Genomes and transcriptomes of partners in plant-fungal- interactions between canola (*Brassica napus*) and two *Leptosphaeria species*. PLoS One **9**(7). doi:10.1371/journal.pone.0103098.

Luna, E., Pastor, V., Robert, J., Flors, V., Mauch-Mani, B., and Ton, J. 2011. Callose Deposition: A Multifaceted Plant Defense Response. Mol. Plant-Microbe Interact. **24**(2): 183–193. doi:10.1094/MPMI-07-10-0149.

Ma, L., and Borhan, M.H. 2015. The receptor-like kinase SOBIR1 interacts with Brassica napus LepR3 and is required for *Leptosphaeria maculans* AvrLm1-triggered immunity. Front. Plant Sci. **6**(October): 1–10. doi:10.3389/fpls.2015.00933.

Ma, L., Djavaheri, M., Wang, H., Larkan, N.J., Haddadi, P., Beynon, E., Gropp, G., and Borhan, M.H. 2018. Leptosphaeria maculans effector protein AvrLm1 modulates plant immunity by enhancing MAP kinase 9 phosphorylation. iScience **3**(May): 177–191. doi:10.1016/j.isci.2018.04.015.

Ma, X., Xu, G., He, P., and Shan, L. 2016. SERKing Coreceptors for Receptors. Trends Plant Sci. **21**(12): 1017–1033. Elsevier Ltd. doi:10.1016/j.tplants.2016.08.014.

Ma, Y., Zhao, Y., and Berkowitz, G.A. 2017. Intracellular Ca2+ is important for flagellin-triggered defense in Arabidopsis and involves inositol polyphosphate signaling. J. Exp. Bot. **68**(13): 3617–3628. doi:10.1093/jxb/erx176.

Malinovsky, F.G., Fangel, J.U., and Willats, W.G.T. 2014. The role of the cell wall in plant immunity. Front. Plant Sci. **5**(May): 1–12. doi:10.3389/fpls.2014.00178.

Marcroft, S.J., Wouw, A.P. Van De, Salisbury, P.A., and Potter, T.D. 2012. Effect of rotation of canola (*Brassica napus*) cultivars with different complements of blackleg resistance genes on disease severity. Plant Pathol. **61**: 934–944. doi:10.1111/j.1365-3059.2011.02580.x.

Marie- Hélène, B., Fudal, I., Ollivier, B., Bally, P., Grandaubert, J., Eber, F., Chèvre, A., Leflon, M., and Rouxel, T. 2013. The dispensable chromosome of *Leptosphaeria maculans* shelters an effector gene conferring avirulence towards *Brassica rapa*. New Phytol. **198**(3): 887–898.

Mauch-Mani, B., Baccelli, I., Luna, E., and Flors, V. 2017. Defense Priming: An Adaptive Part of Induced Resistance. Annu. Rev. Plant Biol. **68**(1): 485–512. doi:10.1146/annurev-arplant-042916-041132.

McLoughlin, A.G., Wytinck, N., Walker, P.L., Girard, I.J., Rashid, K.Y., de Kievit, T., Fernando, W.G.D., Whyard, S., and Belmonte, M.F. 2018. Identification and application of exogenous dsRNA confers plant protection against *Sclerotinia sclerotiorum* and *Botrytis cinerea*. Sci. Rep. **8**(1): 7320. doi:10.1038/s41598-018-25434-4.

Medina-Rivera, A., Defrance, M., Sand, O., Herrmann, C., Castro-Mondragon, J.A., Delerce, J., Jaeger, S., Blanchet, C., Vincens, P., Caron, C., Staines, D.M., Contreras-Moreira, B., Artufel, M., Charbonnier-Khamvongsa, L., Hernandez, C., Thieffry, D., Thomas-Chollier, M., and van Helden, J. 2015. RSAT 2015: Regulatory Sequence Analysis Tools. Nucleic Acids Res **43**(W1): 50–56. doi:10.1093/nar/gkv362.

Mele, G. 2016. Arabidopsis Motif Scanner. BMC Bioinformatics **17**(1): doi:10.1186/s12859-016-0896-x.

Meng, X., and Zhang, S. 2013. MAPK cascades in plant disease resistance signaling. Annu. Rev. Phytopathol. **51**: 245–266.

Millar, J.L., Becker, M.G., and Belmonte, M.F. 2015. Laser Microdissection of Plant Tissues. *In* Plant Microtechniques and Protocols. Springer International Publishing. pp. 337–350. doi:10.1007/978-3-319-19944-3.

Mishina, T.E., and Zeier, J. 2007. Pathogen-associated molecular pattern recognition rather than development of tissue necrosis contributes to bacterial induction of systemic acquired resistance in Arabidopsis. Plant J. **50**(3): 500–513. doi:10.1111/j.1365-313X.2007.03067.x.

Mishra, A.K., Sharma, K., and Misra, R.S. 2012. Elicitor recognition, signal transduction and induced resistance in plants. J. Plant Interact. **7**(2): 95–120. doi:10.1080/17429145.2011.597517.

Mithen, R.F., Lewis, B.G., and Fenwick, G.R. 1986. In vitro activity of glucosinolates and their products against Leptosphaeria maculans. Trans. Br. Mycol. Soc. **87**(3): 433–440. British Mycological Society. doi:10.1016/S0007-1536(86)80219-4.

Mohammed, A.E., You, M.P., and Barbetti, M.J. 2017. New resistances offer opportunity for effective management of the downy mildew (*Hyaloperonospora parasitica*) threat to canola. Crop Pasture Sci. **68**(3): 234–242.

Mortazavi, A., Williams, B.A., McCue, K., Schaeffer, L., and Wold, B. 2008. Mapping and quantifying mammalian transcriptomes by RNA-Seq. Nat. Methods **5**(7): 621–628. doi:10.1038/nmeth.1226.

Mugford, S.G., Yoshimoto, N., Reichelt, M., Wirtz, M., Hill, L., Mugford, S.T., Noji, M., Takahashi, H., Kramell, R., Gigolashvili, T., Flu, U., Saito, K., Kopriva, S., and Gershenzon, J. 2009. Disruption of Adenosine-5 9 -Phosphosulfate Kinase in Arabidopsis Reduces Levels of Sulfated Secondary Metabolites. **21**(March): 910–927. doi:10.1105/tpc.109.065581.

Naito, K., Taguchi, F., Suzuki, T., Inagaki, Y., Toyoda, K., Shiraishi, T., and Ichinose, Y. 2008. Amino Acid Sequence of Bacterial Microbe-Associated Molecular Pattern flg22 Is Required for Virulence. Mol. Plant-Microbe Interact. **21**(9): 1165–1174. doi:10.1094/MPMI-21-9-1165.

Nakano, T., Suzuki, K., Fujimura, T., and Shinshi, H. 2006. Genome-Wide Analysis of the ERF Gene Family. Plant Physiol. **140**(February): 411–432. doi:10.1104/pp.105.073783.currently.

Nakao, M., Nakamura, R., Kita, K., Inukai, R., and Ishikawa, A. 2011. Non-host resistance to penetration and hyphal growth of *Magnaporthe oryzae* in Arabidopsis. Sci. Rep. **1**: 171. doi:10.1038/srep00171.

Nieschlag, H.J., and Regional, N. 1970. Industrial Uses of High Erucic Oils. J. Am. oil Chem. Soc. **48**(September): 723–727.

Nováková, M., Šašek, V., Trdá, L., Krutinová, H., Mongin, T., Valentová, O., Balesdent, M.-H., Rouxel, T., and Burketová, L. 2015. *Leptosphaeria maculans* effector AvrLm4-7 affects SA- and ET-signalling and H2O2 accumulation in *Brassica napus*. Mol. Plant Pathol. **7**(2016): 818–831. doi:10.1111/mpp.12332.

O'Malley, R.C., Huang, S.C., Song, L., Lewsey, M.G., Bartlett, A., Nery, J.R., Galli, M., Gallavotti, A., and Ecker, J.R. 2016. Cistrome and Epicistrome Features Shape the Regulatory DNA Landscape. Cell **165**(5): 1280–1292. doi:10.1016/j.cell.2016.04.038.

Orlando, D.A., Brady, S.M., Koch, J.D., Dinneny, R., and Benfey, P.N. 2009. Manipulating Large-Scale Arabidopsis Microarray Expression Data: Identifying Dominant Expression Patterns and Biological Process Enrichment. *In* Plant Systems Biology. *Edited by* D. Belostotsky. Humana Press. pp. 57–77. doi:10.1007/978-1-60327-563-7.

Osaka, M., Matsuda, T., Sakazono, S., Masuko-Suzuki, H., Maeda, S., Sewaki, M., Sone, M., Takahashi, H., Nakazono, M., Iwano, M., Takayama, S., Shimizu, K.K., Yano, K., Lim, Y.P., Suzuki, G., Suwabe, K., and Watanabe, M. 2013. Cell type-specific transcriptome of Brassicaceae stigmatic papilla cells from a combination of laser microdissection and RNA sequencing. Plant Cell Physiol. **54**(11): 1894–906. doi:10.1093/pcp/pct133.

Pan, R., Satkovich, J., and Hu, J. 2016. E3 ubiquitin ligase SP1 regulates peroxisome biogenesis in Arabidopsis. Proc. Natl. Acad. Sci. U. S. A. **113**(46): E7307-E7316. doi:10.1073/pnas.1613530113.

Parenicova, L. 2003. Molecular and Phylogenetic Analyses of the Complete MADS-Box Transcription Factor Family in Arabidopsis: New Openings to the MADS World. Plant Cell Online **15**(7): 1538–1551. doi:10.1105/tpc.011544.

Parkin, I.A.., Sharpe, A.G., and Lydiate, D.J. 2003. Patterns of genome duplication within the *Brassica napus* genome. Genome **46**(2): 291–303. doi:10.1139/g03-006.

Parlange, F., Daverdin, G., Fudal, I., Kuhn, M.L., Balesdent, M.H., Blaise, F., Grezes-besset, B., and Rouxel, T. 2009. *Leptosphaeria maculans* avirulence gene *AvrLm4-7* confers a dual recognition specificity by the *Rlm4* and *Rlm7* resistance genes of oilseed rape, and circumvents Rlm4-mediated recognition through a single amino acid change. Mol. Microbiol. **71**(4): 851–863. doi:10.1111/j.1365-2958.2008.06547.x.

Pedras, M., C., S., Yaya, E.E., and Glawischnig, E. 2011. The phytoalexins from cultivated and wild crucifers: chemistry and biology. Nat. Prod. Rep. **28**(8): 1381–1405.

Pedras, M.S.C., and Biesenthal, C.J. 1998. Production of the host-selective phytotoxin phomalide by isolates of *Leptosphaeria maculans* and its correlation with sirodesmin PL production. **553**: 547–553.

Pedras, M.S.C., and Jha, M. 2006. Toward the control of *Leptosphaeria maculans*: Design, syntheses, biological activity, and metabolism of potential detoxification inhibitors of the crucifer phytoalexin brassinin. Bioorganic Med. Chem. **14**(14): 4958–4979. doi:10.1016/j.bmc.2006.03.014.

Pedras, M.S.C., Khan, A.Q., and Taylor, J.L. 1998. The phytoalexin camalexin is not metabolized by Phoma lingam, *Alternaria brassicae*, or phytopathogenic bacteria. Plant Sci. **139**(1): 1–8. doi:10.1016/S0168-9452(98)00172-1.

Peluola, C., Fernando, W.G.D., Huvenaars, C., Kutcher, H.R., and Lahlali, R.L. 2013. Effect of flooding on the survival of Leptosphaeria spp . in canola stubble. doi:10.1111/ppa.12036.

Peng, G., Fernando, W.G.D., Kirkham, C.L., Lange, R., Kutcher, R.H., Mclaren, D., and Johnson, E. 2012. Mitigating the risk of blackleg disease of canola using fungicide strategies. *In* Soils and Crops. University of Saskatchewan, Saskatoon, Saskatchewan. pp. 1–7.

Peng, G., Pageau, D., Strelkov, S.E., Gossen, B.D., Hwang, S.-F., and Lahlali, R. 2015. A >2-year crop rotation reduces resting spores of *Plasmodiophora brassicae* in soil and the impact of clubroot on canola. Eur. J. Agron. **70**: 78–84.

Peng, Y., van Wersch, R., and Zhang, Y. 2018. Convergent and Divergent Signaling in PAMP-Triggered Immunity and Effector-Triggered Immunity. Mol. Plant-Microbe Interact. **31**(4): MPMI-06-17-0145.

Petit-houdenot, Y., and Fudal, I. 2017. Complex Interactions between Fungal Avirulence Genes and Their Corresponding Plant Resistance Genes and Consequences for Disease Resistance Management. **8**(June). doi:10.3389/fpls.2017.01072.

Petrie, G.A. 1994. Effects of temperature and moisture on the number, size and septation of ascospores produced by *Leptosphaeria maculans* (blackleg) on rapeseed stubble. Can. Plant Dis. Surv. **74**(2): 141–151.

Pettit, J.H., Slinger, S.J., Evans, E. V., and Marcellus, F.N. 1944. The Utilization of Sunflower Seed Oil Meal, Wheat Distillers' Dried Grains and Rapeseed Oil Meal in Poultry Rations. Sci. Agric. **24**(5): 201–213.

Pitzschke, A., Schikora, A., and Hirt, H. 2009. MAPK cascade signalling networks in plant defence. Curr. Opin. Plant Biol. **12**(4): 421–426.

Plett, J.M., Daguerre, Y., Wittulsky, S., Vayssières, A., Deveau, A., Melton, S.J., Kohler, A., Morrell-Falvey, J.L., Brun, A., Veneault-Fourrey, C., and Martin, F. 2014. Effector MiSSP7 of the mutualistic fungus *Laccaria bicolor* stabilizes the Populus JAZ6 protein and represses jasmonic acid (JA) responsive genes. Proc. Natl. Acad. Sci. U. S. A. **111**(22): 8299–304. National Academy of Sciences. doi:10.1073/pnas.1322671111.

Plissonneau, C., Daverdin, G., Ollivier, B., Blaise, F., Degrave, A., Fudal, I., Rouxel, T., and Balesdent, M. 2016. A game of hide and seek between avirulence genes *AvrLm4-7* and *AvrLm3* in *Leptosphaeria maculans*. New Phytol. **209**: 1613–1624.

Qi, P.F., Balcerzak, M., Rocheleau, H., Leung, W., Wei, Y.M., Zheng, Y.L., and Ouellet, T. 2016. Jasmonic acid and abscisic acid play important roles in host-pathogen interaction between *Fusarium graminearum* and wheat during the early stages of fusarium head blight. Physiol. Mol. Plant Pathol. **93**: 39–48. doi:10.1016/j.pmpp.2015.12.004.

Qiao, M., Sun, J., Liu, N., Sun, T., Liu, G., Han, S., Hou, C., and Wang, D. 2015. Changes of nitric oxide and its relationship with H2O2 and Ca^{2+} in defense interactions between wheat and *Puccinia triticina*. PLoS One **10**(7): 1–19. doi:10.1371/journal.pone.0132265.

Rajaram, S. 2014. Health Benefits of plant-derived α-linolenic acid. Am. J. Clin. Nutr. **100**: 443–448.

Raman, H., Raman, R., Coombes, N., Song, J., Diffey, S., Kilian, A., Lindbeck, K., Barbulescu, D.M., Batley, J., Edwards, D., Salisbury, P.A., and Marcroft, S. 2016. Genome-wide Association Study Identifies New Loci for Resistance to *Leptosphaeria maculans* in Canola Evaluation of Diverse Accessions and. **7**(October): 1–16. doi:10.3389/fpls.2016.01513.

Raman, H., Raman, R., and Larkan, N. 2013. Genetic Dissection of Blackleg Resistance Loci in Rapeseed (*Brassica napus* L.). Plant Breed. from Lab. to Fields: 85–118. doi:10.5772/53611.

Ranf, S., Eschen-Lippold, L., Frhlich, K., Westphal, L., Scheel, D., and Lee, J. 2014. Microbe-associated molecular pattern-induced calcium signaling requires the receptor-like cytoplasmic kinases, PBL1 and BIK1. Ann. Bot. **14**: 1–15. doi:10.1186/s12870-014-0374-4.

Ranf, S., Eschen-Lippold, L., Pecher, P., Lee, J., and Scheel, D. 2011. Interplay between calcium signalling and early signalling elements during defence responses to microbe- or damage-associated molecular patterns. Plant J. **68**(1): 100–113. doi:10.1111/j.1365-313X.2011.04671.x.

Ranty, B., Aldon, D., Cotelle, V., Galaud, J.-P., Thuleau, P., and Mazars, C. 2016. Calcium Sensors as Key Hubs in Plant Responses to Biotic and Abiotic Stresses. Front. Plant Sci. **7**(March): 1–7. doi:10.3389/fpls.2016.00327.

Rao, M. V, Lee, H., Creelman, R. a, Mullet, J.E., and Davis, K.R. 2000. Jasmonic acid signaling modulates ozone-induced hypersensitive cell death. Plant Cell **12**(9): 1633–1646. doi:10.1105/tpc.12.9.1633.

Reyes, J.C., Muro-Pastor, M.I., and Florencio, F.J. 2004. The GATA family of transcription factors in Arabidopsis and rice. Plant Physiol. **134**(April): 1718–1732. doi:10.1104/pp.103.037788.

Rhee, S.Y. 2003. The Arabidopsis Information Resource (TAIR): a model organism database providing a centralized, curated gateway to Arabidopsis biology, research materials and community. Nucleic Acids Res. **31**(1): 224–228. doi:10.1093/nar/gkg076.

Rieu, I., and Powers, S.J. 2009. Real-Time Quantitative RT-PCR: Design, Calculations, and Statistics. Plant Cell Online **21**(4): 1031–1033. doi:10.1105/tpc.109.066001.

Rivas, S., and Thomas, C.M. 2005. Molecular interactions between tomato and the leaf mold pathogen *Cladosporium fulvum*. Annu. Rev. Phytopathol. **43**: 395–436.

Roider, H.G., Kanhere, A., Manke, T., and Vingron, M. 2007. Predicting transcription factor affinities to DNA from a biophysical model. Bioinformatics **23**(2): 134–141. doi:10.1093/bioinformatics/btl565.

Romanus, K., Van Neer, W., Marinova, E., Verbeke, K., Luypaerts, A., Accardo, S., Hermans, I., Jacobs, P., De Vos, D., and Waelkens, M. 2008. Brassicaceae seed oil identified as illuminant in Nilotic shells from a first millennium AD Coptic church in Bawit, Egypt. Anal. Bioanal. Chem. **390**(2): 783–793. doi:10.1007/s00216-007-1704-2.

Rossi, F.R., Gárriz, A., Marina, M., Romero, F.M., Gonzalez, M.E., Collado, I.G., and Pieckenstain, F.L. 2011. The sesquiterpene botrydial produced by *Botrytis cinerea* induces the hypersensitive response on plant tissues and its action is modulated by salicylic acid and jasmonic acid signaling. Mol Plant Microbe Interact **24**(8): 888–896. doi:10.1094/MPMI-10-10-0248.

Roux, B., Rodde, N., Jardinaud, M.F., Timmers, T., Sauviac, L., Cottret, L., Carrère, S., Sallet, E., Courcelle, E., Moreau, S., Debellé, F., Capela, D., De Carvalho-Niebel, F., Gouzy, J., Bruand, C., and Gamas, P. 2014. An integrated analysis of plant and bacterial gene expression in symbiotic root nodules using laser-capture microdissection coupled to RNA sequencing. Plant J. **77**(6): 817–837. doi:10.1111/tpj.12442.

Rouxel, T., Grandaubert, J., Hane, J.K., Hoede, C., van de Wouw, A.P., Couloux, A., Dominguez, V., Anthouard, V., Bally, P., Bourras, S., Cozijnsen, A.J., Ciuffetti, L.M., Degrave, A., Dilmaghani, A., Duret, L., Fudal, I., Goodwin, S.B., Gout, L., Glaser, N., Linglin, J., Kema, G.H.J., Lapalu, N., Lawrence, C.B., May, K., Meyer, M., Ollivier, B., Poulain, J., Schoch, C.L., Simon, A., Spatafora, J.W., Stachowiak, A., Turgeon, B.G., Tyler, B.M., Vincent, D., Weissenbach, J., Amselem, J., Quesneville, H., Oliver, R.P., Wincker, P., Balesdent, M.-H., and Howlett, B.J. 2011. Effector diversification within compartments of the *Leptosphaeria maculans* genome affected by Repeat-Induced Point mutations. Nat. Commun. **2**: 202. doi:10.1038/ncomms1189.

Rouxel, T., Penaud, A., Pinochet, X., Brun, H., and Gout, L. 2003. A 10-year survey of populations of *Leptosphaeria maculans* in France indicates a rapid adaptation towards the *Rlm1* resistance gene of oilseed rape. **109**: 871–881.

Russell, A.R., Ashfield, T., and Innes, R.W. 2015. *Pseudomonas syringae* effector AvrPphB suppresses AvrB-induced activation of RPM1, but not AvrRpm1-induced activation. Mol. Plant. Microbe. Interact. **28**(6): doi:10.1094/MPMI-08-14-0248-R.

Saijo, Y., Loo, E.P., and Yasuda, S. 2017. Pattern recognition receptors and signaling in plant-microbe interactions. Plant J. **93**: 592–613. doi:10.1111/tpj.13808.

Salisbury, P.A. 1995. Blackleg disease on oilseed Brassica in Australia: a review. Aust. J. Exp. Agric. **35**(5): 665–672.

Santi, S., Grisan, S., Pierasco, A., DE Marco, F., and Musetti, R. 2013. Laser microdissection of grapevine leaf phloem infected by stolbur reveals site-specific gene responses associated to sucrose transport and metabolism. Plant. Cell Environ. **36**(2): 343–355. doi:10.1111/j.1365-3040.2012.02577.x.

Sasaki-Sekimoto, Y., Jikumaru, Y., Obayashi, T., Saito, H., Masuda, S., Kamiya, Y., Ohta, H., and Shirasu, K. 2013. Basic helix-loop-helix transcription factors JASMONATE-ASSOCIATED MYC2-LIKE1 (JAM1), JAM2, and JAM3 are negative regulators of jasmonate responses in Arabidopsis. Plant Physiol. **163**(1): 291–304. doi:10.1104/pp.113.220129.

Sašek, V., Nováková, M., Jindřichová, B., Bóka, K., Valentová, O., and Burketová, L. 2012. Recognition of avirulence gene *AvrLm1* from hemibiotrophic ascomycete *Leptosphaeria maculans* triggers salicylic acid and ethylene signaling in *Brassica napus*. Mol. Plant. Microbe. Interact. **25**(9): 1238–50. doi:10.1094/MPMI-02-12-0033-R.

Scarth, R.P.B.E., McVetty, P.B.E., Rimmer, S.R., and Stefansson, B.R. 1988. Stellar low linolenic-high linoleic acid summer rape. Can. J. Plant Sci. **68**(2): 509–511.

Schiffer, R., Görg, R., Jarosch, B., Beckhove, U., Bahrenberg, G., Kogel, K., and Schulze-Lefert, P. 1997. Tissue Dependence and Differential Cordycepin Sensitivity of Race-Specific Resistance Responses in the Barley-Powdery Mildew Interaction. Mol. Plant-Microbe Interact. **10**(7): 830–839. doi:10.1094/MPMI.1997.10.7.830.

Schweighofer, A., Kazanaviciute, V., Scheikl, E., Teige, M., Doczi, R., Hirt, H., Schwanninger, M., Kant, M., Schuurink, R., Mauch, F., and Buchala, A. 2007. The PP2C-type phosphatase AP2C1, which negatively regulates MPK4 and MPK6, modulates innate immunity, jasmonic acid, and ethylene levels in Arabidopsis. Plant Cell **19**(7): 2213–2224.

Serrano, M., Coluccia, F., Torres, M., Haridon, F.L., and Métraux, J. 2014. The cuticle and plant defense to pathogens. Front. Plant Sci. **5**(June): 1–8. doi:10.3389/fpls.2014.00274.

Seybold, H., Trempel, F., Ranf, S., Scheel, D., Romeis, T., and Lee, J. 2014. Ca^{2+} signalling in plant immune response: from pattern recognition receptors to Ca^{2+} decoding mechanisms. New Phytol. **204**(4): 782–790. Wiley/Blackwell (10.1111). doi:10.1111/nph.13031.

Silva, A.T., Ribone, P.A., Chan, R.L., Ligterink, W., and Hilhorst, H.W.M. 2016. A Predictive Coexpression Network Identifies Novel Genes Controlling the Seed-to-Seedling Phase Transition in Arabidopsis thaliana 1. **170**(April): 2218–2231. doi:10.1104/pp.15.01704.

Simon, E.W. 1978. The symptoms of calcium deficiency in plants. New Phytol. **80**(1): 1–15. Wiley/Blackwell (10.1111). doi:10.1111/j.1469-8137.1978.tb02259.x.

Snowdon, R., Lühs, W., and Friedt, W. 2007. Oilseed Rape. *In* Genome Mapping and Molecular Breeding in Plants, Volume 2. pp. 55–114.

Sonah, H., Zhang, X., Deshmukh, R.K., Borhan, M.H., Fernando, W.G.D., and Bélanger, R.R. 2016. Comparative Transcriptomic Analysis of Virulence Factors in *Leptosphaeria maculans* during Compatible and Incompatible Interactions with Canola. Front. Plant Sci. **7**(December): 1784. doi:10.3389/fpls.2016.01784.

Sprague, S.J., Balesdent, M.-H., Brun, H., Hayden, H.L., Marcroft, S.J., Pinochet, X., Rouxel, T., and Howlett, B.J. 2006. Major gene resistance in *Brassica napus* (oilseed rape) is overcome by changes in virulence of populations of *Leptosphaeria maculans* in France and Australia. Eur. J. Plant Pathol. **114**(1): 33–40. doi:10.1007/s10658-005-3683-5.

Srinivasasainagendra, V., Page, G.P., Mehta, T., Coulibaly, I., and Loraine, A.E. 2008. CressExpress: A Tool For Large-Scale Mining of Expression Data from Arabidopsis. Plant Physiol. **147**(3): 1004–1016. doi:10.1104/pp.107.115535.

Staal, J., and Dixelius, C. 2008. RLM3, a potential adaptor between specific TIR-NB-LRR receptors and DZC proteins. Commun. Integr. Biol. **1**(1): 59–61. doi:10.4161/cib.1.1.6394.

Staal, J., Kaliff, M., Persson, M., and Dixelius, C. 2006. Defence components in Arabidopsis against *Leptosphaeria maculans*. Proceedings of the 12th International Rapeseed Congress **4**: 229-231.

Stefansson, B.R., and Hougen, F.W. 1964. Selection of rape plants (*Brassica napus*) with seed oil practically free from erucic acid. Can. J. Plant Sci. **44**: 359–364.

Stefansson, B.R., Hougen, W., and Downey, R.K. 1961. Note on the Isolation of Rape Plants With Seed Oil Free From Erucic Acid. Can. J. Plant Sci. **41**(1): 218–219.

Stender, E.G., O'Shea, C., and Skriver, K. 2015. Subgroup-specific intrinsic disorder profiles of arabidopsis NAC transcription factors: Identification of functional hotspots. Plant Signal. Behav. **10**(6): e1010967. doi:10.1080/15592324.2015.1010967.

Stotz, H.U., Mitrousia, G.K., de Wit, P.J.G.M., and Fitt, B.D.L. 2014. Effector-triggered defence against apoplastic fungal pathogens. Trends Plant Sci. **19**(8): 491–500. Elsevier Ltd. doi:10.1016/j.tplants.2014.04.009.

Tang, W., Coughlan, S., Crane, E., Beatty, M., and Duvick, J. 2006. The Application of Laser Microdissection to In Planta Gene Expression Profiling of the Maize Anthracnose Stalk Rot Fungus *Colletotrichum graminicola*. Mol. Plant-Microbe Interact. **19**(11): 1240–1250. doi:10.1094/MPMI-19-1240.

Tapia-López, R., García-Ponce, B., Dubrovsky, J.G., Garay-Arroyo, A., Pérez-Ruíz, R. V, Kim, S.-H., Acevedo, F., Pelaz, S., and Alvarez-Buylla, E.R. 2008. An AGAMOUS-related MADS-box gene, XAL1 (AGL12), regulates root meristem cell proliferation and flowering transition in Arabidopsis. Plant Physiol. **146**(3): 1182–1192. doi:10.1104/pp.107.108647.

Taylor-Teeples, M., Lin, L., de Lucas, M., Turco, G., Toal, T.W., Gaudinier, A., Young, N.F., Trabucco, G.M., Veling, M.T., Lamothe, R., Handakumbura, P.P., Xiong, G., Wang, C., Corwin, J., Tsoukalas, A., Zhang, L., Ware, D., Pauly, M., Kliebenstein, D.J., Dehesh, K., Tagkopoulos, I., Breton, G., Pruneda-Paz, J.L., Ahnert, S.E., Kay, S.A., Hazen, S.P., and Brady, S.M. 2014. An Arabidopsis gene regulatory network for secondary cell wall synthesis. Nature **517**(7536): 571–575. doi:10.1038/nature14099.

Teper, D., Girija, A.M., Bosis, E., Popov, G., Savidor, A., and Sessa, G. 2018. The Xanthomonas euvesicatoria type III effector XopAU is an active protein kinase that manipulates plant MAP kinase signaling. PLOS Pathog. **14**(1): e1006880. doi:10.1371/journal.ppat.1006880.

The Arabidopsis Genome Initiative. 2000. Analysis of the genome sequence of the flowering plant Arabidopsis thaliana. Nature **408**(6814): 796–815. doi:10.1038/35048692.

Thomma, B.P.H.J., Nürnberger, T., Joosten, M.H.A.J. 2011. Of PAMPs and Effectors: The Blurred PTI-ETI Dichotomy. Plant Cell **23**(1): 4–15. doi:10.1105/tpc.110.082602.

Tian, T., Liu, Y., Yan, H., You, Q., Yi, X., Du, Z., Xu, W., and Su, Z. 2017. AgriGO v2.0: A GO analysis toolkit for the agricultural community, 2017 update. Nucleic Acids Res. **45**(W1): 122–129. doi:10.1093/nar/gkx382.

Tode, H.I. 1791. Fungi Mecklenburgenses Selecti. Fasc. II **51**(Plate XVI): Fig. 126.

Tollenaere, R., Hayward, A., Dalton-morgan, J., Campbell, E., Lee, J.R.M., Michal, T., Manoli, S., Stiller, J., Raman, R., Raman, H., Edwards, D., Batley, J., Lorenc, M.T., Manoli, S., Stiller, J., Raman, R., Raman, H., Edwards, D., and Batley, J. 2012. Identification and characterization of candidate *Rlm4* blackleg resistance genes in *Brassica napus* using next-generation sequencing. Plant Biotechnol. J. **10**(6): 709–715. doi:10.1111/j.1467-7652.2012.00716.x.

Toscano- Underwood, C., Huang, Y.J., Fitt, B.D.L., and Hall, A.M. 2003. Effects of temperature on maturation of pseudothecia of *Leptosphaeria maculans* and *L. biglobosa* on oilseed rape stem debris. Plant Pathol. **52**: 726–730.

Trapnell, C., Roberts, A., Goff, L., Pertea, G., Kim, D., Kelley, D.R., Pimentel, H., Salzberg, S.L., Rinn, J.L., and Pachter, L. 2012. Differential gene and transcript expression analysis of RNA-seq experiments with TopHat and Cufflinks. Nat. Protoc. **7**(3): 562–78. doi:10.1038/nprot.2012.016.

Travadon, R., Bousset, L., Saint-Jean, S., Brun, H., Sache, I., Cedex, L.R., Pg, I., Environnement, U.M.R., Grignon, T., and Umr, I.P.G. 2007. Splash dispersal of *Leptosphaeria maculans* pycnidiospores and the spread of blackleg on oilseed rape. Plant Pathol. **56**(4): 595–603. doi:10.1111/j.1365-3059.2007.01572.x.

Trdá, L., Barešová, M., Šašek, V., Nováková, M., Zahajská, L., Dobrev, P.I., Motyka, V., and Burketová, L. 2017. Cytokinin metabolism of pathogenic fungus *Leptosphaeria maculans* involves isopentenyltransferase, adenosine kinase and cytokinin oxidase/dehydrogenase. Front. Microbiol. **8**(July): 1–20. Frontiers Media SA. doi:10.3389/fmicb.2017.01374.

Tsuda, K., and Somssich, I.E.E. 2015. Tansley review Transcriptional networks in plant immunity. New Phytol. **2**(3): 932–47. doi:10.1111/nph.13286.

U, N. 1935. Genome analysis in Brassica with special reference to the experimental formation of *B. napus* and peculiar mode of fertilization. Japanese J. Bot. **7**(7): 389–452.

Uloth, M.B., You, M.P., and Barbetti, M.J. 2016. Cultivar resistance offers the first opportunity for effective management of the emerging powdery mildew (*Erysiphe cruciferarum*) threat to oilseed brassicas in Australia. Crop Pasture Sci. **67**: 1179–1187.

Vaistij, F.E., Gan, Y., Penfield, S., Gilday, A.D., Dave, A., He, Z., Josse, E.-M., Choi, G., Halliday, K.J., and Graham, I. a. 2013. Differential control of seed primary dormancy in Arabidopsis ecotypes by the transcription factor SPATULA. Proc. Natl. Acad. Sci. U. S. A. **110**(26): 10866–71. doi:10.1073/pnas.1301647110.

Vatsa-Portugal, P., Aziz, A., Rondeau, M., Villaume, S., Morjani, H., Clément, C., and Ait Barka, E. 2017. How Streptomyces anulatus Primes Grapevine Defenses to Cope with Gray Mold: A Study of the Early Responses of Cell Suspensions. Front. Plant Sci. **8**(June): 1–12. doi:10.3389/fpls.2017.01043.

Wan, H., Cui, Y., Ding, Y., Mei, J., Dong, H., Zhang, W., Wu, S., Liang, Y., Zhang, C., Li, J., Xiong, Q., and Qian, W. 2017. Time-Series Analyses of Transcriptomes and Proteomes Reveal Molecular Networks Underlying Oil Accumulation in Canola. Front. Plant Sci. **7**(January): 1–17. doi:10.3389/fpls.2016.02007.

Wang, D., Guo, Y., Wu, C., Yang, G., Li, Y., and Zheng, C. 2008. Genome-wide analysis of CCCH zinc finger family in Arabidopsis and rice. BMC Genomics **9**: 44. doi:10.1186/1471-2164-9-44.

Wang, Y., and Navin, N.E. 2015. Advances and Applications of Single-Cell Sequencing Technologies. Mol. Cell **58**(4): 598–609. Elsevier Inc. doi:10.1016/j.molcel.2015.05.005.

Wang, Y.H. 2008. How effective is T-DNA insertional mutagenesis in Arabidopsis? J Biochem Tech **1**(1): 11–20.

Wang, Z., Meng, P., Zhang, X., Ren, D., and Yang, S. 2011. BON1 interacts with the protein kinases BIR1 and BAK1 in modulation of temperature-dependent plant growth and cell death in Arabidopsis. Plant J. **67**(6): 1081–1093. doi:10.1111/j.1365-313X.2011.04659.x.

Weiberg, A., Wang, M., Lin, F.-M., Zhao, H., Zhang, Z., Kaloshian, I., Huang, H.-D., Jin, H., Khaloshian, I., Huang, H.-D., and Jin, H. 2014. Fungal Small RNAs Suppress Plant Immunity by Hijacking Host RNA Interference Pathways. Science **342**(6154): 118–123. doi:10.1126/science.1239705.

West, J.S., Kharbanda, P.D., Barbetti, M.J., and Fitt, B.D.L. 2001. Epidemiology and management of *Leptosphaeria maculans* (phoma stem canker) on oilseed rape in Australia, Canada and Europe. Plant Pathol. **50**(50): 10–27.

Westermann, A.J., Barquist, L., and Vogel, J. 2017. Resolving host–pathogen interactions by dual RNA-seq. PLoS Pathog. **13**(2): 1–19. doi:10.1371/journal.ppat.1006033.

Winter, M., and Koopmann, B. 2016. Race spectra of *Leptosphaeria maculans*, the causal agent of blackleg disease of oilseed rape, in different geographic regions in northern Germany. Eur. J. Plant Pathol. **145**: 629–641. doi:10.1007/s10658-016-0932-8.

Van de Wouw, A.P., Cozijnsen, A.J., Hane, J.K., Brunner, P.C., McDonald, B. a, Oliver, R.P., and Howlett, B.J. 2010. Evolution of linked avirulence effectors in *Leptosphaeria maculans* is affected by genomic environment and exposure to resistance genes in host plants. PLoS Pathog. **6**(11): e1001180. doi:10.1371/journal.ppat.1001180.

Wouw, A.P. Van De, Howlett, B.J., and Idnurm, A. 2018. Changes in allele frequencies of avirulence genes in the blackleg fungus, *Leptosphaeria maculans*, over two decades in Australia. Crop & Pasture Sci. **69**: 20–29.

Wouw, A.P. Van De, Idnurm, A., Davidson, J.A., Sprague, S.J., Khangura, R.K., Van de Wouw, A.P., Idnurm, A., Davidson, J.A., Sprague, S.J., Khangura, R.K., Ware, A.H., Lindbeck, K.D., and Marcroft, S.J. 2016a. Fungal diseases of canola in Australia: identification of trends, threats and potential therapies. Australas. Plant Pathol. **45**(4): 415–423. Australasian Plant Pathology. doi:10.1007/s13313-016-0428-1.

Wouw, A.P. Van De, Marcroft, S.J., and Howlett, B.J. 2016b. Blackleg disease of canola in Australia. Crop Pasture Sci. **67**: 273–283.

Wouw, A.P. Van De, Marcroft, S.J., Ware, A., Lindbeck, K., Khangura, R., and Howlett, B.J. 2014. Field Crops Research Breakdown of resistance to the fungal disease , blackleg , is averted in commercial canola (*Brassica napus*) crops in Australia. F. Crop. Res. **166**: 144–151. doi:10.1016/j.fcr.2014.06.023.

Van de Wouw, A.P., Elliott, V.L., Ware, A., Lindbeck, K., Howlett, B.J., and Marcroft, S.J. 2016. Infection of canola pods by *Leptosphaeria maculans* and subsequent seed contamination. Eur. J. Plant Pathol. **145**(3): 687–695. doi:10.1007/s10658-015-0827-0.

Van de Wouw, A.P., Lowe, R.G.T., Elliott, C.E., Dubois, D.J., Howlett, B.J. 2014. An avirulence gene, *AvrLmJ1*, from the blackleg fungus, *Leptosphaeria maculans*, confers avirulence to *Brassica juncea* cultivars. Mol. Plant Pathol. **15**(5): 523–530. doi:10.1111/mpp.12105.

Wu, J., van der Burgh, A.M., Bi, G., Zhang, L., Alfano, J.R., Martin, G.B., and Joosten, M.H.A.J. 2018. The Bacterial Effector AvrPto Targets the Regulatory Coreceptor SOBIR1 and Suppresses Defense Signaling Mediated by the Receptor-Like Protein Cf-4. Mol. Plant-Microbe Interact. **31**(1): 75–85. Molecular Plant-Microbe Interactions. doi:10.1094/MPMI-08-17-0203-FI.

Yamada, K., Yamaguchi, K., Yoshimura, S., Terauchi, A., and Kawasaki, T. 2017. Conservation of chitin-induced MAPK signaling pathways in rice and arabidopsis. Plant Cell Physiol. **58**(6): 993–1002. doi:10.1093/pcp/pcx042.

Yamaguchi, K., Yamada, K., Ishikawa, K., Yoshimura, S., Hayashi, N., Uchihashi, K., Ishihama, N., Kishi-Kaboshi, M., Takahashi, A., Tsuge, S., Ochiai, H., Tada, Y., Shimamoto, K., Yoshioka, H., and Kawasaki, T. 2013. A Receptor-like Cytoplasmic Kinase Targeted by a Plant Pathogen Effector Is Directly Phosphorylated by the Chitin Receptor and Mediates Rice Immunity. Cell Host Microbe **13**(3): 347–357. doi:10.1016/J.CHOM.2013.02.007.

Yan, T., Yoo, D., Berardini, T.Z., Mueller, L.A., Weems, D.C., Weng, S., Cherry, J.M., and Rhee, S.Y. 2005. PatMatch: A program for finding patterns in peptide and nucleotide sequences. Nucleic Acids Res. **33**(S2): 262–266. doi:10.1093/nar/gki368.

Yang, D.-H., Hettenhausen, C., Baldwin, I.T., and Wu, J. 2011. BAK1 regulates the accumulation of jasmonic acid and the levels of trypsin proteinase inhibitors in *Nicotiana attenuata*'s responses to herbivory. J. Exp. Bot. **62**(2): 641–652. Oxford University Press. doi:10.1093/jxb/erq298.

Yang, D.-L., Shi, Z., Bao, Y., Yan, J., Yang, Z., Yu, H., Li, Y., Gou, M., Wang, S., Zou, B., Xu, D., Ma, Z., Kim, J., and Hua, J. 2017. Calcium Pumps and Interacting BON1 Protein Modulate Calcium Signature, Stomatal Closure, and Plant Immunity. Plant Physiol. **175**(1): 424–437. doi:10.1104/pp.17.00495.

Yanhui, C., Xiaoyuan, Y., Kun, H., Meihua, L., Jigang, L., Zhaofeng, G., Zhiqiang, L., Yunfei, Z., Xiaoxiao, W., Xiaoming, Q., Yunping, S., Li, Z., Xiaohui, D., Jingchu, L., Xing-Wang, D., Zhangliang, C., Hongya, G., and Li-Jia, Q. 2006. The MYB transcription factor superfamily of Arabidopsis: Expression analysis and phylogenetic comparison with the rice MYB family. Plant Mol. Biol. **60**(1): 107–124. doi:10.1007/s11103-005-2910-y.

Yilmaz, A., Mejia-Guerra, M.K., Kurz, K., Liang, X., Welch, L., and Grotewold, E. 2011. AGRIS: The arabidopsis gene regulatory information server, an update. Nucleic Acids Res. **39**(S1): 1118–1122. doi:10.1093/nar/gkq1120.

Yu, C.-P., Lin, J.-J., and Li, W.-H. 2016. Positional distribution of transcription factor binding sites in Arabidopsis thaliana. Sci. Rep. **6**(April): 25164. doi:10.1038/srep25164.

Yu, X., Zheng, G., Shan, L., Meng, G., Vingron, M., Liu, Q., and Zhu, X.-G. 2014. Reconstruction of gene regulatory network related to photosynthesis in *Arabidopsis thaliana*. Front. Plant Sci. **5**(June): 1–9. doi:10.3389/fpls.2014.00273.

Yuan, P., Jauregui, E., Du, L., Tanaka, K., and Poovaiah, B.W. 2017. Calcium signatures and signaling events orchestrate plant–microbe interactions. Curr. Opin. Plant Biol. **38**: 173–183. Elsevier Ltd. doi:10.1016/j.pbi.2017.06.003.

Zeng, W., Melotto, M., and He, S.Y. 2010. Plant stomata: A checkpoint of host immunity and pathogen virulence. Curr. Opin. Biotechnol. **21**(5): 599–603. Elsevier Ltd. doi:10.1016/j.copbio.2010.05.006.

Zhang, W., Fraiture, M., Kolb, D., Loffelhardt, B., Desaki, Y., Boutrot, F.F.G., Tor, M., Zipfel, C., Gust, A.A., and Brunner, F. 2013. Arabidopsis RECEPTOR-LIKE PROTEIN30 and Receptor-Like Kinase SUPPRESSOR OF BIR1-1/EVERSHED Mediate Innate Immunity to Necrotrophic Fungi. Plant Cell **25**(10): 4227–4241. doi:10.1105/tpc.113.117010.

Zhang, X., and Fernando, W.G.D. 2018. Insights into fighting against blackleg disease of *Brassica napus* in Canada. Crop Pasture Sci. **69**: 40–47.

Zhang, X., Peng, G., Kutcher, H.R., Balesdent, M.H., Delourme, R., and Fernando, W.G.D. 2016. Breakdown of *Rlm3* resistance in the *Brassica napus–Leptosphaeria maculans* pathosystem in western Canada. Eur. J. Plant Pathol. **145**(3): 659–674. doi:10.1007/s10658-015-0819-0.

Zhang, Y., Huai, D., Yang, Q., Cheng, Y., Ma, M., Kliebenstein, D.J., and Zhou, Y. 2015. Overexpression of three glucosinolate biosynthesis genes in *Brassica napus* identifies enhanced resistance to *Sclerotinia sclerotiorum* and *Botrytis cinerea*. PLoS One **10**(10): 1–17. doi:10.1371/journal.pone.0140491.

Zhang, Z., Liu, Y., Huang, H., Gao, M., Wu, D., Kong, Q., and Zhang, Y. 2017. The NLR protein SUMM2 senses the disruption of an immune signaling MAP kinase cascade via CRCK3. EMBO Rep. **18**(2): 292–302. EMBO Press. doi:10.15252/embr.201642704.

Zhao, L., Chen, Y., Yang, W., Zhang, Y., Chen, W., Feng, C., Wang, Q., and Wu, Y. 2018. Polysaccharide Peptide–Induced Virus Resistance Depends on Ca^{2+} Influx by Increasing the Salicylic Acid Content and Upregulating the Leucine-Rich Repeat Gene in *Arabidopsis thaliana*. Mol. Plant-Microbe Interact. **31**(5): MPMI-10-17-0242. doi:10.1094/MPMI-10-17-0242-R.

Zheng, Y., Jiao, C., Sun, H., Rosli, H.G., Pombo, M.A., Zhang, P., Banf, M., Dai, X., Martin, G.B., Giovannoni, J.J., Zhao, P.X., Rhee, S.Y., and Fei, Z. 2016. iTAK: A Program for Genome-wide Prediction and Classification of Plant Transcription Factors, Transcriptional Regulators, and Protein Kinases. Mol. Plant **9**(12): 1667–1670. doi:10.1016/j.molp.2016.09.014.

Zheng, Z., Mosher, S.L., Fan, B., Klessig, D.F., and Chen, Z. 2007. Functional analysis of Arabidopsis WRKY25 transcription factor in plant defense against *Pseudomonas syringae*. BMC Plant Biol. **7**: 2. doi:10.1186/1471-2229-7-2.

Zhou, J., Wu, S., Chen, X., Liu, C., Sheen, J., Shan, L., and He, P. 2014. The *Pseudomonas syringae* effector HopF2 suppresses Arabidopsis immunity by targeting BAK1. Plant J. **77**(2): 235–245. Wiley/Blackwell (10.1111). doi:10.1111/tpj.12381.

Zhou, S., Jia, L., Chu, H., Wu, D., Peng, X., Liu, X., Zhang, J., Zhao, J., Chen, K., and Zhao, L. 2016. Arabidopsis CaM1 and CaM4 Promote Nitric Oxide Production and Salt Resistance by Inhibiting S-Nitrosoglutathione Reductase via Direct Binding. PLOS Genet. **12**(9): e1006255.

Zhou, Y., Sun, L., Wassan, G.M., He, X., Shaban, M., Zhang, L., Zhu, L., and Zhang, X. 2018. GbSOBIR1 confers *Verticillium* wilt resistance by phosphorylating the transcriptional factor GbbHLH171 in *Gossypium barbadense*. Plant Biotechnol. J.: doi:10.1111/pbi.12954.

Zhou, Y., Xu, D., Jia, L., Huang, X., Ma, G., Wang, S., Zhu, M., Zhang, A., Guan, M., Lu, K., Xu, X., Wang, R., Li, J., and Qu, C. 2017. Genome-wide identification and structural analysis of bZIP transcription factor genes in *Brassica napus*. Genes (Basel). **8**(10): 1–24. doi:10.3390/genes8100288.

Zhu, X., Soliman, A., Islam, M.R., Adam, L.R., and Daayf, F. 2017. *Verticillium dahliae*'s Isochorismatase Hydrolase Is a Virulence Factor That Contributes to Interference With Potato's Salicylate and Jasmonate Defense Signaling. Front. Plant Sci. **8**(March): 1–15. doi:10.3389/fpls.2017.00399.

Zou, Z., Zhang, X., Gerard, W., Fernando, D., and Fernando, W.G.D. 2018. Distribution of mating-type alleles and genetic variability in field populations of *Leptosphaeria maculans* in western Canada. J. Phytopathol. **166**(6): 438–447. doi:10.1111/jph.12706.

Zuluaga, A.P., Vega-Arreguín, J.C., Fei, Z., Matas, A.J., Patev, S., Fry, W.E., and Rose, J.K.C. 2016a. Analysis of the tomato leaf transcriptome during successive hemibiotrophic stages of a compatible interaction with the oomycete pathogen *Phytophthora infestans*. Mol. Plant Pathol. **17**(1): 42–54. doi:10.1111/mpp.12260.

Zuluaga, A.P., Vega-Arreguín, J.C., Fei, Z., Ponnala, L., Lee, S.J., Matas, A.J., Patev, S., Fry, W.E., and Rose, J.K.C. 2016b. Transcriptional dynamics of *Phytophthora infestans* during sequential stages of hemibiotrophic infection of tomato. Mol. Plant Pathol. **17**(1): 29–41. doi:10.1111/mpp.12263.

7 Appendices

Appendix I: Characterization of *R*-genes carried in resistant line DF78 and susceptible cv. Westar. A total of 34 characterized *L. maculans* isolates were tested against cv. DF78 and cv. Westar and interaction phenotype was recorded as resistant [R] or susceptible [S]. The genotype of *Avr* genes enclosed in ( ) are not determined.

Isolates	Avirulence genotype	Interaction with DF78	Interaction with Westar
D1	*AvrLm2,5,6,9,(10),S,AvrLepR1, 2*	R	S
D2	*AvrLm5,6,8,(10),11,S,AvrLepR1*	R	S
D3	*AvrLm5,(10),11,AvrLepR1*	R	S
D4	*AvrLm4, 5,6,7,8,(10),11,AvrLepR1,2*	R	S
D5	*AvrLm1,2,4,7,(10),11,S,AvrLepR1,2*	R	S
D6	*AvrLm1,5,6,8,(10),11,S*	R	S
D7	*AvrLm1,3,5,6,8,(10),11,(S),AvrLepR1*	R	S
D8	*AvrLm5,7,(8,10),11, AvrLepR1*	R	S
D9	*AvrLm5,6, 7,(8, 10),11, AvrLepR1*	R	S
D10	*AvrLm5,6,8,9,(10),11,S*	R	S
D13	*AvrLm4,6,7,(8,10),11*	S	S
D14	*AvrLm1,7,(5,8,10),11,S, AvrLepR1*	R	S
S7	*AvrLm1,5,6,7,(8), 11,AvrLepR1*	R	S
ICBN14	*AvrLm5,6,10,AvrLepR1*	R	S
PHW1223	*AvrLm5,6,8,9,11*	R	S
R2	*AvrLm5,7,10,(8), AvrLepR1*	R	S
AD746	*AvrLm3,6,(8), AvrLepR1*	R	S
JN2	*AvrLm5,6,7,8, 11,AvrLepR1*	R	S
JN3	*AvrLm1,4,5,6,7,8,11*	R	S
J3	*AvrLm2,3,5,6,(8,10),11,S*	R	S
J20	*AvrLm2,3,6,(8,10),11,S,AvrLepR1*	R	S
Q12	*AvrLm2, 4,5,7,(8,10), 11,AvrLepR1*	R	S
L-MD7-14	*AvrLm4,5,6,7,(8,10),11*	S	S
L-PC4-1	*AvrLm2,4,(8,10),11*	S	S
L-MP1-8	*AvrLm2,4,5,6,7,(8,10),11*	S	S
L-Sb1	*AvrLm2,3,5,6,7, (8,10),S,11*	R	S
L-MP1-6	*AvrLm4,5,6,7,(8,10),11*	S	S
L-Sb7-6	*AvrLm4,5,6,7,(8,10),11, LepR1*	R	S
L-Br17-1	*AvrLm5,6,7,(4,8,10),11,LepR1*	R	S
L-Mo5-1	*AvrLm2,4,5,6,7, (8,10),11, LepR2*	S	S
L-Br1-16	*AvrLm1,4,5,6,7,(8,10, S),11*	S	S
RL25	*AvrLm5,6,7,(8,10),11,S*	S	S
DS103	*AvrLm5,9,(8,10),11*	S	S
CV8-7	*AvrLm2,4,5,6,7,(5,8,10),11,S*	S	S

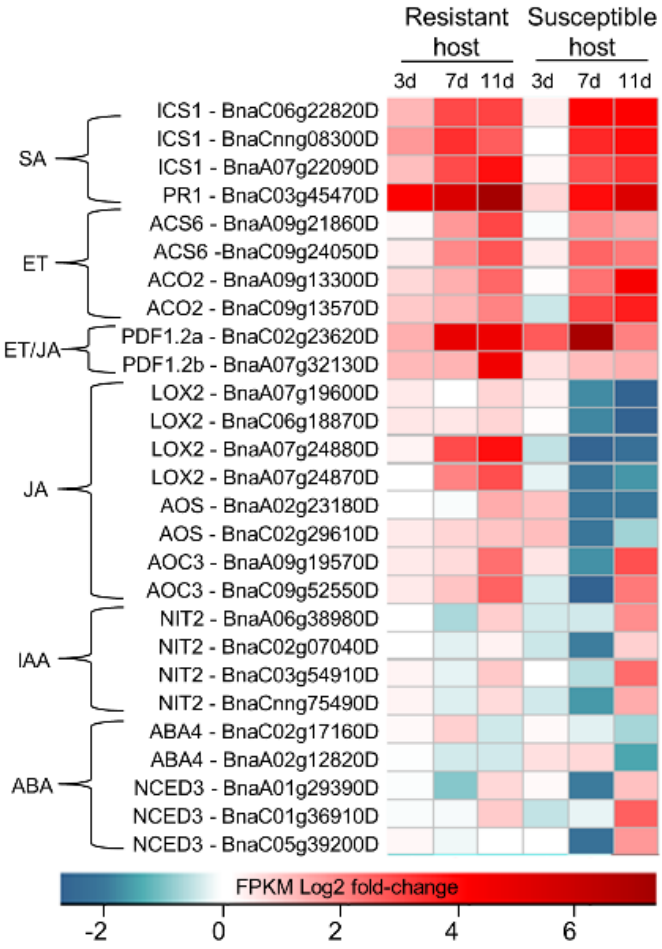

Appendix II: Expression levels of hormone biosynthetic genes and hormone signaling markers in response to *L. maculans*. Heatmap of Log2 transcript level fold-change vs. mock controls in resistant (R) and susceptible (S) cotyledons at 3, 7, and 11 days post *L. maculans* inoculation.

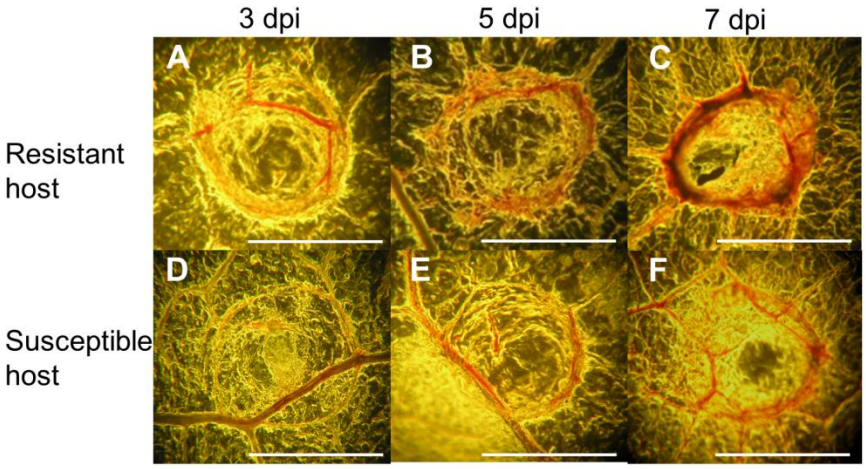

Appendix III: Deposition of lignified plant materials at the infection site in resistant and susceptible hosts. Cotyledons are infected with *L. maculans* and stained with phloroglucinol-HCL. Lignified plant materials appear dark orange/red. Scales = 1 mm.

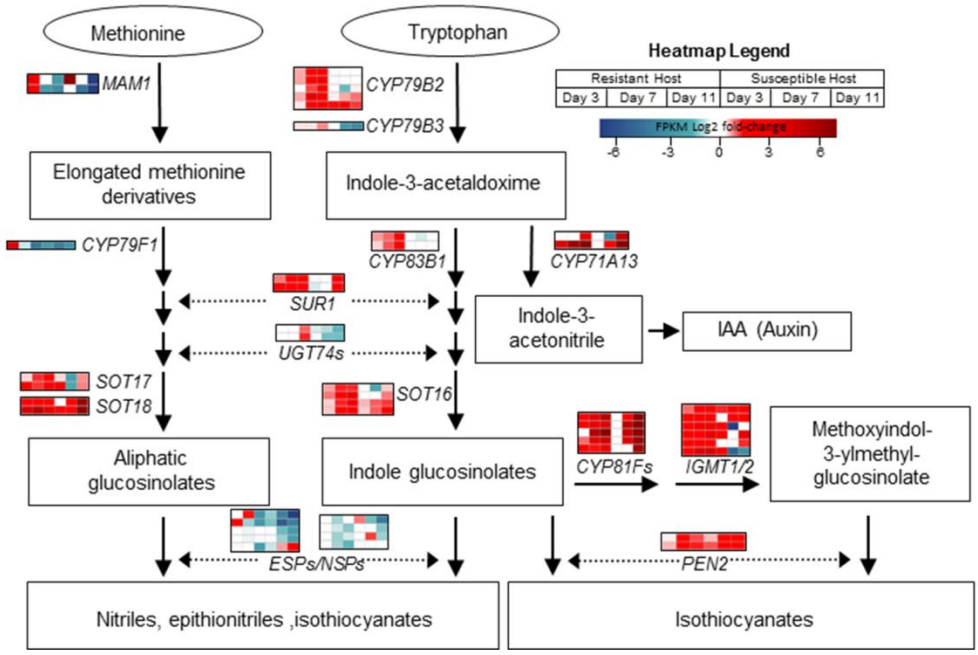

Appendix IV: Differentially expressed ($p < 0.05$) glucosinolate and indole glucosinolate biosynthetic genes in *B. napus* cotyledons infection with *L. maculans*. Changes in expression of biosynthetic gene homologs are shown across their respective biosynthetic pathways. Fluctuations in gene expression are recorded as FPKM [Fragments Per Kilobase of transcript per Million mapped reads] deviation from mock controls. A more intense red colour reflects gene activation, a more intense blue colour represents gene repression.

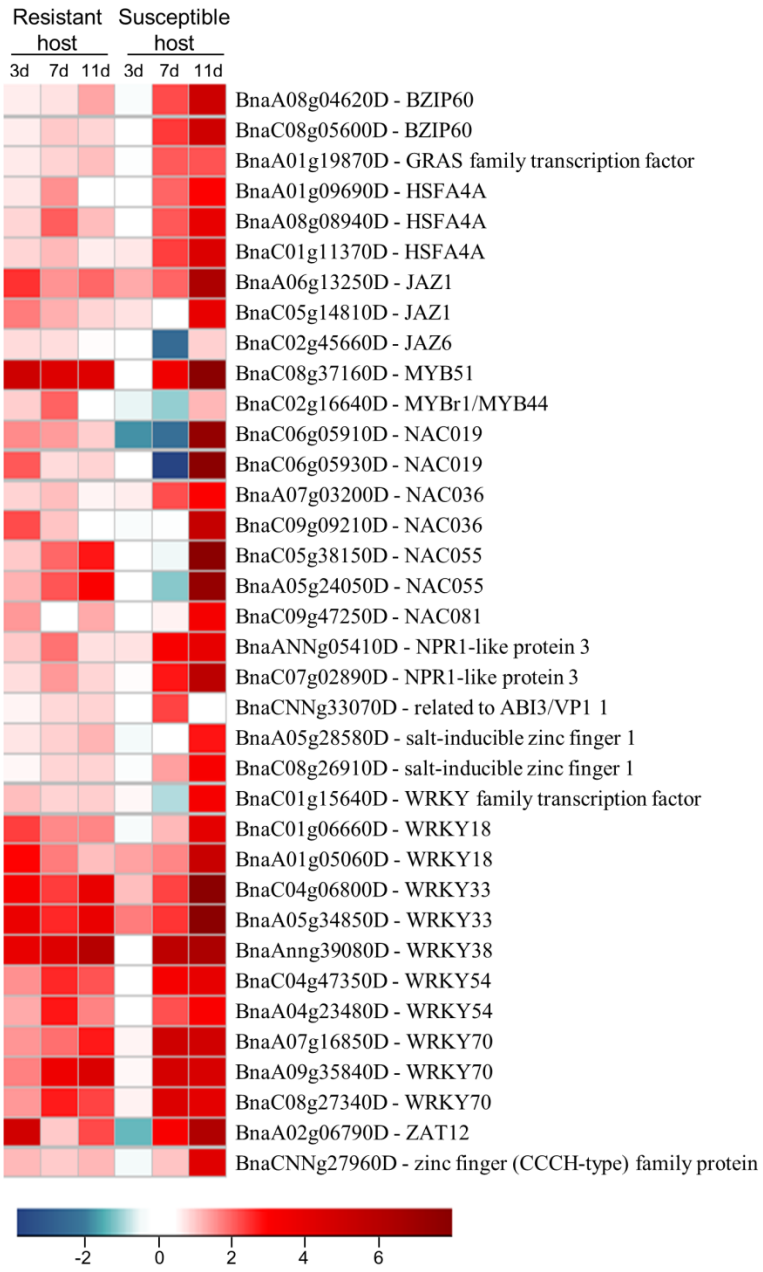

Appendix V: Transcript levels of transcription factors expressed in response to *L. maculans*. Heatmap of Log2 transcript level fold-change vs. mock controls in resistant (R) and susceptible (S) cotyledons at 3, 7, and 11 days post *L. maculans* inoculation.

Appendix VI: Complete list of 54 genes with significantly (P < 0.5) elevated expression in response to *L. maculans* at every time point specifically in resistant line DF78, and their putative Arabidopsis homolog and annotation. Genes with no identifiable Arabidopsis homolog from nucleotide or protein BLAST searches are marked as 'no hit' and are of unknown function.

B. napus locus	Putative Arabidopsis homolog	Putative Annotation
BnaC05g38740D	AT3G14840	LYSM RLK1-interacting kinase 1
BnaA01g12650D	AT4G23190	cysteine-rich RLK (RECEPTOR-like protein kinase) 11
BnaAnng25570D	AT4G23290	cysteine-rich RLK (RECEPTOR-like protein kinase) 21
BnaCnng49020D	AT4G04540	cysteine-rich RLK (RECEPTOR-like protein kinase) 39
BnaA03g25470D	AT4G04540	cysteine-rich RLK (RECEPTOR-like protein kinase) 39
BnaC07g06130D	AT2G17120	lysm domain GPI-anchored protein 2 precursor
BnaC03g71330D	AT5G01950	Leucine-rich repeat protein kinase family protein
BnaA02g12640D	AT1G66880	Protein kinase superfamily protein
BnaA03g36540D	AT4G11850	phospholipase D gamma 1
BnaA07g22750D	AT1G73260	Kunitz Trypsin Inhibitor 1
BnaA07g30760D	AT1G73260	Kunitz Trypsin Inhibitor 1
BnaA06g12220D	AT3G05360	receptor like protein 30
BnaA03g43720D	AT4G18250	Putative receptor kinase
BnaC04g27200D	AT3G53490	Putative receptor kinase
BnaA10g07090D	AT1G11330	S-locus lectin protein kinase family protein
BnaCnng55880D	AT1G11330	S-locus lectin protein kinase family protein
BnaAnng21280D	AT4G17500	ethylene responsive element binding factor 1
BnaA02g25110D	AT5G47220	ethylene responsive element binding factor 2
BnaA09g50010D	AT1G06160	octadecanoid-responsive Arabidopsis AP2/ERF 59
BnaC07g23070D	AT3G25882	NIM1-interacting 2
BnaA03g04410D	AT5G13550	sulfate transporter 4.1
BnaC07g51290D	AT4G39940	APS-kinase 2
BnaCnng04780D	AT1G25220	anthranilate synthase beta subunit 1
BnaA01g34610D	AT4G39950	cytochrome P450, family 79, subfamily B, polypeptide 2
BnaC01g00800D	AT4G39950	cytochrome P450, family 79, subfamily B, polypeptide 2
BnaA04g12790D	AT2G22330	cytochrome P450, family 79, subfamily B, polypeptide 3
BnaA08g04520D	AT4G31500	cytochrome P450, family 83, subfamily B, polypeptide 1
BnaC08g05690D	AT4G31500	cytochrome P450, family 83, subfamily B, polypeptide 1
BnaA04g27110D	AT2G46650	cytochrome B5 isoform C
BnaC04g50950D	AT2G46650	cytochrome B5 isoform C
BnaC06g21620D	AT1G76790	Indole Glucosinolate O-methyltransferase 5
BnaA03g58530D	AT4G21120	amino acid transporter 1

BnaA07g23890D	AT1G70260	Usually multiple acids movie in and out transporter 36
BnaA06g31460D	AT3G28480	Oxoglutarate/iron-dependent oxygenase
BnaC03g62400D	AT4G35630	phosphoserine aminotransferase
BnaAnng33720D	AT1G20160	Response secreted protease
BnaC01g41020D	AT4G19810	Chitinase C
BnaAnng42000D	AT4G29700	Alkaline-phosphatase-like family protein
CUFF.2933.3	AT5G14930	senescence-associated gene 101
BnaA05g29820D	AT3G14040	Pectin lyase-like superfamily protein
BnaA06g37630D	AT4G04775	zinc ion binding
BnaA04g17910D	AT2G30860	glutathione S-transferase PHI 9
BnaA09g28900D	AT1G26420	FAD-binding Berberine family protein
BnaA05g07460D	AT2G36970	UDP-Glycosyltransferase superfamily protein
BnaC07g47720D	AT4G38540	FAD/NAD(P)-binding oxidoreductase family protein
BnaC06g18710D	AT1G21310	extensin 3
BnaC04g55140D	AT3G60420	Phosphoglycerate mutase family protein
BnaC04g21680D	AT3G61640	arabinogalactan protein 20
BnaC09g52960D	AT5G53110	RING/U-box superfamily protein
BnaA09g19740D	AT5G01750	Protein of unknown function (DUF567)
BnaC06g28720D	no hit	N/A
BnaC02g31360D	no hit	N/A
BnaC06g41090D	no hit	N/A
BnaA03g08620D	no hit	N/A

Appendix VII: Results of Arabidopsis mutant susceptibility screening for blackleg disease. A total of 49 loss-of-function Col-0 background Arabidopsis mutants were screened for blackleg disease susceptibility. Blackleg resistance evaluation: R, resistant, infected plants showed small lesions with clear black borders; +, some visual evidence for marginal breakdown of non-host resistance where fungal load increase not significant in qPCR assays; ++ lesions spread into host tissues and infected hosts have significantly ($p < 0.05$) higher fungal loads; +++ reproductive structures (pycnidia) of fungus are visible and hosts have significantly higher ($p < 0.05$) fungal loads.

Mutant	T-DNA insertion line	Gene name	Insertion site	Blackleg resistance
N/A	Col-0	N/A	N/A	R
at3g11820	SALK_087016C	*PEN1*	Promoter	++
at3g53490	SALK_036238	u/c	Promoter	+
at3g14840	SALK_030855C	*LIK1*	Exon	+
at4g18250	SALK_043853C	u/c	Intron	++
at4g18250	SALK_072295C	u/c	Promoter	++
at1g73260	SALK_131716C	*KTI1*	Promoter	+++
at4g39940	SALK_025296C	*APK2*	Exon	++
at4g39940	SALK_060023C	*APK2*	Promoter	+
at3g14840	SALK_056862	*LIK1*	Promoter	R
at1g02930	SALK_026398C	*GSTF6*	Intron	R
at4g21120	SALK_087921C	*AAT1*	Exon	R
at4g21120	SALK_059873C	*AAT1*	Intron	R
at1g33950	SALK_000761C	u/c	Intron	R
at1g02930	SALK_065940C	*GSTF6*	Exon	R
at4g17500	SALK_036267	*ERF-1*	Promoter	R
at4g04540	SALK_098187C	*CRK39*	Exon	R
at3g60420	SALK_057524C	u/c	promoter	R
at3g60420	SALK_059036C	u/c	promoter	R
at3g61640	SALK_092212C	*AGP20*	promoter	R
at3g05360	SALK_008911C	*RLP30*	Exon	R
at3g05360	SALK_145342C	*RLP30*	Exon	R
at4g23290	SALK_022512C	*CRK21*	Exon	R
at4g23290	SALK_035263C	*CRK21*	Exon	R
at4g22880	SALK_120680C	*LDOX*	Promoter	R
at4g22880	SALK_073183	*LDOX*	Exon	R
at4g04540	SALK_036225C	*CRK39*	Exon	R
at4g11850	SALK_089968	*LPLDGAMMA1*	Promoter	R
at3g53490	SALK_645697C	u/c	5' UTR	R
at5g14930	SALK_022911C	*SAG101*	Exon	R

at5g01750	SALK_089519C	u/c	Promoter	R
at5g01750	CS372146	u/c	Promoter	R
at4g23190	SALK_054888	*CRK11*	Exon	R
at4g23190	SALK_054880	*CRK11*	Exon	R
at5g53110	SALK_136256	u/c	Exon	R
at5g53110	SALK_004123	u/c	Intron	R
at3g25882	SALK _148447C	*NIMI-2*	Exon	R
at3g25882	SALK_06674C	*NIMI-2*	Promoter	R
at2g30860	SALK_148672C	*GSTF9*	Promoter	R
at2g30860	SALK_001519C	*GSTF9*	Exon	R
at1g66880	SALK_034755	u/c	Exon	R
at1g66880	SALK_137021	u/c	Exon	R
at5g17220	SALK_105779C	u/c	Intron	R
at5g17220	SALK_113805C	u/c	Promoter	R
at5g41020	SALK_108569C	u/c	Promoter	R
at1g74650	CS2104374	*MYB31*	Promoter	R
at4g39950	SALK_113348C	*CYP79B2*	Exon	R
at4g31500	SALK_102615	*CYP83B1*	Promoter	R
at1g26420	SALK_079007	u/c	Promoter	R
at2g46650	SALK_027748C	*CYTB5-C*	Exon	R
at1g11330	SALK_076543C	u/c	Promoter	R

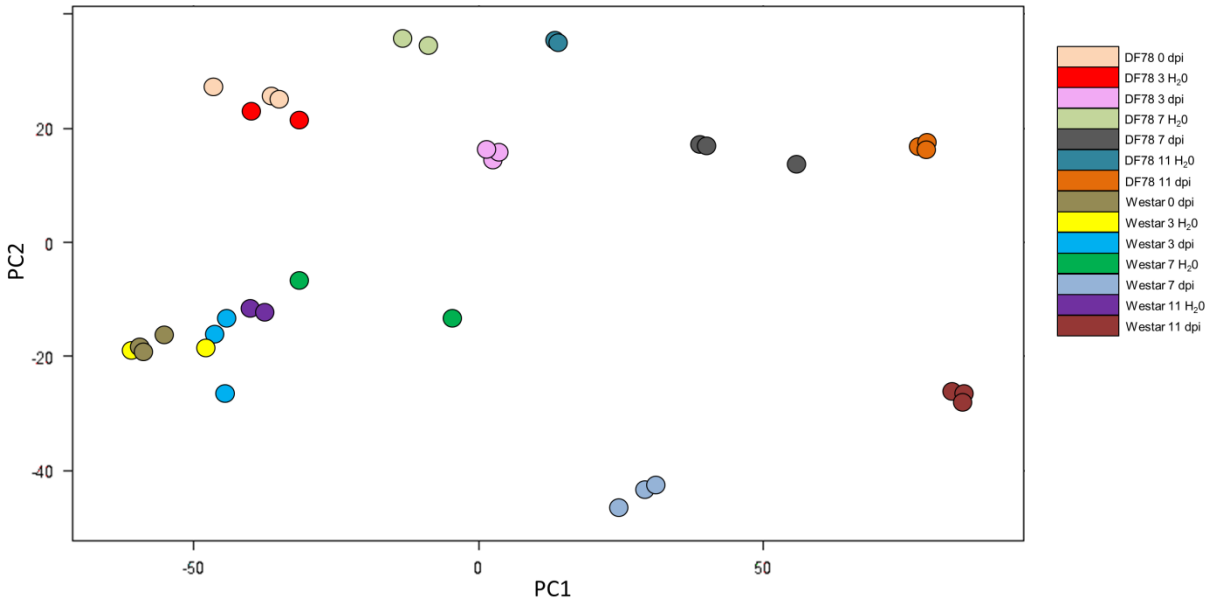

Appendix VIII: Principle component analysis of raw counts for each individual treatment. Legend on right of graph shows representative colour for each treatment group.

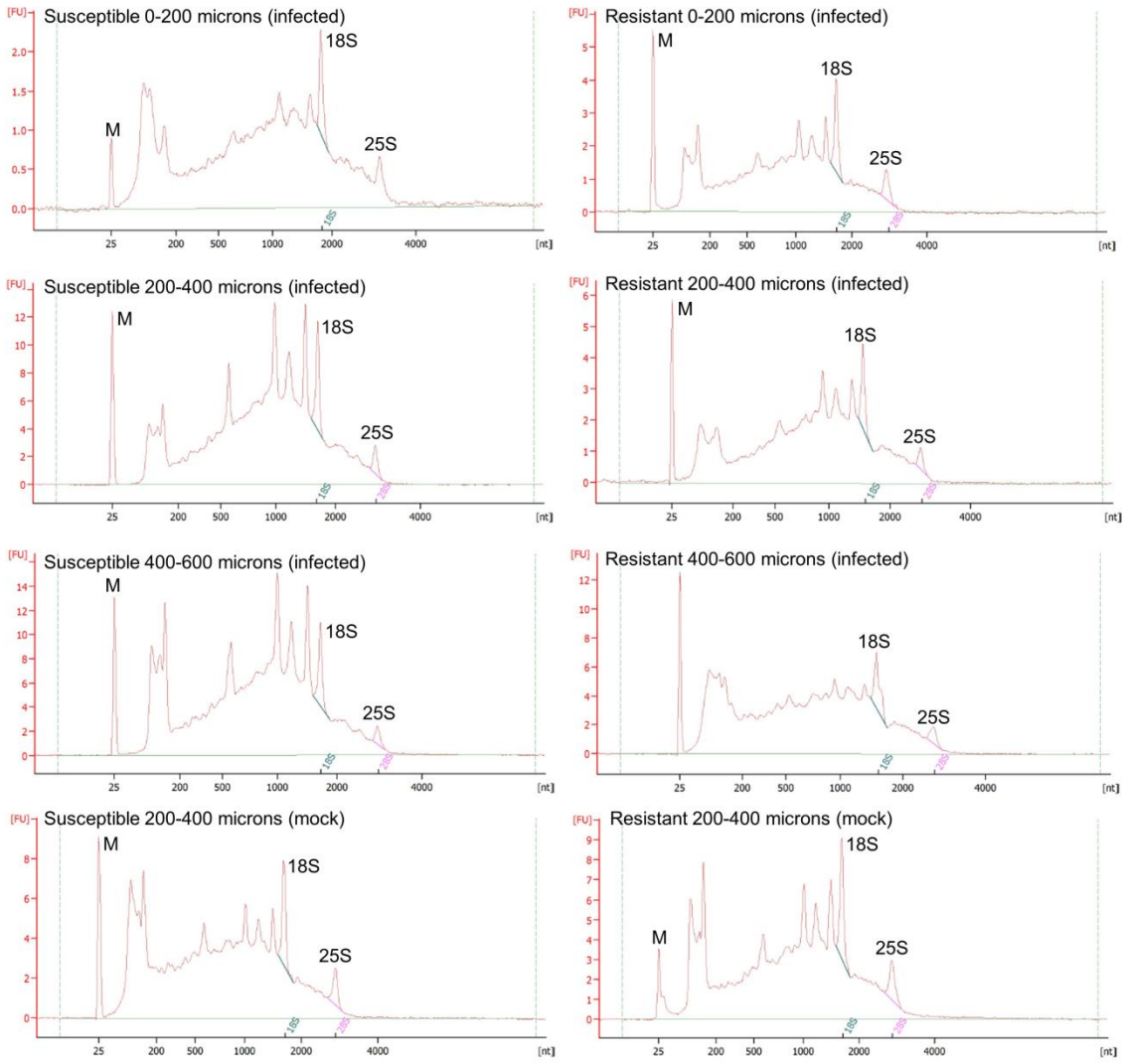

Appendix IX: RNA quality following tissue processing and laser microdissection. Representative electropherograms were recorded using a microfluidic PicoChip on the Agilent 2100 Bioanalyzer. Ribosomal peaks (18S and 25S) and chip marker have been superimposed onto electropherograms to aid interpretation.

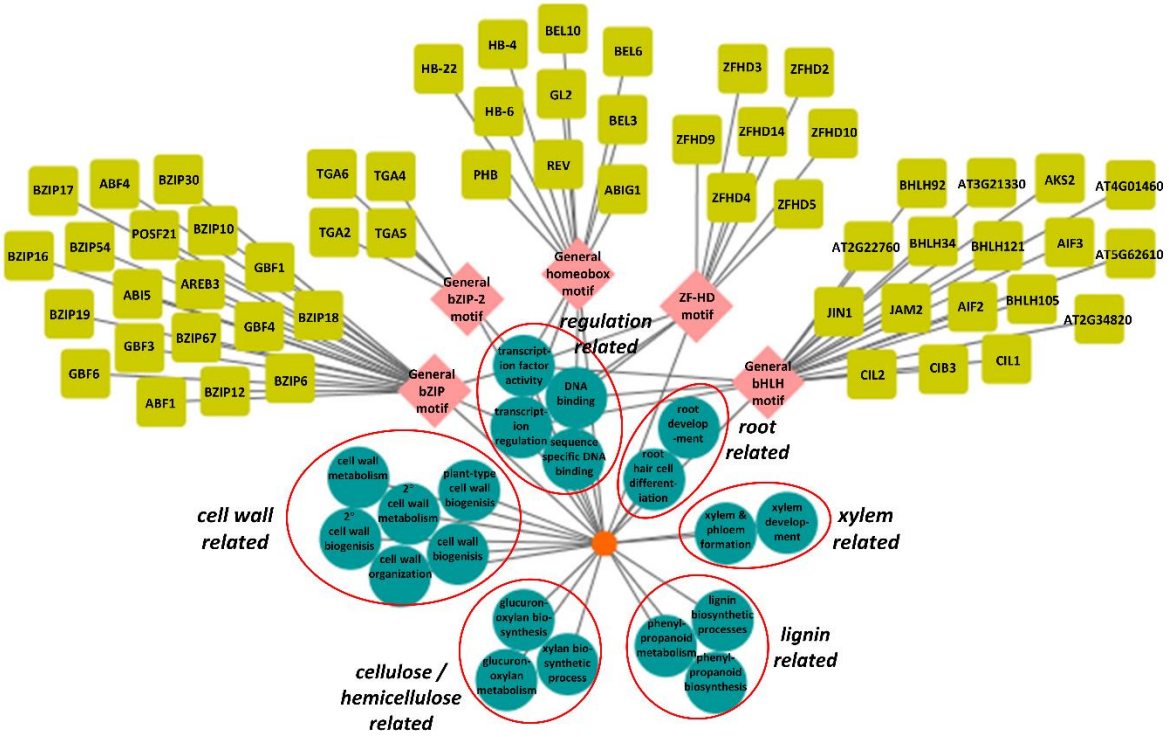

Appendix X: Transcriptional module produced with SeqEnrich. Input data was TFs and target genes involved in root specification and secondary cell wall synthesis, as identified in Taylor-Teeples et al. (2015). Data show enriched bZIP and Homeobox TF families, targeting genes associated with cell wall, cellulose and hemicellulose, xylem, lignin, root development, and regulation of transcription.

Appendix XI: Primer sequences used in LMD-RNA-Seq study.

Primer Name	Primer Sequence (5’ -> 3’)
CAM1.forward	TTGGCTAACCCATCGTTTTC
CAM1.reverse	ACTCCGAAATTTGGATGCTG
CPK5.forward	CGGCTAAGCGTGTAGAGGTC
CPK5.reverse	TCCCCAAAGAAGCTCACAAC
CNGC12.forward	CTTCATGCCCCTTAATCGAA
CNGC12.reverse	GACCCCACCAAAAGCAGTAA
PR1.forward	TGTGGCAAAGCAAGGTGTAA
PR1.reverse	TTCCCCGAGGATCATAGTTG
SOBIR1.forward	GGCATAGGAGGAACCCTCTC
SOBIR1.reverse	AACGCTTCTTCGTTCTCCAA
MEKK1.forward	AGTCACCACCACCTTCGTTC
MEKK1.reverse	TACCTCCGACAATGGAGAGG
MPK4.forward	TGGTGATCAGAGCACGAAAG
MPK4.reverse	CCCGTCTCTGAGTTGGTAGC
MPK6.forward	CGGCTATCGATGTTTGGTCT
MPK6.reverse	GCAAACGAAGCTGATGAACA
JAM1.forward	CAAGCTCAAGAACACCAGCA
JAM1.reverse	TAACCACGGAGAAGGTGGTC
MYC3.forward	TGGGGAGACGGGTACTACAG
MYC3.reverse	ACGAGTTAAGCTCCCGGATT
Lmac18S.forward	ATCTCTTGGTTCTGGCATCG
Lmac18S.reverse	GCAATGTGCGTTCAAAGATT

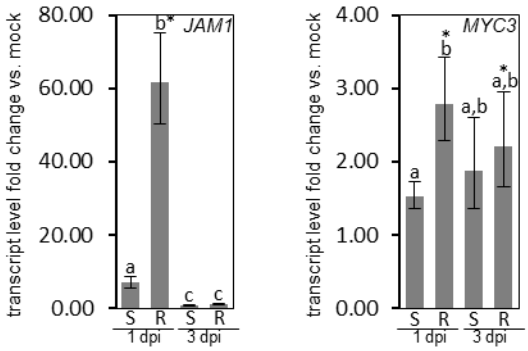

Appendix XII: Combined LMD and qPCR of select transcription factors from SeqEnrich regulatory networks. Expression levels of *JASMONIC ACID-ASSOCIATED 1* and *MYC3* at 1 day post inoculation (dpi) and 3 dpi, in resistant (R) or susceptible (S) hosts. Gene expression is compared to mock-inoculated controls treated with water. Significance of qPCR results for each target individually was determined with a one-way ANOVA ($p < 0.05$) between treatments, where significance is indicated by different letters. Significant deviation from mock controls is denoted by an (*), as determined by a Student's t-test ($p < 0.05$).

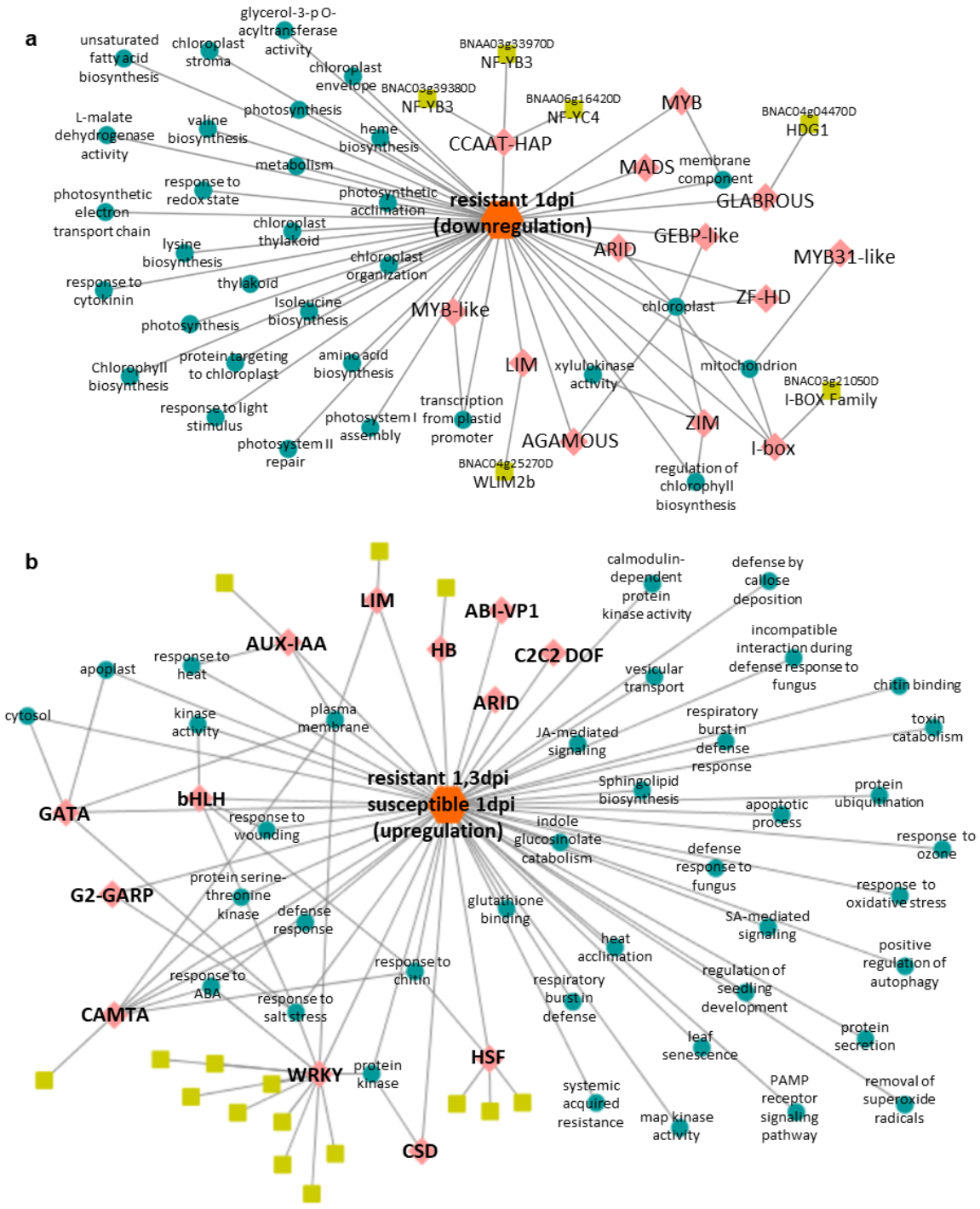

Appendix XIII: Predictive transcription factor networks identified from differentially expressed gene sets. A) Predicted network showing genes specifically downregulated in resistant hosts at 1 dpi. B) Predicted network showing transcription factors (chartreuse squares), DNA binding motifs (pink diamonds), and gene ontology terms (blue circles) enriched in upregulated differentially expressed in both infected hosts at 1 dpi and the resistant host only at 3 dpi. Grey lines show predicted connections between transcription factors, motifs, gene ontology terms, or the resistant-specific gene set.

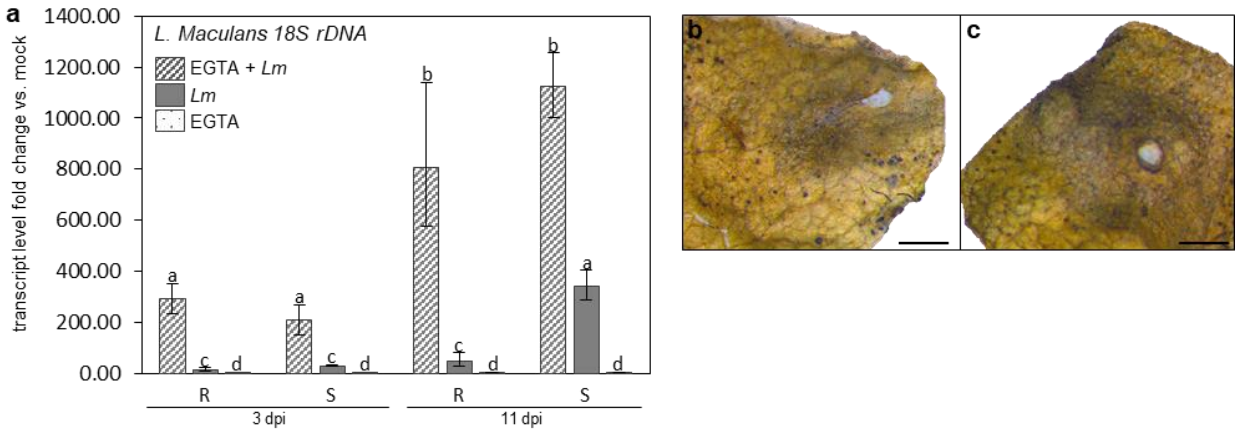

Appendix XIV: *L. maculans* fungal load in all treatments. (A) Relative mRNA abundance of *L. maculans* 18S rDNA in all treatment combinations at 3 and 11 days post inoculation (dpi). (B) Resistant Rlm2 cotyledons at 14 dpi, treated with EGTA and infected with *L. maculans.* (C) Susceptible Topas cotyledons at 14 dpi, treated with EGTA and infected with *L. maculans*. Scale = 2mm.

Appendix XV: List of abbreviations.

ABA	Abscisic acid
AGRIS	Arabidopsis Gene Regulatory Information Server
ANOVA	Analysis of variance
Avr	Avirulence
BAR	Bio-analytic resource
ChIP-Seq	Chromatin immunoprecipitation sequencing
CAM	Calmodulin
DEG	Differentially expressed Gene
DPI	Days post inoculation
EGTA	ethylene glycol-bis(β-aminoethyl ether -tetraacetic acid
ET	Ethylene
ETD	Effector-triggered defense
ETI	Effector-triggered immunity
FPKM	Fragments Per Kilobase of gene per Million mapped reads
GO	Gene ontology
HD	Homeobox domain
HR	Hypersensitive response
IAA	Auxin
IGS	Indole glucosinolates
JA	Jasmonic acid
LMD	Laser microdissection
MAPK	Mitogen-activated protein kinase

MKK	MAPK kinases
MEKK	MAPKK Kinase
NBS-LRR	Nucleotide-binding site leucine-rich repeats
NGS	Next-generation sequencing
ORF	Open reading frame
PAD3	Phytoalexin-deficient 3
PAMP	Pathogen-associated molecular pattern
PCA	Principle component analysis
PCD	Programmed cell death
PCR	Polymerase chain reaction
PRRs	Pattern recognition receptors
PTI	PAMP-triggered immunity
R	Resistant/Resistance
Rlm	Resistance to *L. maculans*
RLP	Receptor-like protein
RNA-Seq	RNA sequencing
ROS	Reactive oxygen species
S	Susceptible
SA	Salicylic acid
TAIR	The Arabidopsis Information Server
TF	Transcription factor
WAK	Wall-associated kinase

Appendix XVI: List of supplemental datasets.

Available from https://doi.org/10.1111/tpj.13514:

Data S1. Gene annotation and expression levels in all treatments.

Data S2. Differentially expressed genes in cv. Westar or line DF78 following *Leptosphaeria maculans* infection.

Data S3. Gene Ontology term enrichment output.

Data S4. Genome coordinates of novel transcripts.

Data S5. Primer sequences used for laser microdissection-qPCR and 18s rDNA detection.

Available from https://doi.org/10.1371/journal.pone.0178256:

Data S6. SeqEnrich program. Updated versions of the SeqEnrich program will be deposited as they become available at http://www.belmontelab.com.

Data S7. SeqEnrich source code. Updated versions of the SeqEnrich source code will be deposited as they become available at the SourceForge open-source repository (https://sourceforge.net/).

Data S8. SeqEnrich Java file and usage information.

Data S9. Arabidopsis and *B. napus* query lists used as test data for the SeqEnrich program.

Available pre-submission from https://dropbox.com/sh/un46ftkcbsztp19/AAD7qO55YMTlI3VOPNwN3ui1a?dl=0:

Data S10. *L. maculans* differential gene expression analysis summary.

Data S11. Genes coding for putative secreted proteins and their expression values.

Data S12. FPKM of all genes in all treatments.

Data S13. Raw data from SeqEnrich analysis.

Accessions: All RNA sequencing data are available from the Gene Expression Omnibus (GEO) data repository (accession GSE77723 and PRJNA477556)